D-MEM
PhD-UNIMI

Doctorate program
Milan
EXPERIMENTAL
MEDICINE

Università degli Studi di Milano

PhD Course in Experimental Medicine

CYCLE XXXVIII

BIOS-11/A

PRIMING STRATEGIES TO ENHANCE THE EFFECT OF THE SECRETOME OF MESENCHYMAL STEM/STROMAL CELLS IN COUNTERACTING OSTEOARTHRITIS THROUGH THE ACTION OF THE EVS

Candidate: **Dr. Francesca Cadelano**

Matr. ID: R13934

Orcid ID: 0000-0002-1658-8932

Tutor: **Prof. Anna Teresa Brini**

Supervisor: **Dr. Stefania Niada**

Director: **Prof. Nicoletta Landsberger**

Academic Year 2024-2025

Table of Content

1. Abstract

Osteoarthritis (OA) is the most prevalent form of joint disease, affecting millions worldwide and leading to chronic pain, stiffness, and functional disability due to progressive degeneration of articular cartilage, synovial inflammation, and exposure of subchondral bone and nervous terminals. Further, OA is increasingly recognized as being influenced by “inflammaging”, an emerging concept describing the chronic, low-grade inflammation associated with aging that contributes to tissue degeneration and impaired repair mechanisms. Despite its multifactorial pathophysiology, current OA treatments primarily address symptoms without targeting the underlying biological processes, ultimately necessitating surgical intervention. Additionally, OA can affect any individual since its early stages of aging, and considering the increasing average lifespan, disease-modifying or even disease-reverting approaches are urgently required, to overcome this social and economic burden.

Among emerging therapeutic strategies, mesenchymal stem cell (MSC)-derived conditioned medium (CM) has gained significant attention for its ability to recapitulate many of the regenerative, immunomodulatory, and anti-inflammatory properties of stem cells through its complex cargo of cytokines, growth factors, and extracellular vesicles. However, translating CM into clinical practice is hindered by production variability and the absence of preclinical models and guidelines to test its efficacy, safety and dosage. With this project, we established a standardized protocol to produce CM from adipose-derived MSC (ASCs) and characterized it comprehensively. CM was then evaluated into increasingly complex OA models, both bidimensional (2D) and three-dimensional (3D), where the pathology was recapitulated by the exposure to inflammatory cytokines, namely TNFα and/or IL-1β. These platform were used to test the effects of both naïve and primed CM on cellular and tissue responses, focusing on key molecular markers related to inflammation, matrix degradation, and tissue remodelling. CM treatment resulted in a significant downregulation of catabolic enzymes such as MMPs in cartilage representative models, moreover it demonstrated anti-inflammatory properties in both cartilage and synovial membrane representative ones. Importantly, in ex vivo settings, the response to CM varied among donors, with some explants exhibiting marked improvement while others showed minimal modulation, revealing inter-individual differences in therapeutic responsiveness.

These findings not only confirm the potential of MSC-derived CM as a promising disease-modifying agent in OA but also underscore the value of patient-specific ex vivo

models as predictive tools for therapeutic screening and for stratifying patients based on their molecular response profiles, paving the way toward personalized approaches in OA management.

2. Disclosure for research integrity

This research was carried out in line with the principles of the European Code of Conduct for Research Integrity. Throughout the project, I have aimed to maintain high standards of reliability and rigor in the design, methods, and analysis. I have been committed to being honest and transparent in how the work was planned, conducted, and presented, including the proper acknowledgment of sources and contributions. Respect for colleagues, research participants, and ethical standards has guided every part of this work. I have also followed the necessary protocols to protect data and ensure responsible handling of all research materials. There has been no fabrication, falsification, plagiarism, or other forms of research misconduct during this study. The text in this thesis is my own (unless otherwise specified) and AI-assisted tools have only been used for grammar editing. I have reviewed and edited the content as needed and I take full responsibility for the content of the thesis

3. Abbreviations

A

AA: Arachidonic Acid

ACAN: Aggrecan

ACLT: Anterior Cruciate Ligament Transection

ADAMTS: A Disintegrin And Metalloproteinase with Thrombospondin motifs

AFU: Arbitrary Fluorescence Unit

ALP: Alkaline Phosphatase

AMPK: Adenosine Monophosphate-activated Protein Kinase

ANOVA: Analysis of Variance

APMA: 4-Aminophenyl Mercuric Acetate

ASC: Adipose-derived Stem/stromal Cell

ATMP: Advanced Therapeutic Medicinal Product

B

BCA: Bicinchoninic Acid

BDNF: Brain-Derived Neurotrophic Factor

BMAC: Bone Marrow Aspirate Concentrate

BMI: Body Mass Index

BMP: Bone Morphogenetic Protein

C

CAD: Computer Assisted Design

CCL: C-C motif Chemokine Ligand

CD: Cluster of Differentiation

CER: Ceramides

CFSE: Carboxyfluorescein Diacetate Succinimidyl Ester

CFU: Colony Forming Unit

CM: Conditioned Medium

COL2A1: Collagen type II α chain 1

COL11A1: Collagen type XI α chain 1

COX2: Cyclooxygenase-2

COVID-19: Coronavirus disease 2019

CT: Computed Tomography

CTGF: Connective Tissue Growth Factor

CXCL: C-X-C motif Chemokine Ligand

D

DAMPs: Damage Associated Molecular Patterns

DHA: Docosahexaenoic acid

DHCER: Dihydroceramides

DKK-1: Dickkopf-1

DLP: Digital Light Processing

DMEM: Dulbecco Modified Eagle Medium

DMM: Destabilization of the Medial Meniscus

DMMB: 1,9-Dimethylmethylene Blue

DMOAD: Disease Modifying Osteoarthritis Drug

E

ECM: Extracellular Matrix

EICO: Eicosanoids

ELISA: Enzyme-Linked Immunosorbent Assay

EMA: European Medicines Agency

ENA: Epithelial Neutrophil-Activating Peptide 78

EPA: Eicosapentaenoic Acid

ERK: Extracellular signal-Regulated Kinase

EVs: Extracellular Vesicles

F

FA: Fatty Acids

FBS: Fetal Bovine Serum

FDA: Food and Drug Administration

FDR: False Degree Rate

FGF: Fibroblasts Growth Factor

FN1: Fibronectin 1

G

G-CSF: Granulocyte Colony Stimulating Factor

GAG: Glycosaminoglycans

GAPDH: Glyceraldehyde-3-Phosphate Dehydrogenase

GB3: Globotriaosylceramides

GMP: Good Manufacturing Practices

H

HIF: Hypoxia Inducible Factor

HGF: Hepatocyte Growth Factor

HLA-DR: Human Leukocyte Antigen – DR isotype

I

IDO: Indoleamine 2,3-dioxygenase

IFN: Interferon

IGF: Insulin-like Growth Factor

IHH: Indian Hedgehog

IκB: Inhibitor of nuclear factor kappa B

IKK: IκB kinase

IL: Interleukin

IL-1ra: IL-1 receptor antagonist

ISCT: International Society for Cell and Gene Therapy

J

JNK: c-Jun N-terminal Kinase

K

KL: Kellgren-Lawrence

KOOS: Knee Injury and Osteoarthritis Outcome Score

L

LacCer: Lactosyleramides

LCA: Leukocyte Common Antigen

LPA: Lipoaspirate

LPS: Lipopolysaccharide

LRP5/6: Low-density Receptor related Protein 5 or 6

M

M-CSF: Macrophage Colony Stimulating Factor

MAPK: Mitogen-Activated Protein Kinase

MCP-4: Monocyte Chemotactic Protein 4

miRNA: microRNA

MIA: Monosodium Iodoacetate

MHC-II: Major Histocompatibility Complex class 2

MISEV: Minimal Information for Studies of EV

MMP: Matrix Metalloproteinases

MRI: Magnetic Resonance Imaging

MSC: Mesenchymal Stem/Stromal Cell

mTOR: mechanistic Target Of Rapamycin

N

NF-κB: Nuclear Factor kappa-light-chain-enhancer of activated B cells

NO: Nitric Oxide

NSAIDs: Non-Steroidal Anti-Inflammatory Drugs

NTA: Nanoparticle Tracking Analysis

O

OA: Osteoarthritis

OC: Osteocalcin

OPN: Osteopontin

OPG: Osteoprotegerin

ORO: Oil Red-O

P

PBS: Phosphate-Buffered Saline

PCM: Pericellular Matrix

PDGF-AA: Platelet-Derived Growth Factor-AA

PGE2: Prostaglandin E_2

pNP/pNPP: P-Nitrophenol/ P-Nitrophenyl Phosphate

PTGS2: Prostaglandin-endoperoxide synthase 2

Prg4: Proteoglycan 4

PRP: Platelet-Rich Plasma

Q

QC: Quality Control

R

RA: Rheumatoid Arthritis

RAGE: Receptor for Advanced Glycation Endproducts

RANK/L: Receptor activator of nuclear factor kappa-B/ Ligand

ROS: Reactive Oxygen Species

RPMI: Roswell Park Memorial Institute

RT-qPCR: Real Time quantitative Polymerase Chain Reaction

Runx2: Runt-related transcription factor 2

S

SASP: Senescence-Associated Secretory Phenotype

SDS-PAGE: Sodium Dodecyl Sulphate-Polyacrylamide Gel Electrophoresis

SEM: Standard Error of the Mean

SM: Sphingomyelins

SMAD: Suppressor of Mothers Against Decapentaplegic

SOP: Standard Operating Procedure

SOX9: SRY-Box Transcription Factor 9

STRING: Search Tool for Retrieval of Interacting Genes/proteins

SVF: Stromal Vascular Fraction

T

TAK1: TGFβ−Activated Kinase 1

TAZ: Transcriptional coactivator with PDZ-binding motif

TBP: TATA Binding Protein

TCF/LEF: T-Cell Factor/Lymphoid Enhancer-binding Factor

TEM: Transmission Electron Microscopy

TGFβ: Transforming Growth Factor-β

THR: Total Hip Replacement

TIMP: Tissue Inhibitor of Matrix Metalloproteinases

TKR: Total Knee Replacement

TLR: Toll Like Receptor

TNFα: Tumor Necrosis Factor alpha

TNF-RI: TNF Receptor 1

TRAP: Tartrate-resistant Acid Phosphatase

TSG-6: TNF Stimulated Gene-6

U

UHPLC: Ultrahigh-Pressure Liquid Chromatography

V

VEGF: Vascular Endothelial Growth Factor

W

Wnt: Wingless

WOMAC: Western Ontario and McMaster Universities Osteoarthritis Index

Y

YAP: Hippo-Yes-Associated Protein

4. Introduction

Due to the multidisciplinary nature of this project, the introduction will separately address the following main sections: the first introducing conditioned medium as part of the cell-free approach in regenerative medicine, whereas the second part will cover osteoarthritis pathology, treatment and modelling.

4.1 Introduction on conditioned medium potential

The therapeutic potential of mesenchymal stromal cells (MSCs) has generated considerable interest over the past decades, particularly due to their regenerative and immunomodulatory properties. More recently, the focus has shifted to their paracrine modulatory capacity, to the point that a change in nomenclature has been proposed to better reflect their mechanism of action. In 2019, the International Society for Cell & Gene Therapy (ISCT) recommended the term Medicinal Signaling Cells, mainly through the work of Arnold Caplan (1,2), to underscore the ability of MSCs to exert therapeutic effects primarily through the secretion of bioactive factors, collectively known as the secretome. This shift in perspective highlighted a broader role for MSCs as dynamic modulators of the tissue microenvironment, rather than simply as progenitor cells for tissue repair. The following paragraphs will cover the foundation of MSC research and introduce the principal derivatives of their secretome, namely conditioned medium and extracellular vesicles.

4.1.1 What are MSCs, where do they come from, how are they used

MSCs are a heterogeneous population of multipotent, fibroblast-like cells capable of self-renewal and differentiation into multiple mesenchymal lineages, including osteoblasts, chondrocytes, and adipocytes (3). Originally isolated from the bone marrow by Friedenstein and colleagues in the 1970s (4), MSCs have since been identified in a wide variety of adult and perinatal tissues, such as adipose tissue, bone marrow, dental pulp, synovial membrane, periosteum, umbilical cord and placenta (5,6). These diverse sources have allowed the development of tissue-specific MSC populations that may vary in their proliferation, differentiation, and secretory capacities (7), while still fulfilling the minimal criteria defined by the ISCT: plastic adherence in standard culture conditions, expression of surface markers (CD73, CD90, and CD105) in the absence of hematopoietic markers (CD34, CD45, CD14 or CD11b, CD79α or

CD19, and HLA-DR), and in vitro trilineage differentiation potential (8,9). MSCs have gained significant attention in regenerative medicine and immunotherapy due to their ability to modulate immune responses, secrete trophic and anti-inflammatory factors, and contribute to tissue repair (10). Their applications range from treatment of immune-mediated disorders, including graft-versus-host disease, Crohn's disease, and systemic lupus erythematosus, to degenerative diseases, such as osteoarthritis (11–13). Their broad application is supported by the diminished immunogenicity, due to the absence of MHC-II antigen expression (14). In orthopaedic and musculoskeletal settings, MSCs have been investigated for their potential to promote bone regeneration, cartilage repair, and tendon healing, often through local injection or scaffold-based delivery strategies (15,16). Despite their original characterization as stem cells with differentiation capabilities, current evidence suggests that their primary therapeutic mechanism involves paracrine signalling, where secreted molecules influence the surrounding microenvironment, reduce inflammation, and promote endogenous repair processes (17,18). This has led to increasing interest in cell-free therapies, such as the MSC-derived secretome or extracellular vesicles, as alternatives to cell transplantation, potentially reducing safety and regulatory concerns.

4.1.2 Derivate of MSCs: cell free products, secretome focus

Initially, MSCs therapeutic potential was attributed to direct differentiation and engraftment into damaged tissues. However, accumulating evidence indicates that the primary mechanism behind their therapeutic action lies in the bioactive molecules they secrete rather than cellular integration. This has shifted attention toward cell-free MSC-derived products, comprehensively referred to as the secretome. The term secretome encompasses the totality of molecules secreted by MSCs, including soluble proteins such as cytokines, chemokines, and growth factors; lipids and metabolites; extracellular vesicles (EVs) such as exosomes and microvesicles; and nucleic acids including mRNAs and microRNAs (miRNAs) (19,20). Within this context, conditioned medium (CM)—the culture supernatant containing all the bioactive factors and particles released by MSCs, thus making it a synonym for secretome—has emerged as a promising therapeutic candidate, offering advantages in terms of safety, storage, and regulatory compliance compared to cell-based therapies. These components act

synergistically to orchestrate various biological effects, including immunomodulation, anti-apoptotic signalling, angiogenesis, macrophage polarization, enhancing wound healing and tissue remodelling (21). Importantly, the secretome is believed to mediate many of the therapeutic outcomes observed in MSC-based therapies, independent of cell engraftment or long-term survival (22).

CM and other stem cell-derived acellular products treatments, such as EVs, offer important safety advantages over cell transplantation ones. By acting mainly through paracrine mechanisms, they bypass critical risks associated with live cell administration, including immune rejection, tumorigenicity, uncontrolled proliferation, undesired differentiation, embolization, or vascular obstruction (23,24). CM is also compatible with scalable, off-the-shelf production and –possibly– with more straightforward regulatory pathways, particularly taking as examples the frameworks for biologics and advanced therapy medicinal products (ATMPs). A major strength of CM lies in its flexibility and tunability. The composition and biological potency of CM can be modulated by altering cell culture parameters, such as oxygen tension, serum content, passage number, or 3D growth systems (25). Additionally, preconditioning or priming strategies, including exposure to inflammatory cytokines (e.g., IFNγ, TNFα), hypoxia, or mechanical stimulation, have been shown to enhance the immunomodulatory and trophic profiles of the secretome (26). This adaptability enables researchers to tailor CM to specific disease contexts. Moreover, to highlight an apparently obvious concept, the secretome therapeutic potential extends beyond the anatomical origin of its source cells, enabling the use of accessible and abundant MSC sources to treat physiologically distant tissues. An example, is the recent interest in MSCs derived from menstrual blood, whose secretome has been applied to treat COVID-19 severe patients to reduce hypoxia, cytokine storm and restore immune function (27).

Despite its promise, CM-based therapy also faces significant challenges. Its complex and variable composition makes it difficult to define potency assays and release criteria. Inter-donor variability, heterogeneity in MSC source (e.g., adipose tissue, bone marrow, umbilical cord), and culture protocol inconsistencies introduce batch-to-batch variation that complicates standardization and reproducibility. Furthermore, while although CM contains EVs, it differs from EV-enriched products in

terms of isolation, stability, and regulatory considerations — highlighting the need for clear definitions and product characterization in clinical translation pathways. Recent findings in osteoarthritis models underscore CM's therapeutic relevance, showing reduced synovial inflammation, preserved cartilage integrity, and modulation of chondrocyte metabolism (28). These results, coupled with its favourable safety profile, position MSC-derived CM as a compelling next-generation product in regenerative medicine. Moving forward, efforts toward standardization, mechanistic insight, and clinical validation—supported by advances in omics technologies, functional assays, and ex vivo disease modelling—will be crucial for its successful integration into precision therapies (29)

4.2 Conditioned medium/secretome production

4.2.1 Strategies for production

The production of conditioned medium presents several challenges that must be addressed to enable its clinical application. Various strategies exist for secretome collection and conditioning, including modifications to culture conditions, stimulation protocols, and preconditioning with inflammatory or hypoxic signals. Each of these factors can profoundly influence the composition and efficacy of the final product.

4.2.1.1 Culture conditions

CM can be collected from cells cultured using a wide range of in vitro methods. To date, no specific culture condition has been identified as incompatible with CM collection, which further supports its versatility as a therapeutic product. CM can be obtained from virtually any cell type, provided their specific culture requirements are respected. There are examples of CM harvested from both bidimensional (2D) and three-dimensional (3D) cultures, as well as from tissue explants (30–32). Furthermore, cultures can be maintained under static or dynamic conditions, with CM collected either at a single endpoint or continuously, resulting in a final "cumulative" product. Typically, standard culture media such as DMEM or RPMI are employed, with supplements adapted depending on whether the goal is basic research, compliance with good manufacturing practices (GMP), or suitability for in vivo administration. Importantly, it is critical to distinguish between the conditions used for cell expansion and those intended for CM production. Cells or tissue explants may initially be cultured

under optimized conditions to promote growth and limit contamination (e.g. using antibiotics), before transitioning to more minimal or defined conditions for CM collection (33,34). A commonly implemented step in CM production is serum starvation, wherein growth factor sources like foetal bovine serum (FBS) or platelet lysate are removed. This serves a dual purpose: reducing the presence of undefined or exogenous components in the final product and stimulating the cells to enhance their secretory activity (26). Notably, serum deprivation has been shown to induce a more robust secretory phenotype, simulating the cellular response to physiological stress or injury, but also modifies mitochondria morphology in order to compensate to the energy demand (26,35).

4.2.1.2 Stimulation and pre-conditioning

CM represents a valuable therapeutic option due to its high degree of personalization, which can be achieved by selecting different MSC sources. Its composition and potency can be further modulated through exposure to specific chemical, biological, or physical stimuli (36,25). The rationale behind these approaches is to enhance the therapeutic efficacy of the secretome by tuning the cellular response to mimic disease-specific environments or to replicate the conditions the cells would encounter in vivo if administered as part of a cell-based therapy rather than a cell-free product. As outlined by Ferreira et al. (37), biological stimulation may involve the use of cytokines, growth factors, or other bioactive molecules; chemical stimulation relies on pharmacological agents; and physical stimulation includes modifications to culture surface properties, dimensionality (2D vs. 3D), gas composition, or exposure to electromagnetic fields. Each type of stimulus can selectively enhance specific functions of the secretome — such as promoting cell adhesion, proliferation, or differentiation — and influence its capacity to modulate immune, endocrine, musculoskeletal, and other physiological systems. Representative examples of preconditioning strategies, along with the observed effects, are summarized in Supplementary Table 1.

4.2.2 Standardization challenges

One of the major challenges in CM production lies in the validation of standardised protocols, which significantly hampers reproducibility and slow down

clinical translation. Variability can arise from multiple factors, including the tissue source and donor variability of MSCs, differences in culture conditions (such as media composition, oxygen tension, and confluence at harvest), and inconsistencies in the duration and method of conditioning. Furthermore, downstream processing steps—such as centrifugation, filtration, and storage—can greatly influence the final composition of CM, particularly in terms of extracellular vesicle and protein content (38). This heterogeneity complicates comparisons between studies and consequently, a second major issue in CM production is the establishment of quality control measures essential for regulatory approval and therapeutic application. The complexity of this product in terms of soluble factors and vesicles content, poses a challenge to current quality prerequisites, since it would be impossible and more importantly limiting, comparing the CM with other biological drugs. Addressing these issues requires the development of robust, scalable, and harmonised production and characterisation protocols (39). Standardization efforts are essential to minimize batch variability and ensure reproducibility. Defining optimal culture parameters, harvest timing, and processing techniques is critical to produce conditioned medium suitable for therapeutic use (29,40).

4.2.3 Regulatory framework

The regulatory framework for the clinical application of CM and other cell-free products such as EVs remains an evolving landscape. The closest comparable biotherapeutics are the Advanced Therapy Medicinal Product (ATMP), which include gene therapies, somatic cell therapies, and tissue-engineered products (41). As neither CM and EVs currently fall within this classification, under the European Medicines Agency (EMA) or the U.S. Food and Drug Administration (FDA), their regulatory framework cannot be applied but can serve as a preliminary guide to follow (42,43). Moreover, both agencies adopt a case-by-case evaluation, particularly focusing on the manufacturing process, intended use, and degree of manipulation. This kind of plasticity by the regulators is needed in ATMPs as well as for CM and EVs, since they are produced ad hoc for several pathologies and adopting unique protocols. For what concerns ATMPs, they must comply with stringent standards aimed at ensuring quality, safety, and efficacy, such as:

1. Defined identity and potency: the product must be well-characterised with clear biological activity related to its mechanism of action.
2. Batch-to-batch consistency: reproducibility must be ensured through validated and controlled processes.
3. Purity and safety: products must be free from contaminants (e.g., endotoxins, pathogens, residual nucleic acids) and be manufactured under sterile conditions.
4. Stability and traceability: shelf-life, storage conditions, and complete traceability of donor materials and production records must be guaranteed.

When comparing CM and EVs to these criteria, several gaps become evident. Particularly, CM is a complex mixture of soluble proteins, lipids, nucleic acids, and vesicles, which poses significant challenges in complying with the first two points. Its composition varies depending on many factors, as previously discussed, however a possible approach could be to determine specific threshold and ranges for beneficial and dangerous components and adapting it to the context of application. Moreover, in order to better assess potency and safety, a panel of different *in vitro*/*ex vivo* assays could be implemented, that comprehend all major systemic toxicity effects: this could better include the 3Rs (Reduce, Refine, Replace) approach to the clinical translation of such products, thus helping in reducing the *in vivo* assays. EVs, being a more specific and physically distinguishable component of CM, offer relatively greater promise in terms of standardisation. Advances in EV isolation and characterisation techniques have improved the reproducibility and purity of EV-based products, starting with the implementation of dynamic and automatic culturing methods of the donor cells (44). However, the lack of consensus on potency assays and quality markers remains a regulatory bottleneck. While EVs may be closer to fulfilling the ATMP quality criteria, both CM and EVs currently require further standardisation, validated bioactivity assays, and controlled manufacturing pipelines to approach regulatory approval.

4.3 Musculoskeletal inflammatory diseases

Musculoskeletal inflammatory diseases are a group of conditions characterized by chronic inflammation affecting joints, muscles, and connective tissues, often

leading to pain, stiffness, and progressive functional impairment. They include both autoimmune disorders, such as rheumatoid arthritis (RA) and psoriatic arthritis, driven by systemic immune dysregulation, and non-autoimmune forms like osteoarthritis (OA), where inflammation arises locally in response to mechanical and biochemical joint stress. Other disorders such as ankylosing spondylitis, and gout also contribute significantly to disease burden and disability.

4.3.1 Overview of diseases: OA, RA, others

Musculoskeletal inflammatory diseases encompass a broad group of conditions characterized by chronic inflammation of the joints, connective tissues, and supporting structures. Among these, OA and RA are the most prevalent and clinically relevant. While these pathologies share some overlapping features—such as joint pain, stiffness, and impaired mobility—they differ markedly in their underlying aetiology, inflammatory mechanisms, and clinical progression. OA is the most prevalent musculoskeletal disorder worldwide and a leading cause of disability among older adults. Traditionally considered a degenerative joint disease caused by mechanical wear and tear, OA is now recognized as a complex and multifactorial condition involving mechanical, biochemical, and inflammatory components. It primarily affects load-bearing joints such as the knees, hips, and spine, but may also involve the hands and other joints. The hallmark of OA is the progressive degradation of articular cartilage, accompanied by subchondral bone remodelling, synovial inflammation, and osteophyte formation, as well recapitulated in Figure 1 from the work of Tang et al (45). Joint integrity depends on the interplay of different periarticular tissues. Under physiological conditions, the synovial membrane and fluid ensure lubrication and metabolic exchange, the infrapatellar fat pad contributes mechanical support and immune regulation, and the menisci aid in shock absorption and stability. In osteoarthritis, the dysfunction of these structures amplifies cartilage degeneration: synovial inflammation alters fluid composition, the fat pad becomes a source of pro-inflammatory mediators, and meniscal damage disrupts load distribution (45–47).

Altogether, these changes accelerate the loss of joint homeostasis and exacerbate disease progression.

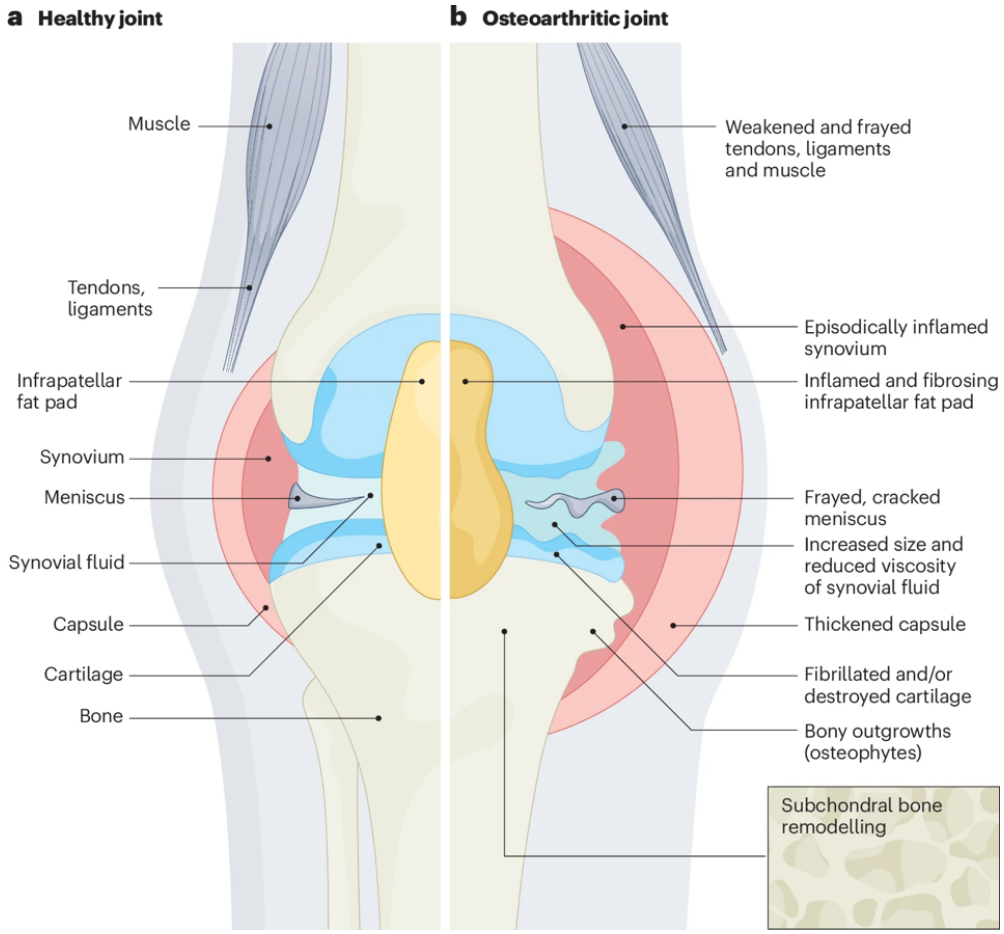

Figure 1 – Osteoarthritis in a knee joint *– In the image from Tang et al. are represented all the anatomical structures involved in OA disease. On the left side, the healthy joint is represented, whereas the damaged and affected joint is depicted in the right ride.*

Although OA is not classified as an autoimmune disease, low-grade chronic inflammation plays a significant role in its onset and progression. Chondrocytes and synoviocytes respond to joint stress or injury by releasing pro-inflammatory cytokines such as IL-1β, TNF-α, and IL-6, which in turn stimulate the production of matrix-degrading enzymes like MMPs and ADAMTSs. These molecular events accelerate cartilage breakdown and impair tissue repair mechanisms. Additionally, the infiltration of immune cells, the presence of damage-associated molecular patterns (DAMPs), and the activation of innate immune receptors such as TLRs contribute to sustaining the inflammatory environment within the joint. OA is also considered a disease of the whole joint, involving not only cartilage but also the synovium, subchondral bone, menisci, ligaments, and periarticular muscles (48). It is important to acknowledge such

definition in order to improve appropriate therapeutic strategies. Aging, obesity, prior joint injury, and genetic predisposition are key risk factors; however, the management of the modifiable ones is not enough to eradicate the risk of contracting this condition. Notably, the concept of inflammaging—the age-related, low-grade chronic activation of the immune system—has been increasingly implicated in OA pathogenesis, linking dysregulated immune response to tissue degeneration in elderly patients (49). From a biological point of view, in cartilage such alterations cause the formation of a peculiar chondrocyte phenotype that responds to inflammatory insults and accelerates cartilage degradation, in the process of chondrosenescence (50). Current OA treatments are primarily symptomatic and include pharmacological pain relief, lifestyle modifications, intra-articular injections, and ultimately surgical joint replacement (51). However, these approaches do not halt disease progression. As a result, there is growing interest in regenerative and anti-inflammatory strategies, including MSC-derived therapies and their secretome, as potential disease-modifying options. In contrast, RA is a systemic autoimmune disease characterized by persistent synovial inflammation, immune cell infiltration, and autoantibody production (e.g., rheumatoid factor, anti-citrullinated protein antibodies) (52). It often presents as symmetric polyarthritis and leads to rapid joint destruction if untreated. RA affects multiple joints and can also involve other systemic organs, reflecting its inflammatory and immune-mediated nature (53). Other inflammatory joint diseases, including psoriatic arthritis and ankylosing spondylitis, belong to the spondyloarthropathy group, which inflammatory arthropathies that interest also extra-articular regions. The spondyloarthropathies comprehend indeed also inflammatory bowel disease-related arthritis and psoriatic arthritis (54). Understanding the pathophysiological distinctions between these diseases is critical for therapeutic development, especially in the context of regenerative and anti-inflammatory strategies such as MSC-derived secretome. Tailoring treatment approaches requires not only addressing the inflammatory component but also the tissue-specific mechanisms driving disease progression in each condition.

4.3.2 Symptomatology and diagnosis

Symptomatically, OA is characterized by pain and functional limitation of the affected sites, and its diagnosis is primarily clinical, supported by imaging and, in some cases, laboratory investigations. More specifically, patients typically present with joint pain, stiffness, and limited mobility, especially after periods of inactivity or excessive use. Pain is usually subtle at the onset and worsens with activity and disease progression. Commonly affected sites include load-bearing joints, such as knees, hips, and spine, or highly mobile joints like hands and elbows. On physical examination, crepitus –the noise produced by unhealthy joints that seem to crack or crunch when moving–, joint tenderness, bony enlargement, and reduced range of motion may be noted (55). Imaging has a supportive role in diagnosis, with plain radiography remaining the first-line tool for OA evaluation. Radiographic features include joint space narrowing, osteophyte formation, subchondral sclerosis, and subchondral cysts. From this parameter, Kellgren and Lawrence defined a grading scheme for OA severity, that has five degrees of intensity. It starts at 0, with none OA detected, and progressively pass from (I) doubtful, (II) minimal, (III) moderate and (IV) severe (56).

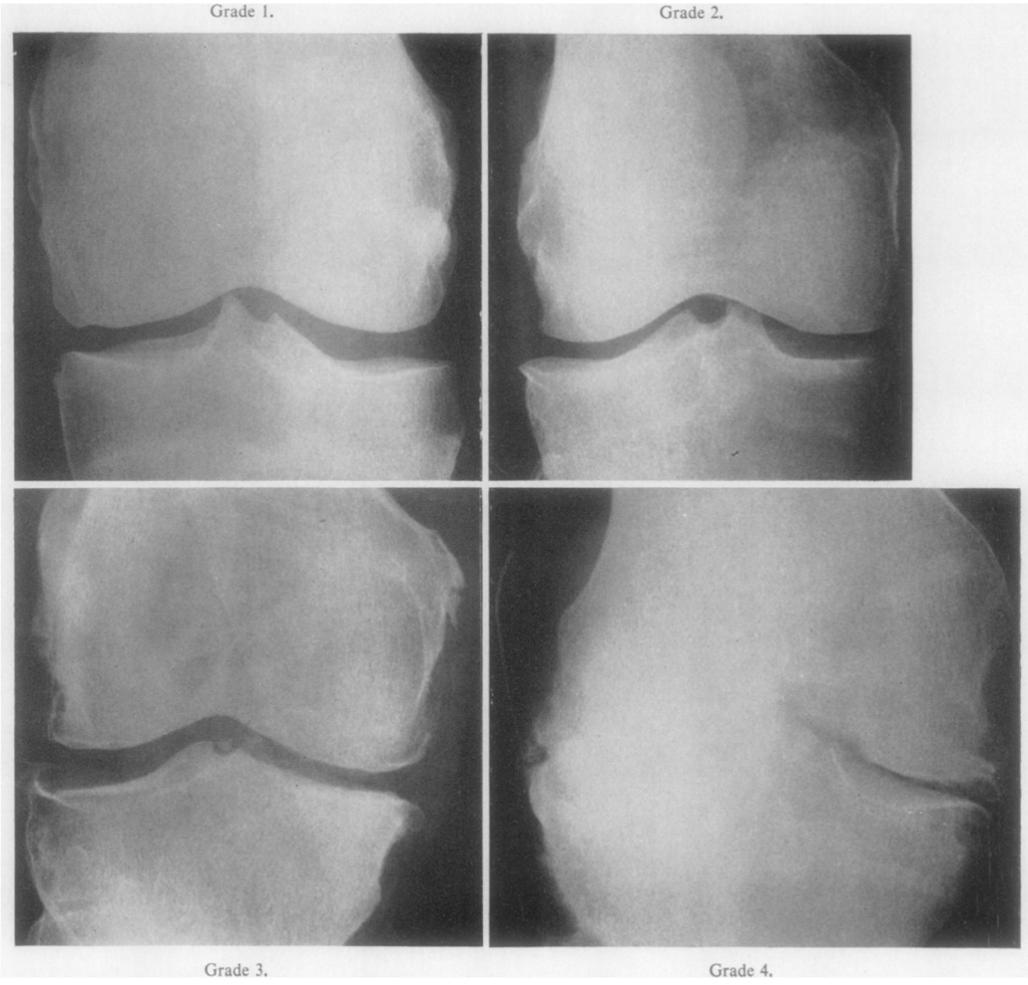

Figure 2 – Radiological assessment of osteoarthritis severity using the Kellgren–Lawrence (KL) grading system *– Original Figure 8 from the Kellgren and Lawrence publication illustrates four progressive stages of knee OA. Scoring is based on the presence and extent of osteophyte formation, joint space narrowing, subchondral bone sclerosis, bone contour deformities, and loss of definition in the joint space.*

A representative image from the original article has been selected, to highlight the differences detectable through x-rays evaluation (Figure 2). Other imaging techniques comprehend magnetic resonance imaging (MRI), that can provide more sensitive detection of early cartilage damage, bone marrow lesions, and synovitis, and is particularly useful in research or ambiguous cases (57). Laboratory testing may be performed on synovial fluid, collected through arthrocentesis, mainly to differentiate inflammatory or crystal induced- arthritis, and immune cell or bacterial infiltrate (58). There are no specific biomarkers for OA in routine clinical use, but ongoing research seeks to identify molecular signatures in blood, urine, that may aid in early detection, monitoring, or stratification (59). In terms of quality of life and patient symptomatology WOMAC and KOOS are standardized questionnaires used to assess pain, stiffness, and physical function in patients with osteoarthritis. WOMAC focuses on the hip and knee, while KOOS expands to include sport-related aspects and general quality of life (60). Overall, OA diagnosis is based on a combination of clinical features, risk factors, and imaging, with an increasing emphasis on identifying the disease in its early, potentially modifiable stages.

4.3.3 Focus on OA pathogenesis

Understanding OA pathogenesis is crucial for the development of effective treatments. OA is characterized by a complex interplay of mechanical, biochemical, and inflammatory processes leading to progressive cartilage degradation, subchondral bone remodelling, and synovial inflammation.

4.3.3.1 Tissues involved

Osteoarthritis is increasingly recognized as a disease of the entire joint, involving not only articular cartilage but also the synovial membrane, subchondral bone, menisci, ligaments, and periarticular muscles. Cartilage degradation is a hallmark feature, driven by an imbalance between anabolic and catabolic processes in chondrocytes. The synovium often exhibits low-grade inflammation, contributing to

pain and the release of pro-inflammatory mediators. Subchondral bone undergoes sclerosis and remodelling, influencing mechanical stress distribution and further affecting cartilage integrity. Structural damage to the menisci and ligaments compromises joint stability, while alterations in periarticular muscles can contribute to functional decline. The interplay among these tissues is critical to the initiation and progression of OA. How the tissues are involved, and at which stage, has been summarised in Supplementary Table 2.

4.3.3.2 Molecular pathways

Osteoarthritis is driven by a multifaceted set of pathways, that ultimately cause the onset of a chronic inflammatory environment. One of the central signalling cascades in OA pathogenesis is the nuclear factor kappa B (NF-κB) pathway (61), which is activated in response to inflammatory cytokines such as IL-1β and TNF-α. The inhibitors of NF-κB, mainly IκB proteins such as IκBα, are present in the cytoplasm and block its phosphorylation and nuclear import. When inflammatory stimuli activate the IKK complex and promote IκB degradation, NF-κB is released, most commonly in the form of the p65 (RelA)/p50 dimer, which then translocates into the nucleus and promotes the expression of target genes including cytokines (IL-1β, TNF-α, IL-6), chemokines, and catabolic enzymes (MMPs, ADAMTS) all contributing to the pathological matrix degradation (62). Additionally, NF-κB regulates cyclooxygenase-2 (COX-2) and inducible nitric oxide synthase (iNOS), leading to increased production of prostaglandin E_2 (PGE_2) and nitric oxide (NO), which amplify inflammation, oxidative stress, and cartilage degradation in osteoarthritis (63,64).

The wingless (Wnt)/β-catenin canonical pathway also plays a critical role in OA. In healthy cartilage, the β-catenin is degraded by proteasome and the Wnt signalling is inhibited. In pathological chondrocytes, Wnt binds the transmembrane receptor Frizzled and low-density receptor related protein 5 or 6 (LRP5/6) complex and starts the signalling cascade that inhibit β-catenin degradation. Then β-catenin translocate in the nucleus and binds to TCF/LEF and control the expression of several genes important for cartilage tissue: collagen type II α chain (Col2a1), collagen type XI α chain (Col11a1), MMP13, p53 and ADAMTS. However, a normal level of Wnt/β-catenin signalling is necessary for cartilage development, health and repair (65). Similarly, the mitogen-activated protein kinase (MAPK) pathway—including the ERK,

JNK, and p38 MAPKs—is activated by stress stimuli and cytokines, leading to the phosphorylation of transcription factors that enhance catabolic and inflammatory gene expression (66).

The transforming growth factor β and bone morphogenetic protein, TGF-β/BMP, pathway exhibits a dual and context-dependent role in OA. The cascade is activated when they bind respective transmembrane receptor that can induce Suppressor of Mothers Against Decapentaplegic (SMAD) phosphorylation and its consequent nuclear translocation or activate TGFβ−activated kinase 1 (TAK1) and extracellular signal-regulated kinase 1 and 2 (ERK1/2). In healthy cartilage, TGF-β signalling maintains chondrocyte phenotype and ECM integrity through canonical (SMAD dependent) and non-canonical (SMAD independent) pathway. However, in OA, the pathway is altered mainly due to the abnormal expression of BMP-2 and BMP-4 (67).

Other involved pathways are related to the presence in chondrocytes and other joint cells of specific receptors—including those for Wnt, NF-κB, TGF-β/BMP, and other signalling pathways such as FGF signalling pathways, as well as focal adhesion (FA) proteins—that enable them to detect and respond to biochemical and mechanical stimuli (68). Upon activation, these pathways interact in a complex regulatory network involving key signalling molecules such as AMPK, mTOR, FGF, BMP, HIFs, and NF-κB (69). Through complex crosstalk and feedback loops, they modulate the expression of critical downstream targets in articular cartilage and synovial tissue, including transcription factors like Runx2 and catabolic enzymes such as MMP13, ADAMTS4, and ADAMTS5, along with protective factors like Prg4 (69). Recent evidence also highlights the role of oxidative stress and mitochondrial dysfunction in OA. Excessive production of reactive oxygen species (ROS) activates catabolic signalling pathways and impairs mitochondrial bioenergetics, accelerating chondrocyte senescence and matrix breakdown (70). Furthermore, TLR-mediated innate immune signalling contributes to synovial inflammation and pain initiation and maintenance, via recognition of damage-associated molecular patterns (DAMPs) released from degraded cartilage (71). The onset of OA can be triggered by diverse factors—such as chronic mechanical overload, inflammation, and aging—which initiate disease

progression through distinct molecular pathways that characterize the early stages of OA.

The mechanotransduction is mainly due to the pericellular matrix (PCM), which provide a surrounding controlled region for chondrocytes, by maintaining optimal mechanical stress and general homeostasis. When the mechanical stress is excessive, the Hippo-Yes-associated protein (YAP)/transcriptional coactivator with PDZ-binding motif (TAZ), TGF-β1, mitogen-activated protein kinase/extracellular signal-regulated kinase (MAPK)-ERK, Wnt and Indian hedgehog (IHH) pathways are activated. They respond to PCM slimming and overload by incrementing MMP expression, thus causing major damages to the matrix (72).

Collectively, these interconnected molecular pathways represent potential therapeutic targets and provide a mechanistic rationale for the use of anti-inflammatory and regenerative agents, including MSC-derived secretome, to modulate OA progression.

4.3.4 Role of inflammaging

In osteoarthritis, inflammation is not a passive byproduct of tissue damage but actively contributes to joint degeneration from the early stages. This occurs in the form of sustained, low-grade inflammation that favours catabolic and destructive pathways over reparative responses. Recently, the concept of “inflammaging,” a term describing the gradual accumulation of systemic inflammatory mediators with age, has been acknowledged as a predisposing factor for degenerative joint diseases like OA—even in the absence of overt pathology (49,50). This phenomenon results from the cumulative activation of several aging hallmarks, such as the innate immune system due to cellular senescence, mitochondrial dysfunction, microbiome alterations, and chronic antigenic load (73). In the context of OA, inflammaging contributes to the degradation of cartilage, synovial inflammation, and subchondral bone remodelling. Senescent cells within joint tissues secrete a pro-inflammatory secretome known as the senescence-associated secretory phenotype (SASP), further fuelling local inflammation and tissue degeneration (74). Therefore, OA can be considered not only a mechanical and degenerative condition but also a manifestation of age-related, inflammation-driven joint dysfunction. Targeting inflammatory pathways involved in

inflammaging represents a promising approach for modifying OA progression and improving outcomes in elderly patients.

4.4 OA therapy

4.4.1 Current therapies: drugs, surgery

As previously discussed in chapter *4.3.1*, current therapeutic options for OA mainly aim at symptom relief. Pharmacological treatments include pain management drugs, while surgical interventions such as joint replacement are reserved for advanced stages. The first line pharmacological approach consists in the administration of analgesics, non-steroidal anti-inflammatory drugs (NSAIDs) and is usually supported by substantial lifestyle modification, physiotherapy, electromagnetic field therapy. However, up to now, disease modifying drugs (DMOADs) aren't available (75). Intraarticular injection of corticosteroid and gel-like lubricant –referred to as viscosupplementation– can help improving the pain management but for short periods (76). The surgical approach starts with the application of arthroscopy techniques to obtain reliable data on the state of disease progression and to perform minimally invasive procedures. Other steps involve joint preservation and joint fusion (arthrodesis). Joint replacement, or arthroplasty, is the final option, and also the most frequent in elder population. This kind of surgery is the one that creates the most expensive patients in terms of socioeconomic burden for national health systems (77). The estimated annual cost per patient, in 2019, were of 2,180 ± 5,305€, and this value doesn't include the indirect costs related to work absence, compensation costs, caregiver involvement (78). This, and other techniques were reviewed in the work of Brumat et al., (79).

4.4.2 Novel approaches: Orthobiologics

Given the limited efficacy of conventional therapies in altering disease progression, orthobiologics, including MSC-derived products like conditioned medium, have emerged as promising strategies aimed at modulating the underlying pathological processes. Among the most studied orthobiologics are platelet-rich plasma (PRP), the stromal vascular fraction (SVF), bone marrow aspirate concentrate (BMAC), and extracellular vesicles (EVs). PRP delivers a concentrated mix of autologous growth factors with analgesic and anti-inflammatory potential (80); SVF,

derived from adipose tissue, contains a heterogeneous cell population capable of immunomodulation and trophic support (81); and BMAC provides MSCs together with hematopoietic and endothelial progenitors, as well as a wide spectrum of bioactive molecules, thus contributing to both regenerative and immunoregulatory processes (82). Differently, EVs provide a cell-free system for delivering bioactive molecules that can influence key signalling pathways implicated in OA (83). Given the multifactorial nature of osteoarthritis, MSC-derived secretome holds promise as a multimodal therapeutic capable of modulating several key pathological pathways simultaneously. One of the most direct effect observed is the anticatabolic and anti-inflammatory activity of this product: indeed, it has matrix-protective properties by reducing aggrecan breakdown, MMP activity, and exerts anti-inflammatory effects by reducing synovia infiltration of immune cells and swelling (69). Secretome-derived factors such as interleukin-10 (IL-10), TNF stimulated gene-6 (TSG-6), and prostaglandin E2 (PGE2) are known to inhibit NF-κB signalling, whose activation drives the production of catabolic enzymes and inflammatory cytokines (84,85). Additionally, CM anti-inflammatory cytokines may downregulate the MAPK pathway, particularly p38 and JNK, thus attenuating stress-induced catabolism and chondrocyte apoptosis (86). Antioxidant and mitochondrial-stabilizing components within the secretome (e.g., HGF, IGF-1, and extracellular vesicle cargo) can also help mitigate oxidative stress, which is a major contributor to chondrocyte senescence and matrix degradation in OA (87,88). This broad, pleiotropic activity makes MSC secretome-based approaches attractive candidates for disease-modifying OA therapy, particularly in stages characterized by inflammation, matrix loss, and altered joint homeostasis.

4.5 Modelling of OA and testing novel therapeutics

OA as a whole-joint disease, represents a challenge in terms of pathology modelling. The plethora of available models has increased in recent years, and it is shifting towards more standardised, human-based, replicable models.

4.5.1 In vitro models

Modelling OA pathophysiology in vitro presents several challenges, albeit this approach offers controlled and reproducible platforms to investigate disease mechanisms and evaluate therapeutic agents, making them valuable tools for drug

testing. Typically adopted models are 2D cultures of articular chondrocytes, osteoblasts and osteoclasts, and synoviocytes (89). In vitro models have evolved through the integration of various biomaterials and technologies aimed at creating tissue constructs that more accurately mimic the pathological features of the disease (90). Compared to traditional 2D cultures, contemporary 3D models provide enhanced relevance by supporting cell–cell and cell–matrix interactions within a more physiologically accurate microenvironment. These advancements allow for a better understanding of OA-related molecular mechanisms and more reliable preclinical evaluation of therapeutic strategies. Further, the induction of OA in vitro often involves the application of specific cytokines, growth factors, or chemical stimuli, with the possibility to integrate mechanical stimuli only in certain conditions (91). To overcome some of the remaining limitations, advanced platforms such as organ-on-chip systems, microfluidic devices, and dynamic bioreactors are being explored (89,92,93). These technologies enable fine control over mechanical loading, fluid flow, and spatial organization of tissues, offering a more standardized approximation to in vivo conditions. Their use enhances the physiological relevance of OA models and may improve the simulation of chronic disease progression, contributing to the development of more predictive and translatable in vitro systems. Although these models hold significant promise, particularly for personalized medicine, ongoing challenges such as standardization, chronic disease simulation, and translational consistency underscore the need for further refinement before an in vitro model could be accepted for supporting clinical application.

4.5.2 In vivo models

Animal models provide important insights but often fail to fully recapitulate the human disease, due to species-specific differences and ethical concerns. The most commonly used models are of surgical nature and include the destabilization of the medial meniscus (DMM) and the anterior cruciate ligament transection (ACLT), both typically performed in mice or rats (94). The DMM model, is obtained by transecting the medial meniscotibial ligament and induces joint instability that ultimately leads to progressive cartilage degradation, osteophyte formation, subchondral bone sclerosis, and synovial inflammation. It is widely used for studying early to moderate stages of OA due to its relatively slow and reproducible disease progression (95). The ACLT

model is obtained by cutting the anterior cruciate ligament, causing a more rapid and severe joint degeneration. Indeed it is adopted when studying post-traumatic or advanced OA (96). Another frequently employed model is the monosodium iodoacetate (MIA) model, which involves intra-articular injection of MIA, a glycolysis inhibitor that causes chondrocyte death and rapid cartilage breakdown. While the MIA model is highly reproducible and useful for pain studies, it lacks the mechanical and inflammatory components of spontaneous OA and is considered less representative of its multifactorial pathogenesis (97). Thus, the DMM model is generally preferred for preclinical studies aiming to mimic the progressive and multifaceted nature of human OA. As reviewed in the work of Kuyinu et al., in addition to the widely used DMM, ACLT, and MIA models, several other animal models of OA are employed to capture different aspects of the disease (98). Spontaneous OA models, such as those using guinea pigs or STR/Ort mice, naturally develop OA with age and are particularly valuable for studying primary OA, as they closely mimic the slow, idiopathic progression seen in humans. Similarly, transgenic or knockout mice help elucidate the genetic drivers of OA by targeting specific genes involved in cartilage homeostasis, such as collagen genes (99). Non-invasive post-traumatic OA models involve the application of mechanical loading (e.g., cyclic compression or tibial axial loading) to induce joint damage without surgical intervention, offering a reproducible and less invasive alternative for studying early OA (100).

Although animal models remain indispensable for preclinical research in OA, their use is accompanied by significant limitations. A primary concern is the inter-species variability in disease onset, progression, and symptom manifestation. The molecular and cellular mechanisms underpinning OA differ between humans and commonly used animal models, particularly rodents, limiting the translational relevance of findings (101,102). Furthermore, the fact that all standard OA models rely on quadrupedal species, often small in size, introduces discrepancies in joint biomechanics and load distribution, which are critical in the pathogenesis of OA—a disease heavily influenced by mechanical stress (98,103). Another major limitation concerns the age of the animals used in experiments; preclinical studies typically utilize young animals, which do not replicate the aged, degenerative joint environment characteristic of human OA (104). In addition, the development of non-invasive imaging techniques (such as MRI and ultrasound) for assessing human joint health,

along with advanced in vitro systems—including organ-on-chip and 3D tissue-engineered models—offer alternative platforms for assessing the safety and efficacy of therapeutic interventions (105). From an ethical perspective, this raises the question of whether the continued use of animal models is justified for a non-lethal, age-related condition like OA, especially once a therapy has been confirmed to be non-toxic. Given that OA predictive human-based models are increasingly available, it is worth critically evaluating the necessity of animal experimentation to determine therapeutic potency, particularly when species-specific responses may limit translational outcomes.

4.5.3 Ex vivo models

"Out of the living" is the literal translation of ex vivo, which therefore can include all cell culture conditions that we consider as in vitro models. However as conventionally found in literature, this culture approach is referred to tissue explants, isolated and then transferred in laboratory conditions to test several parameters. Unlike 2D cultures, ex vivo systems maintain crucial cell–matrix and inter-tissue interactions, allowing a more realistic replica of OA as a whole joint disease, particularly in response to inflammatory stimuli with the possibility to assess patient-specific variability in disease severity and treatment response. Indeed, ex vivo models have been increasingly adopted across various fields of biomedical research as tools for testing therapeutic responses prior to clinical application, exemplifying their potential in functional precision medicine. In cancer research, ex vivo platforms are exploited to screen investigational drugs in systems that retain the complexity of the tumour microenvironment. In hematologic malignancies for instance, patient-specific ex vivo assays have been used to predict chemotherapy outcomes in acute myeloid leukaemia, allowing clinicians to personalize treatment strategies based on observed drug responsiveness (106). Similarly, in ovarian cancer, in the OVAREX study, patient-derived ex vivo models from tumour tissues were produced to assess treatment efficacy and integrated with data from other tissues, to obtain a personalized therapeutic strategy (107). In OA research, the models are typically composed of joint tissues such as cartilage, synovial membrane, and subchondral bone, either in isolation or in combination, where the native tissue architecture and extracellular matrix are preserved. Currently adopted ex vivo models comprehend cartilage explants, osteochondral plugs and co-cultures with synovial tissue (108–110).

Similarly, in musculoskeletal drug development, an ex vivo model of synovial membrane has been used to study drug permeability to produce intraarticular therapies (111). Together, these diverse applications highlight the translational value such models hold in converting bench research into patient-specific therapeutic strategies. Inter donor variability is the strength but simultaneously the weak point of these models, since it can hide whatsoever effect of a certain drug, from a statistical point of view. This can be solved by finding stratification key factor that allows for the separation in population with more defined drug responses.

5. Aims

5.1 Characterization of conditioned medium

To perform a comprehensive molecular and biological characterization of the CM derived from mesenchymal stromal cells. The focus was on identifying factors relevant to osteoarticular regeneration and inflammation, such as those providing chondroprotective, anticatabolic, immunoregulatory effects. Particular attention was given to extracellular vesicle, and soluble bioactive factors involved in these effects. The characterization process also addressed procedural variations—such as the impact of freezing prior to downstream manipulation or the pre-conditioning of ASC by inflammatory cytokines—on CM composition and efficacy. Batch-to-batch consistency, production parameters, and quality control metrics were defined to support the development of CM as a standardized and clinically translatable product.

5.2 Validation of ex vivo models

To establish and validate ex vivo models that mimic the osteoarthritic joint environment, enabling the evaluation of non-conventional therapeutic strategies. These models aim to provide a physiologically relevant platform that closely mimics the osteoarthritic joint environment, using human cartilage, osteochondral and synovial membrane explants. These models were assessed for tissue-specific markers related to inflammation, matrix degradation, and regeneration. Additionally, the intrinsic variability of the explants—due to donor heterogeneity or anatomical site—were systematically evaluated and accounted for.

5.3 Evaluation of conditioned medium in the osteoarthritic context

To assess the anti-inflammatory and regenerative potential of mesenchymal stromal cell-derived CM within the validated ex vivo osteoarthritis model. Both standard and primed CM were tested under inflammatory conditions that simulate pathological osteoarthritic scenarios. The study analysed the response of joint tissues, in terms of extracellular matrix turnover, catabolic and anabolic activity, and inflammatory mediator expression. The analysis integrated molecular, biochemical, and histological assessments to elucidate the mechanisms of action and therapeutic potential of CM in a clinically relevant setting.

6. Materials and Methods

6.1 Biological samples collection

All the samples collected from patients were obtained after written informed consent, with ethical approval (TENET – IRCCS Ospedale San Raffaele Ethics Committee, approval number 38/int/2022; ASC-OA – IRCCS Ospedale San Raffaele Ethics Committee, approval Number 187/int/2019 – ClinicalTrials.gov (Identifier NCT04223622); protocol no. 160998 – Ethics Committee of the University of Ferrara and S. Anna Hospital) or Institutional Review Board approval (PQ 7.5.125, version 4), and in accordance with the Helsinki regulation.

6.2 ASC isolation and culture conditions

ASC were isolated from subcutaneous adipose tissue collected as waste material of aesthetic or orthopaedic prosthetic surgery (total hip replacement). Adipose tissue was shredded with a scalpel, digested with 0.75 mg/ml collagenase type I (Worthington Biochemical Corporation, Lakewood, NJ, USA) for 30 min at 37 °C, and filtered through a 100 µm cell strainer (Corning Incorporated, Corning, NY, USA). ASCs were plated at a density of 10^4 cells/cm^2 in a culture medium consisting of high-glucose DMEM supplemented with 10% Fetal Bovine Serum (FBS HyClone, Euroclone, Pero, IT), 2 mM glutamine, 50 µg/ml streptomycin, and 50 U/ml penicillin. Cells were used between the 4th and 10th passage, spanning approximately from 5 to 25 cumulative population doublings. Of note, the only batch expanded up to passage 10, showed consistent proliferation rate and preserved MSC features such as elongated spindle-shaped morphology and differentiation ability. Details of ASCs donor are collected in Table 1, along with the relative CM and how they were employed.

Cell population	Passage	CM ID	Surgery	Sex	Age	Application
LPA60	7	CM138	LPA	F	22	Cartilage explants (CE) and synovial membrane (SM) treatments
ASC95	7	CM141	THR	F	56	
ASC103	4	CM149	THR	F	26	
ASC114	7	CM154	THR	F	62	
ASC106	5	CM168	THR	F	70	
ASC121	4	CM155	THR	F	74	

ASC 153	5	CM173	THR	M	50	Cartilage explants (CE) co-cultured with synovial membrane (SM) treatments
ASC165	5	CM175	THR	M	74	
ASC166	5	CM176	THR	F	64	
ASC162	5	CM179	THR	F	57	
ASC176	5	CM180	THR	M	80	
ASC183	4	CM183	THR	M	64	
LPA78	7	p/CM13	LPA	F	38	Production of CM/pCM for characterization and osteochondral explants (OCh) treatments
ASC89	6	p/CM14	THR	F	65	
ASC92	6	p/CM15	THR	F	73	
ASC127	6	p/CM16	THR	M	66	
ASC134	5	p/CM19	THR	M	63	
ASC114	7	F-/T-CM164	THR	F	62	Production of CM from fresh (F-CM) or thawed (T-CM) pre-concentrated media
ASC114	7	F-/T-CM164_(M)	THR	F	62	
ASC112	7	F-/T-CM165	THR	M	72	
ASC121	6	F-/T-CM166	THR	F	74	
ASC115	6	F-/T-CM167	TKR	M	55	
ASC118	6	F-/T-CM169	THR	M	51	
LPA67	3	F-/T-CM170	LPA	F	35	
ASC121	5	F-/T-CM171	THR	F	74	

Table 1: ASC donor characteristics

6.3 ASCs characterization

ASCs were characterized according to the minimal criteria defined by the International Society for Cell & Gene Therapy (ISCT), including plastic adherence, specific surface antigen expression, and multipotent differentiation potential. MSCs were assessed for their differentiation capacity toward adipogenic and osteogenic lineages using standard induction protocols, following protocols as described in Niada et al. 2018 (30).

6.3.1 Clonogenic potential

Cells were observed to check morphology and adherence to standard tissue culture-treated plastic using phase-contrast microscopy. To assess the clonogenic potential of MSCs, a colony-forming unit (CFU) assay was performed. Cells were seeded in triplicate into 6-well plates at decreasing densities using a serial 1:2 dilution starting from 1,000 cells per well. Dilutions were carried out for six steps, resulting in the following seeding densities: 1,000; 500; 250; 125; 62; and 31 cells/well. Cells were

cultured in control medium supplemented with 20% FBS for 14 days without medium changes. At the end of the incubation period, cells were fixed with methanol and stained with 0.5% crystal violet. Colonies (with at least 20/25 cells) were counted manually and the clonogenic efficiency was calculated as the number of colonies divided by the number of cells seeded x100.

6.3.2 Cell Immunophenotyping

Cells were stained for positive markers CD73, CD90, and negative markers CD34, CD45, as per ISCT recommendations. The antibodies were used at 1:100 dilution (BioLegend, San Diego, CA, USA). Appropriate controls were included. Flow cytometric analysis was performed using flow cytometer CytoFLEX (Beckman Coulter, Brea, CA, USA), and data were analysed using CytExpert software.

6.3.3 Adipogenic differentiation

Cells were cultured in 24-well plates for 14 days either in control or adipogenic medium (control medium plus 1 µM dexamethasone, 10 µg/ml insulin, 500 µM 3-isobutyl-1-methyl-xanthine and 200 µM indomethacin). Lipid vacuoles were stained by Oil Red-O (ORO, Bio-Optica).

6.3.4 Osteogenic differentiation

ASCs were cultured in 24-well plates ($1.5x10^4$ cells/well) either in control or osteogenic medium (control medium plus 10 nM dexamethasone, 10 mM glycerol-2-phosphate, 150 µM l-ascorbic acid-2-phosphate and 10 nM cholecalciferol). After 14 days, collagen production was evaluated. Collagen production was evaluated through the Sirius Red method. Bouin's solution-fixed cells were stained with 0.1% Sirius Red (Fast Red 80 in 98% picric acid) for 60 min, then washed with 10 mM HCl.

6.4 CM production

Once cells reached confluence, they were used for conditioned medium (CM) production. Cells were rinsed thoroughly with phosphate-buffered saline (PBS), and 8mL of starving medium was added to each flask. The starving medium consisted of DMEM without phenol red, supplemented with 2 mM glutamine, 50 µg/mL streptomycin, and 50 U/mL penicillin. Cells were then incubated at 37°C for 5 minutes.

Following this, two additional PBS washes were performed, and 10 mL of starving medium was added to each flask. The starvation period lasted between 24 and 72 hours. At the end of the incubation, the CM was collected and centrifuged at 2500g for 10 minutes at 4°C to remove cellular debris. In parallel, cells were detached and counted to normalize the collected CM based on the number of donor cells. The resulting supernatant was then concentrated using Amicon Ultra-15 centrifugal filter units with a 3 kDa molecular weight cut-off (Millipore, Burlington, MA, USA), by centrifugation at 4000g for 2 hours at 4°C. The concentrated CM was aliquoted and stored at –80°C until further use.

6.4.1 Priming protocol

To produce primed CM (pCM), cells are rinsed with PBS and then incubated for 5 minutes at 37°C in starving medium containing 10 ng/ml TNFα and/or 10 ng/ml IL-1β. Finally, they are rinsed twice with PBS and then starved as per normal protocol.

6.5 Total protein concentration

The total protein content of CM was quantified by Bradford Assay following standard procedures. Briefly 2-4 µl of each CM sample were added to a 96-well plate. Then, 200 µL of Bradford reagent (Bio-Rad Laboratories, Hercules, CA, USA) was added to each well. After gentle mixing, the plate was incubated at room temperature for 10 minutes. Absorbance was measured at 570 nm using a microplate reader, and protein concentrations were calculated inferring it from the standard curve, obtained using bovine serum albumin (BSA).

6.6 Nanoparticles Tracking Analysis (NTA)

Aliquots of CM corresponding to $4x10^5$ ASCs were diluted in 0.22 Ø µm triple-filtered PBS for the NTA. For each sample, three recordings of 1 minute were taken. All measurements were checked for the quality criteria of 20–120 particles/frame, a concentration range of 10^6 to $4x10^9$ particles/ml, and a number of valid tracks > 20 %. After capture, the videos were analysed by the in-built NanoSight Software NTA.

6.7 Cytofluorimetry for EVs markers evaluation

For cytofluorimetric analysis, diluted CM samples were stained with 1μM carboxyfluorescein diacetate succinimidyl ester (CFSE, Biotium Fremont, CA, USA). Instrument was calibrated using Megamix-Plus SSC and FSC (Biocytex, Marseille, France), a mixture of FITC fluorescent beads of known dimensions (100 nm, 160 nm, 200 nm, 240 nm, 300 nm, 500 nm, and 900 nm). After 1 hour incubation at 37 °C, samples were analysed to confirm successful staining. CFSE-positive (CFSE+) samples were analysed in Violet SSC–H and FITC–H channels, following the coordinates provided by the standardization beads. CFSE+ samples were then marked with APC-conjugated antibodies αCD9, αCD63, and αCD81 (BioLegend, San Diego, CA, USA, dilution 1:20) and incubated for 30 min at 4 °C in the dark. Finally, samples were acquired for 150 seconds at a medium flow rate. DMEM-diluted antibodies and unlabelled samples were used as appropriate controls.

6.8 Bioactive factor concentration analyses (arrays, lipidomic, Luminex, ELISA)

CM samples underwent protein characterization where 200 analytes between cytokines, chemokines, receptors, and inflammatory and growth factors were investigated using the Quantibody® Human Cytokine Array 4000 Kit, a combination of Human Cytokine Array Q4, Human Chemokine Array Q1, Human Receptor Array Q1, Human Inflammation Array Q3, and Human Growth Factor Array Q1. Samples were analysed by RayBiotech facility (RayBiotech, Norcross, GA, USA). The concentration obtained were normalized on donor cell number.

The lipidomic analysis was performed in collaboration with the laboratory of Forensic Toxicology of the Department of Biomedical, Surgical and Dental Sciences of University of Milan, following previously published protocols (112–114). Polyunsaturated fatty acids, eicosanoids, endocannabinoids, and N-acylethanolamides were quantified on a QTRAP 5500 triple quadrupole linear ion trap mass spectrometer (Sciex, Darmstadt, Germany) coupled with an Agilent 1200 Infinity pump ultrahigh-pressure liquid chromatography (UHPLC) system (Agilent Technologies, Palo Alto, CA, USA) using the UHPLC-MS/MS. Briefly, undiluted samples (approximately 200 μl/sample) were spiked with deuterated internal standards and 1 ml of cold acetonitrile was added for protein precipitation. After centrifugation, the supernatants were extracted with a 4 ml of dichloromethane/isopropanol (8 : 2; v/v) and centrifuged again. The organic layer was

separated, dried, and reconstituted in 60 µl methanol. 3 µl aliquot was analysed for endocannabinoids and N-acylethanolamides. The remaining solution was added with 500 µl hydrochloride acid (0.125 N) and 4 ml ethyl acetate/n-hexane (9 : 1; v/v). The organic phase was dried, and the residue was reconstituted in 60 µl acetonitrile. 30 µl aliquot of methanol obtained from the neutral extraction and 30 µl aliquot from acid extraction were merged, and 10 µl was analysed for polyunsaturated fatty acids and eicosanoid determination. Data acquisition and processing were performed using Analyst®1.6.2 and MultiQuant®2.1.1 software (Sciex, Darmstadt, Germany), respectively.

The Luminex Discovery assay was performed using the following assays: the Human Magnetic Luminex Screening Assay Rk4yTGNI (R&D Systems, Minneapolis, MN, USA) was customized to contain 5 molecules: MCP-4, PDGF-AA, TNF RI, DKK-1, and RAGE. Additional panels applied included the Human Premixed Multi-Analyte Kit LXSAHM and the Human Luminex Discovery Assay LXSAHM14 (R&D Systems, Minneapolis, MN, USA). The first kit was designed to detect and quantify CCL2, CCL3, IL4, IL8, HGF, M-CSF, OPG, and VEGFA. The second kit was customised for: CCL2, CXCL1, HGF, IL-1ra, IL8, M-CSF, TIMP-1, CCL3, G-CSF, IFN-γ, IL4, IL10, Osteoprotegerin, and VEGF-A. Samples were diluted accordingly and read through Bio-Plex Multiplex System (Bio-Rad, Milan, Italy) following standard procedures. Data analysis was performed with MAGPIX xPONENT 4.2 software (Luminex Corporation, Austin, TX, USA).

Factors that were incompatible with Luminex technology were evaluated with sandwich enzyme-linked immunosorbent assay (ELISA) kit. In particular secreted TGF-β1 and PGE2 were determined with the Human TGF-β1 Immunoassay (DB100C, R&D Systems, Minneapolis, MN, USA) and the Prostaglandin E2 Express ELISA Kit (500141, Cayman Chemical, Michigan, MI, USA), respectively. Data were analysed with MyAssays software

6.9 Raman spectroscopy

Raman analysis of CM was performed in collaboration the Laboratory of Nanomedicine and Clinical Biophotonics (LABION) of IRCCS Fondazione Don Gnocchi, following established protocols (115,116). Briefly, CM samples were diluted

1:10 in sterile saline solution, deposited on a calcium fluoride slide, and acquired following a previously optimized protocol for EVs and CM analysis with a LabRAM Aramis Raman microspectroscope (Horiba Jobin Yvon S.A.S., Lille, France) equipped with a 532 nm laser line. Polynomial baseline correction and unit vector normalization were performed using Labspec 6 software (Horiba)

6.10 Transmission Electron Microscopy (TEM)

Particles in CM were analysed for vesicles morphology, using TEM at the UNITECH facility of University of Milan.

6.11 Experimental in vitro models

6.11.1 Bone turnover model

The 3D dynamic co-culture bone turnover model was set up by the Department of Neuroscience and Rehabilitation of University of Ferrara, by using the RCCS-4TM bioreactor (Synthecon™, Inc., Houston, TX, USA), with a High Aspect Ratio Vessel (HARV™; Synthecon™, Inc., Houston, TX, USA) (117). The co-culture was implemented starting from human osteoblasts (hOBs) isolated from bone fragments of vertebral lamina and human monocytes from healthy donors (hMCs) as osteoclasts precursors. hMCs and hOBs were cultured in basal medium until the co-culture. Briefly, 2×10^6 hOBs and 1×10^6 hMCs (2:1 ratio) were inoculated in 2 ml HARV, inserted into the rotary bioreactor incubated for 24 h. After that, the presence of aggregates was observed, and the vessels were filled with osteogenic medium alone or in the presence of CM derived from 5×10^5 cells. Treatment was refreshed twice a week, while the spent culture media were collected. After 14 days in incubation, the hOBs/hOCs aggregates were collected, fixed in 4% PFA, and embedded in paraffin for further analysis.

6.12 Ex vivo 3D models

All models developed in our laboratory derive from biological samples obtained through the TENET and ASC-OA study, as previously mentioned in *6.1* section.

6.12.1 Cartilage explants

Cartilage explants (CE) were obtained from patients diagnosed with progressive hip arthritis and undergoing hip replacement surgery. They were classified as grade III osteoarthritis according to the KL classification system. Donors' features are summarised in Table 2.

CE ID	Age (years)	Sex	Surgery
CE-1	76	M	THR
CE-2	80	F	THR
CE-3	60	M	THR
CE-4	66	F	THR
CE-5	81	F	THR
CE-6	76	M	THR
CE-7	75	F	THR
CE-8	67	M	THR
CE-9	67	F	THR
CE-10	49	M	THR
CE-11	51	F	THR
CE-12	74	F	THR

Table 2: CE donors

The cartilage specimens were excised using a scalpel from macroscopically preserved regions of the femoral head, avoiding arthritic lesions. The selected portions exhibited a polished surface, translucent appearance, and semi-white cartilage. To mitigate any potential bias linked to severe tissue damage, areas displaying visible deformities and calcified cartilage were deliberately excluded. Following excision, the samples underwent a thorough washing in PBS. Subsequently, 4 mm Ø biopsy punch explants were obtained and cultured for one week. The collection procedure is graphically summarised in Figure 3. The culture medium comprised high-glucose DMEM supplemented with 10% FBS, 2 mM L-Glutamine, 150 U/ml penicillin, 150 µg/ml streptomycin, 2.5 µg/ml amphotericin-β, and 110 µg/ml of sodium pyruvate. For OA modelling, culture medium was switched to high-glucose DMEM without phenol red, 1% FBS, 2 mM L-Glutamine, 150 U/ml penicillin, 150 µg/ml streptomycin, 2.5 µg/ml amphotericin-β, and 110 µg/ml of sodium pyruvate. Explants were challenged with either 10ng/ml TNFα and/or 1ng/ml IL-1β. CM treatment was applied in a dose corresponding to $1x10^6$ donor cells. All experimental settings lasted 3 days. At the endpoint, supernatants were collected and centrifuged for at 2000g, 4°C, for 5

minutes. The new supernatants were transferred into new tubes and stored at -20°C

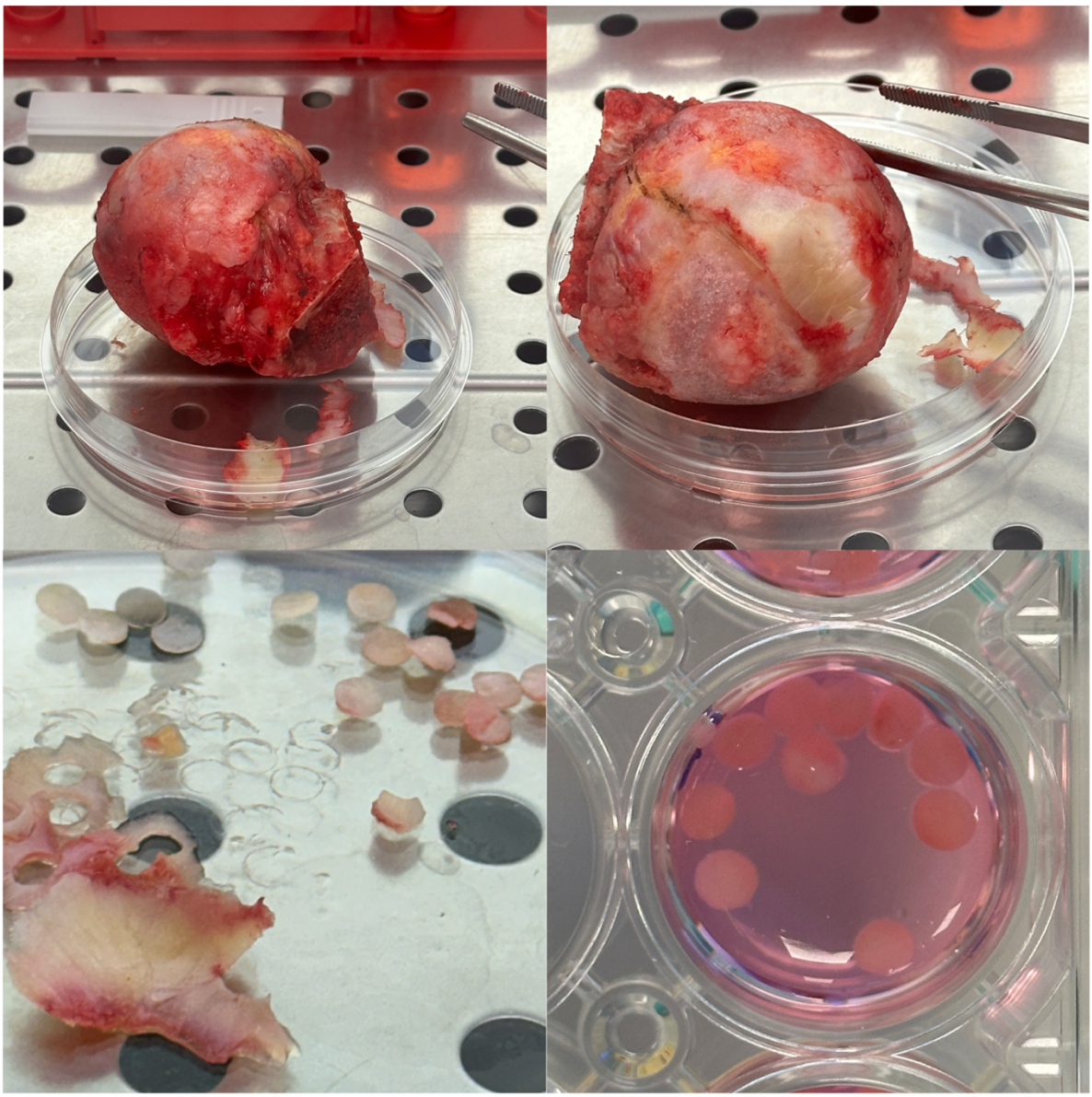

for further analyses.

Figure 3 – CE model
From left up to right bottom, harvest of CE from femur head. After collecting the cartilage from preserved areas, it was punched, and the resulting discs were placed in culture.

6.12.2 Synovial membrane explants

Synovial membrane (SM) explants were obtained from membrane sections of three patients (two female and one male, aged 62-76 years old, grade 3 OA), cleaned

from cauterization and infiltrated adipose tissue, then cut into pieces approximately 2-3 mm in size using a scalpel and weighed. A minimum of 40mg was used for each group. Subsequently, they were cultured in standard medium (DMEM, 10% FBS, 2 mM L-Glutamine, 150 U/ml Penicillin, 150 µg/ml Streptomycin, 2.5 µg/ml Amphotericin-β) for one week. After this period, samples were shifted to a medium containing 1% FBS and supplemented with inflammatory cytokines (10ng/ml TNFα + 1ng/ml IL-1β) and/or CM for 3 days. At the endpoint, supernatants were collected, centrifuged and stored at -20°C for further analyses

6.12.3 Cartilage and synovial membrane co-culture

The CE and SM obtained as previously described, were co-cultured in a transwell system to obtain the CESM model. Donors' features are presented in Table 3.

CE ID	Age (years)	Sex	Surgery
CESM-1	65	F	THR
CESM-2	44	M	THR
CESM-3	52	F	THR
CESM-4	52	M	THR
CESM-5	66	F	THR
CESM-6	75	F	THR
CESM-7	51	M	THR
CESM-8	58	M	THR
CESM-9	76	M	THR

Table 3: CESM donors

Briefly, CE and SM from the same patient were kept separately for a buffer period, in DMEM without phenol red, 1% FBS, 2 mM L-Glutamine, 150 U/ml Penicillin, 150 µg/ml Streptomycin, 2.5 µg/ml Amphotericin-β. Subsequently, 60mg of CE and SM were placed in the bottom and upper chamber –respectively– of a 0.4µm pores 12-well transwell plate (Corning, NY, USA). A graphic summary of the model composition is represented in Figure 4. After 24 hours, media were collected for further analyses and then samples were treated as control (CTR), with 100mM dexamethasone (DEX) or with CM from $0.5x10^6$ cells (CM). At the endpoint, media were collected and stored for further analyses while samples were washed and stored until nucleic acid and protein extraction

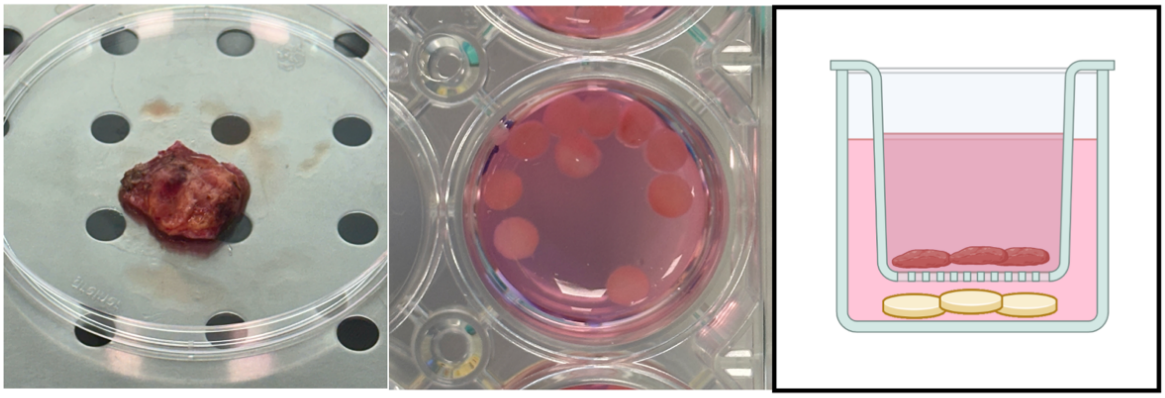

Figure 4 – CESM model
The synovial membrane and cartilage samples are cultured as indicated in the last panel

6.12.4 Osteochondral explants

Osteochondral (OCh) explants were extracted, using a trephine, from the macroscopically preserved regions of tibial plateaus and femoral condyles during knee replacement surgery (TKR). Donors' characteristics are summarised in Table 3.

OCh ID	Sex	Age (years)	Weight (kg)	Height (m)	BMI
ASC-OA #26	F	69	52,0	1,60	20,31
ASC-OA #28	M	83	59,6	1,67	21,37
ASC-OA #29	M	59	85,0	1,78	26,83
ASC-OA #30	F	72	79,0	1,65	29,02
ASC-OA #31	F	81	85,0	1,66	30,85
ASC-OA #32	M	73	104,0	1,80	32,10
ASC-OA #33	F	75	81,0	1,70	28,03
ASC-OA #36	F	50	78,0	1,52	33,76
ASC-OA #37	F	70	72,0	1,60	28,13
ASC-OA #38	F	76	69,0	1,63	25,97
ASC-OA #39	F	56	63,0	1,57	25,56
ASC-OA #40	M	58	70,0	1,73	23,39
ASC-OA #41	M	76	83,0	1,70	28,72

Table 3: Osteochondral (OCh) explants donors features

OCh explants, each of 10 mm Ø and comprising both cartilage and bone, underwent thorough washing in PBS before being equilibrated for one week in a culture medium consisting of high-glucose DMEM, 10% FBS, 2 mM L-glutamine, 50 U/ml penicillin, 50 µg/ml streptomycin, and 2.5 µg/ml amphotericin β. For the OA

modelling, they were cultured in custom-designed inserts, which were designed by our collaborators from the Cell and Tissue Engineering Laboratory (IRCCS Istituto Ortopedico Galeazzi) through Computer Assisted Design (CAD) software and fabricated employing an Asiga Max X 3D printer (ASIGA) that uses Digital Light Processing (DLP) technology. The resin used for printing was the Freeprint® model 2 (Detax Gmbh, Germany). The insert consists of two interlocking parts: the first part (A) is seated with a biocompatible UV resin within each well of a 12-well plate, while the second part (B) is used to fit the OCh explant through a silicone O-ring. The O-ring creates a tight seal between two compartments that delimits regions containing bone and cartilage. In each region, the tissue-specific medium is used: cartilage specific medium consisted in high-glucose DMEM, 1% FBS, 2 mM L-glutamine, 50 U/ml penicillin, 50 µg/ml streptomycin, 2.5 µg/ml amphotericin β, and 110 µg/ml sodium pyruvate. The bone counterpart contained high-glucose DMEM, 1% FBS, 2 mM L-glutamine, 50 U/ml penicillin, 50 µg/ml streptomycin, 2.5 µg/ml amphotericin β, 100 nM dexamethasone, 50 µg/ml ascorbic acid, and 10 mM β glycerophosphate. Inflammatory cytokines were applied to the cartilage side using 10 ng/ml for TNFα and 1 ng/ml for IL-1β, while treatments with CM and pCM derived from $5x10^5$ cells. The workflow of the model set-up is represented in Figure 5.

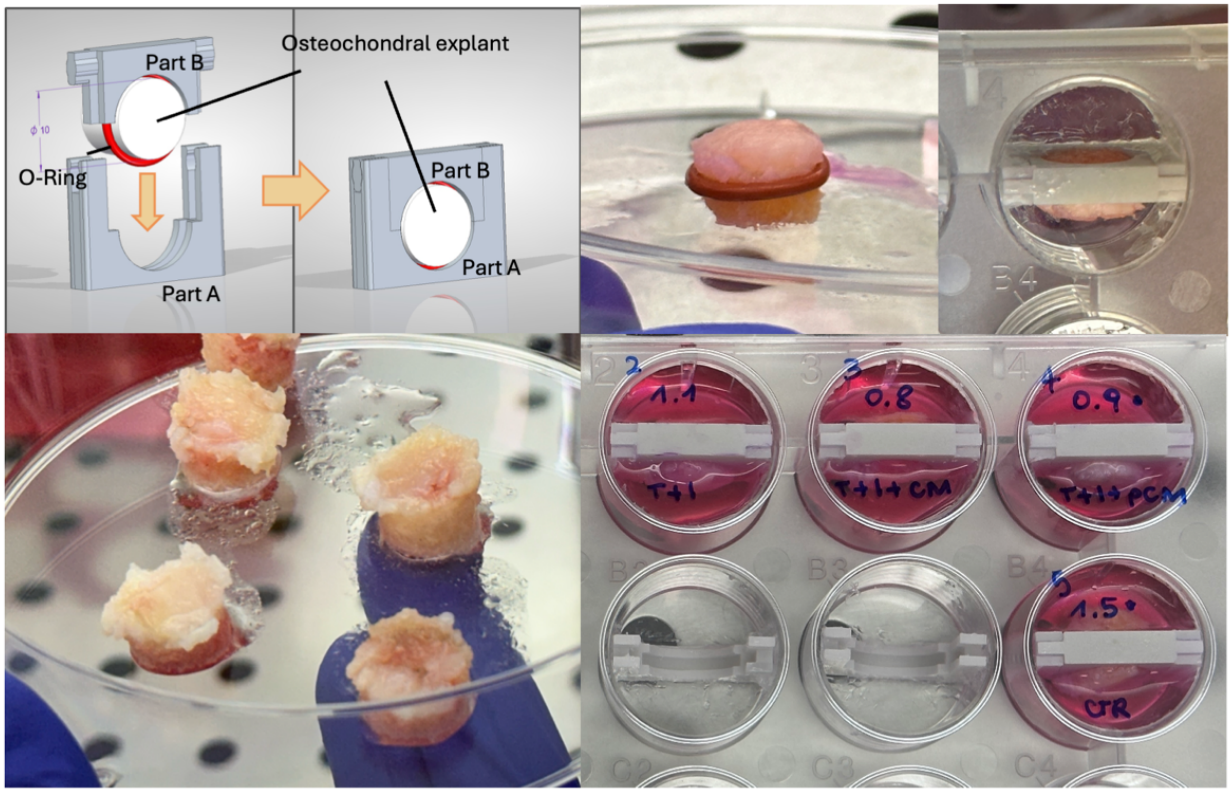

Figure 5 – OCh model
First panel represents the 3D printed insert project. Down, the selection of the explants. In the right half of the image, an explant with the silicone ring, ready to be place in the insert (to its left). Finally, in the bottom image, the complete set-up with specific culture media.

6.13 Supernatants assay

6.13.1 Metabolic activity

To monitor tissue viability, the AlamarBlue assay (Thermo Fisher Scientific, Waltham, MA, USA) was adopted. 10% AlamarBlue reagent was added to the culture medium and incubated for 3 hours at 37 °C in the dark. An aliquot of 100µl was then transferred in triplicate into black-bottom 96 well plates, and fluorescence (excitation λ = 530 nm, emission λ = 590 nm) was evaluated. Comparative analysis of viability at different timepoints served to prove tissue metabolic health. Results were expressed as Arbitrary Fluorescent Units (AFUs).

6.13.2 MMP activity

The metalloproteinases activity in supernatants was assessed through the SensoLyte 520 Generic MMP Assay Kit (AnaSpec Inc., Fremont, CA, USA) following manufacturer's protocol. Samples of spent media underwent pre-activation with 4-aminophenyl mercuric acetate (APMA), for 40 minutes at 37 °C (specific for MMP13 activation, as per protocol guidelines). Activated samples were then transferred in a black-bottom 96 wells plate and substrate was added. After 45 minutes incubation, fluorescence was read at Ex/Em = 490 nm/520 nm.

6.13.3 Sulphated GAG release

The levels of sulphated glycosaminoglycans (sGAG) released in the media were evaluated through the 1,9-dimethylmethylene blue (DMMB assay. Briefly, samples were tested in duplicates. The absorbance was measured at 500 nm, and GAG concentrations were extrapolated using a chondroitin sulphate standard curve.

6.13.4 Alkaline phosphatase activity

The activity of ALP was evaluated through a colorimetric assay, exploiting the conversion of the substrate p-nitrophenyl phosphate (pNPP) into its yellow product, p-

nitrophenol (pNP). The assay was conducted in a buffer solution composed of 100 mM diethanolamine and 0.5 mM MgCl2, adjusted to pH 10.5. Following colour development, absorbance at 405 nm was quantified using a Wallac Victor II microplate reader. Absorbance values were then correlated to a standard curve of pNP concentrations ranging from 4 mM to 0.06 mM. Enzymatic activity was subsequently determined by calculating the amount of pNP produced, divided by the reaction time, and expressed as picomoles/minutes/µl (pmol/min/µl).

6.13.5 Tartrate-resistant acid phosphatase activity

The enzymatic activity of TRAP was evaluated using a colorimetric assay. Samples (50 µl each) were transferred into a 96-well plate, followed by the addition of 100 µl of assay buffer per well. The assay buffer consisted of 0.1 M sodium acetate, 0.1% Triton X-100 in PBS, 30µl/ml of tartrate solution (Sigma-Aldrich, Saint Louis, MO, USA), and the substrate, pNPP, at a final concentration of 1 mg/ml. Final solution was adjusted to pH 5.5. To quantify the reaction product, a standard curve was prepared using pNP diluted in assay buffer at concentrations ranging from 4 mM to 0.03 mM. Absorbance at 405 nm was measured after 90 minutes to calculate the enzymatic activity, expressed as pmol/min/µl.

6.13.6 Osteocalcin release

OC levels were quantified using the Human Osteocalcin Simple Step ELISA Kit (ab270202, Abcam, Cambridge, UK), following standard procedures. Samples were tested either undiluted when collected from the cartilage side or 1:25 diluted when derived from the bone side. Absorbance readings were taken at 450 nm with a Wallac Victor II microplate reader. The resulting values were then interpolated to a standard curve obtained with recombinant protein concentrations ranging from 62.5 pg/ml to 2 ng/ml

6.13.7 Nitric oxide release

NO release in supernatants was analysed utilizing the Nitric Oxide Assay kit from Abcam (ab272517, Abcam, Cambridge, UK). Undiluted samples underwent processing in accordance with the provided protocol. Samples were deproteinized, incubated for 10 minutes at 60 °C, and finally the oxidized NO content was quantified

by measuring the optical density at 540nm. Extrapolation of NO levels was inferred from a nitrite standard curve (0–200 μM)

6.14 Chemotaxis assay

Conditioned media effects on immune cells were assessed in a chemotaxis model of THP-1 monocytes. Briefly, THP-1 cells (ATCC TIB-202) were starved for 24 hours, then labelled with 0.5 μM Calcein AM for 20 min at 37 °C. After the incubation, cells were washed, resuspended in serum-free RPMI and loaded in 24-well plates with 8 μm pore size inserts (353097, Corning, Glendale, AZ, USA). A total of $5x10^5$ THP-1 cells were seeded in the upper chamber, while serum-free RPMI, alone (negative control) or containing the CM, was added to the lower chamber. A medium containing 10 % FBS was considered the positive control. At different time points, the fluorescence (excitation λ = 485 nm, emission λ = 535 nm) emitted from cells that migrated to the lower chamber was measured.

6.15 Gene expression

RNA extraction was performed with the TRIzol-Chloroform extraction method, utilizing PreCellys Mini Tubes (Bertin Technologies, Montigny-le-Bretonneux, FR). The resulting RNAs were then retrotranscribed using the High-Capacity cDNA Reverse Transcription kit (Applied Biosystems, Foster City, CA, USA), following the manufacturer's protocol. Subsequently, the expression levels of different genes were quantified through reverse transcription quantitative polymerase chain reaction (RT-qPCR) employing TaqMan technology using the following probes: ACAN (HS00153936_m1), COL2A1 (hs10060345_m1), CTGF (hs00170014_m1), FN1 (hs01549976_m1), IL-1β (hs01555410_m1), MMP3 (hs00968305_m1), MMP13 (hs00233992_m1), PTGS2 (hs00153133_m1), SOX9 (hs00165814_m1), TIMP1 (hs99999139_m1), and TBP (hs00427600_m1) (Thermo Fisher Scientific, Waltham, MA, USA). The RT-qPCR assays were conducted on the QuantStudio Real-Time PCR systems (Thermo Fisher Scientific, Waltham, MA, USA). Data normalization was performed using TBP as a reference, and relative quantification was determined employing the 2^{-ddCT} method.

6.16 Protein expression

From the TRIzol method is possible to retrieve also tissue protein. For inflammatory pathway activation evaluation, ASCs were lysed in Lysis Buffer 6 (RD system, Minneapolis, MN, USA), with 10µg/ml Aprotinin, 10µg/ml Leupeptin, 10µg/ml Pepstatin, in order to detect the phosphorylated proteins. Proteins were quantified with BCA assay (Thermo Fisher Scientific, Waltham, MA, USA), and 5-20µg of protein, depending on the application, were loaded and separated on a 10% SDS-PAGE gel. Western Blotting was performed using standard protocols. The primary antibodies used are summarised in Table 4. After an overnight incubation at 4°C, specific signals were visualized after incubating the membranes to the appropriate secondary antibodies conjugated to horseradish peroxidase, followed by detection with ECL Westar Supernova (Cyanagen, Bologna, IT). Signal acquisition was performed using a Chemidoc Imaging System, and densitometry analysis was carried out using Image Lab Software (Bio-Rad, Milan, IT).

Protein Name	***Brand***	***Code***	***Animal***	***Dilution***
COL2A1	Abcam	ab34712	rabbit	1:2000
COX2	Cell Signaling	12282S	rabbit	1:1000
MMP3	Cell Signaling	14351S	rabbit	1:1000
MMP13	ThermoFisher Scientific	MA5-14238	mouse	1:100
IDO	Cell Signaling	86630	rabbit	1:1000
GAPDH	Santa Cruz	sc-47724	mouse	1:1000
ACTB	Sigma-Aldrich	A2228	mouse	1:5000
NF-κB p65	Cell Signaling	8242	rabbit	1:1000
Phospho-IkB-a (Ser32)	Cell Signaling	2859	rabbit	1:1000
Phospho-IKKa/b (Ser176/180)	Cell Signaling	2697	rabbit	1:1000
Phospho-NF-kB p65	Cell Signaling	3033	rabbit	1:1000
IkBa	Cell Signaling	4814	mouse	1:1000
IKKα	Cell Signaling	11930	mouse	1:1000
IKKβ	Cell Signaling	8943	rabbit	1:1000

Table 4: Antibodies specifics

6.17 Bioinformatics and statistical analysis

6.17.1 STRING

The Search Tool for the Retrieval of Interacting Genes/proteins (STRING) was used to analyse the pathways related to the protein detected within our CM. After

giving the protein list as an input and selecting *Homo sapiens* as reference organism, the list generated was carefully checked. To continue the analysis, the following parameters were adjusted: i) removed the textmining from active interaction sources; ii) minimum required interaction score was set at 0.700 (high confidence). Only pathways with an FDR <0.05 were considered significantly enriched.

6.17.2 Statistics

All statistical analyses were performed using GraphPad Prism version 10. Data were expressed as mean ± standard error of the mean (SEM), as bar plot with single values or not, depending on data numerosity. Before further analysis, the normality of data was assessed using the D'Ambrosio-Pearson test. For comparisons between two groups, the Student's t-test was used for normally distributed data, while the Mann–Whitney U test was applied for non-parametric data. In the case of paired data, the paired t-test or Wilcoxon signed-rank test was used accordingly. For comparisons involving more than two groups, one-way ANOVA followed by Tukey's post hoc test was used for parametric data, while the Kruskal–Wallis test followed by Dunn's multiple comparisons test was applied for non-parametric data. Simple linear regression was used to assess the relationship between two variables. In datasets with missing values, pairwise deletion or multiple imputation was applied, depending on the context and extent of the missing data. When appropriate, outlier values were identified and discarded after Grubbs' test, with a 0.05 confidence setting. A p-value $\leq$ 0.05 was considered statistically significant.

7. Results

7.1 Characterization of ASCs and CM production

As recommended by International Society for Cell & Gene Therapy (ISCT) guidelines, all MSCs should be characterized in terms of differentiation capacity towards mesodermal lineages, as well as for their clonogenicity and expression of mesenchymal markers whilst being free of hematopoietic lineage markers. ASCs grew in adhesion and presented the classical fibroblast-like MSC morphology (data not shown). In Figure 6a are reported representative images of osteogenic and adipogenic differentiation, where the collagen deposits are highlighted by the Sirius Red staining (left panel) and the adipose vacuoles are dyed in a brilliant red hue with the Oil-Red-O staining (right panel). Clonogenicity was confirmed in the Colony Forming Unit assay (CFU-F), here represented in panel Fig.6b. Finally, the expression of mesenchymal markers CD90 (Thy-1) and CD73 (ecto-5'-nucleotidase) (Fig.6c, left panels), and absence of hematopoietic ones CD14 (LPS receptor) and CD45 (LCA) (Fig.6c, right panels), were confirmed.

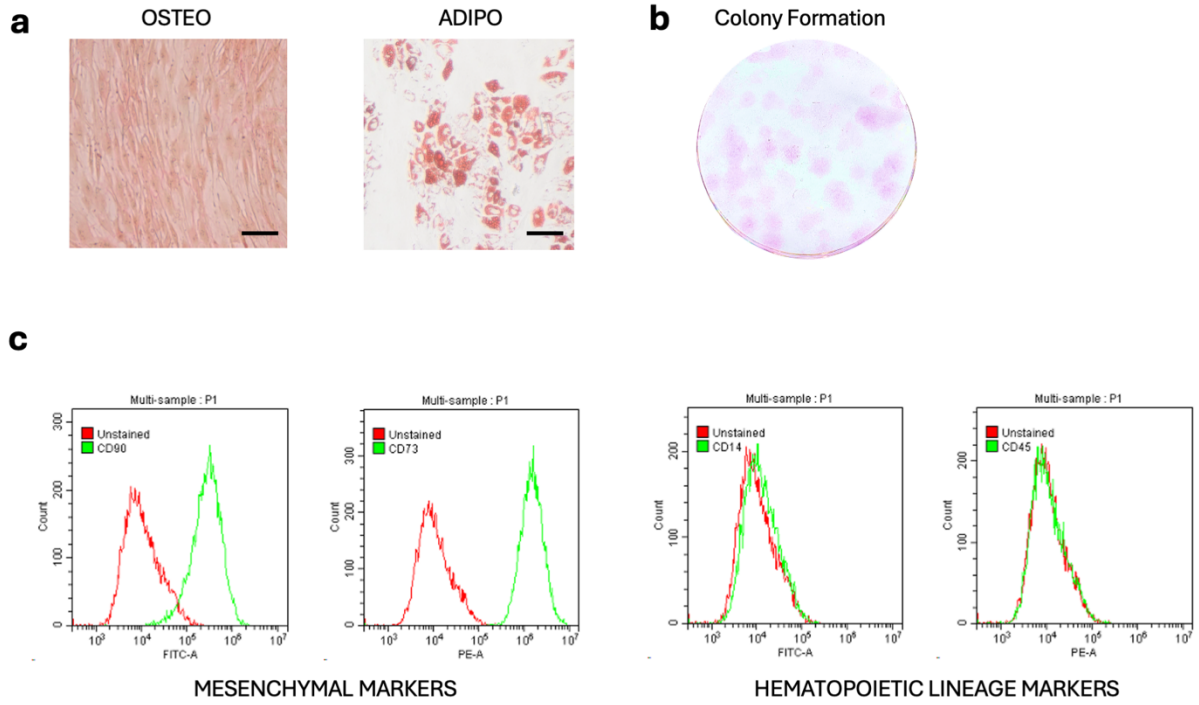

Figure 6 – ASC characterization

a) *Representative images of osteogenic, and adipogenic differentiation of ASCs used for CM production. Cells were stained with Sirius Red and Oil Red O, respectively. Scale bar:100 µm.* ***b)*** *Representative image of the clonogenic assay showing colony-forming ability of donor-derived ASCs. Staining: crystal violet.* ***c)*** *Flow cytometry profiles showing ASC surface markers. Mesenchymal markers (CD73 and CD90) are*

shown in the first panels; Hematopoietic lineage markers (CD14 and CD45) are shown in the last ones.

As part of the internal quality assessment, protein and particles content were assessed in CM. Quantification data are always normalized per 10^6 donor cells in order to align with dosing practices commonly used in cell therapy. Total protein content is in the range of 64,4 ± 6,2 µg/10^6 cells. NTA data show that mean particles size is 164,5 ± 2,6 nm, but the most represented population has a size of 110,7 ± 2,1 nm. Other dimensional information retrieved are the D10, D50 and D90. They represent the size value under which the 10/50/90% of the particles falls. The average values are 95,3 ± 1,4 nm, 142,2 ± 2,9 nm, and 262,4 ± 5,6 nm, respectively. Finally, normalized average particles concentration is around 1,5x10^9 ± 1,5 x10^8 particles/10^6 cells (Fig. 7a). All these data are considered as a whole to define whether a batch of CM is comprised in the standard particles distribution obtained with our protocol. Flow cytometry analysis validated the presence of canonical EV markers. Gating was defined using a mixture of calibration beads to establish size parameters (Fig. 7b, left panel). Histograms for CD63, CD81, and CD9 demonstrated clear positive signals (Fig. 7b, right panel), with the summary table indicating the positivity percentages, confirming the presence of EVs within the CM (Fig. 7b, lower table). Protein yield stratified by donor sex (Figure 7c) did not reveal significant differences, suggesting that sex does not influence CM protein content. Similarly, correlation analysis between donor age and normalized protein yield (Figure 7d) showed no significant association, suggesting that age does not critically affect CM production efficiency in terms of protein content. Lastly, protein levels normalized to cell number were comparable across different ASC passage numbers at the time of CM production (Figure 7e), indicating that moderate in vitro expansion does not substantially impact CM protein output.

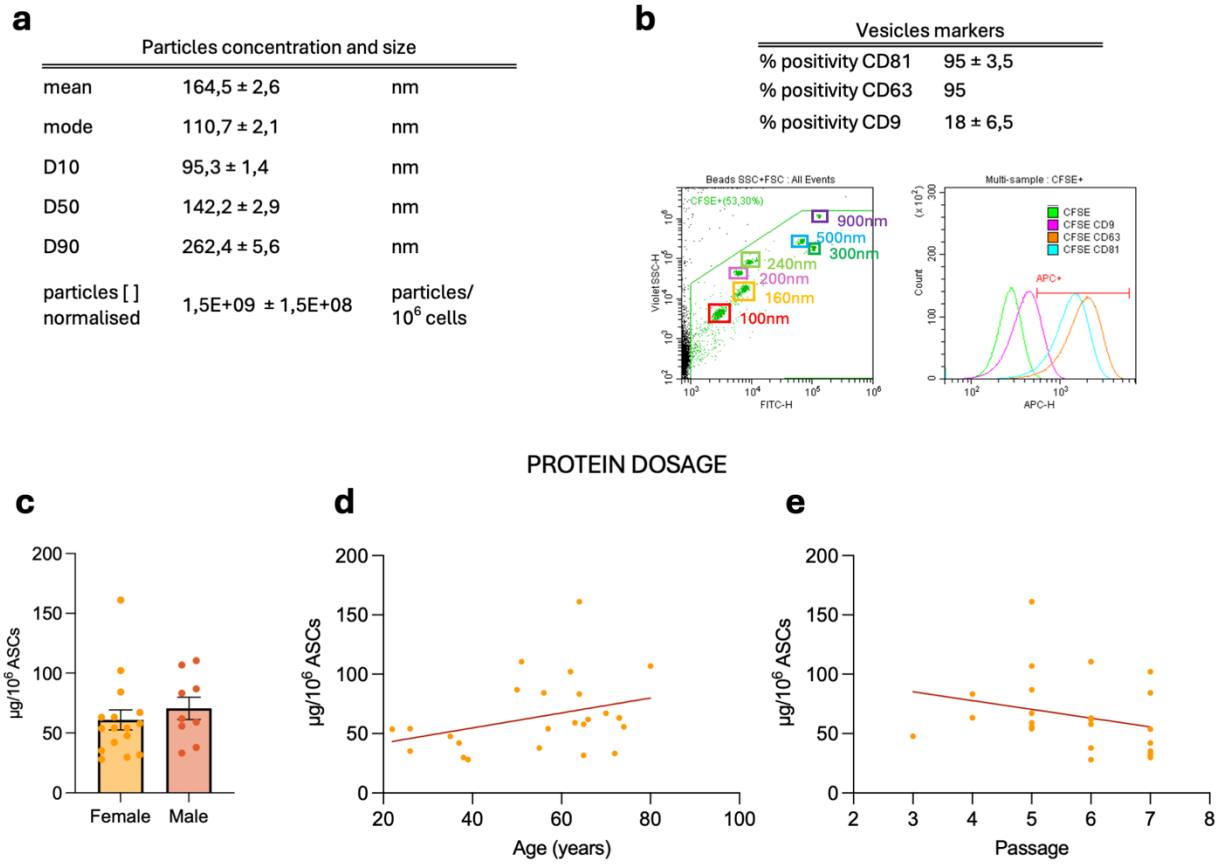

Figure 7 – CM protein dosage and particles quantification
a) *Table showing Nanoparticle tracking Analysis (NTA) results for particle quantification and dimensions in standard CM, normalized per million donor ASCs. n = 11.* ***b)*** *Flow cytometry profiles of canonical EV-positive markers. The first panel shows a mixture of calibration beads used to define the appropriate size gating. The following panel displays histograms for CD63, CD81, and CD9. Below: table summarizing the mean percentages of positive events for each marker. n = 2.* ***c)*** *Bar plot showing normalized protein dosage stratified by donor sex. Mean ± SEM. n= 24.* ***d)*** *Correlation plot between normalized protein dosage and donor age. Simple linear regression is shown; data did not follow a significant trend. n=24.* ***e)*** *Correlation plot of protein dosage stratified by ASC passage number at the time of CM production. For poli represented populations the average value was calculated. Simple linear regression is shown; data did not follow a significant trend. n=24*

7.1.1 Freezing variable influences final product

As part of the protocol standardization process, we analysed the effect of a freezing pre-concentration step, due to storage needs While proper freezing and thawing practices may seem like a minor detail, they can significantly impact protein and particle content during the CM production process. The total protein yield and other specific factors levels, were compared between F-CM ad T-CM (fresh and

thawed CM), revealing that protein dosage and IL4 and VEGFA are significantly reduced in T-CM (Fig. 8a-c). Additionally, CCL2, CCL3, IL8, HGF, M-CSF and OPG also appear to be reduced in the T-CM samples (Fig. 8d-i).

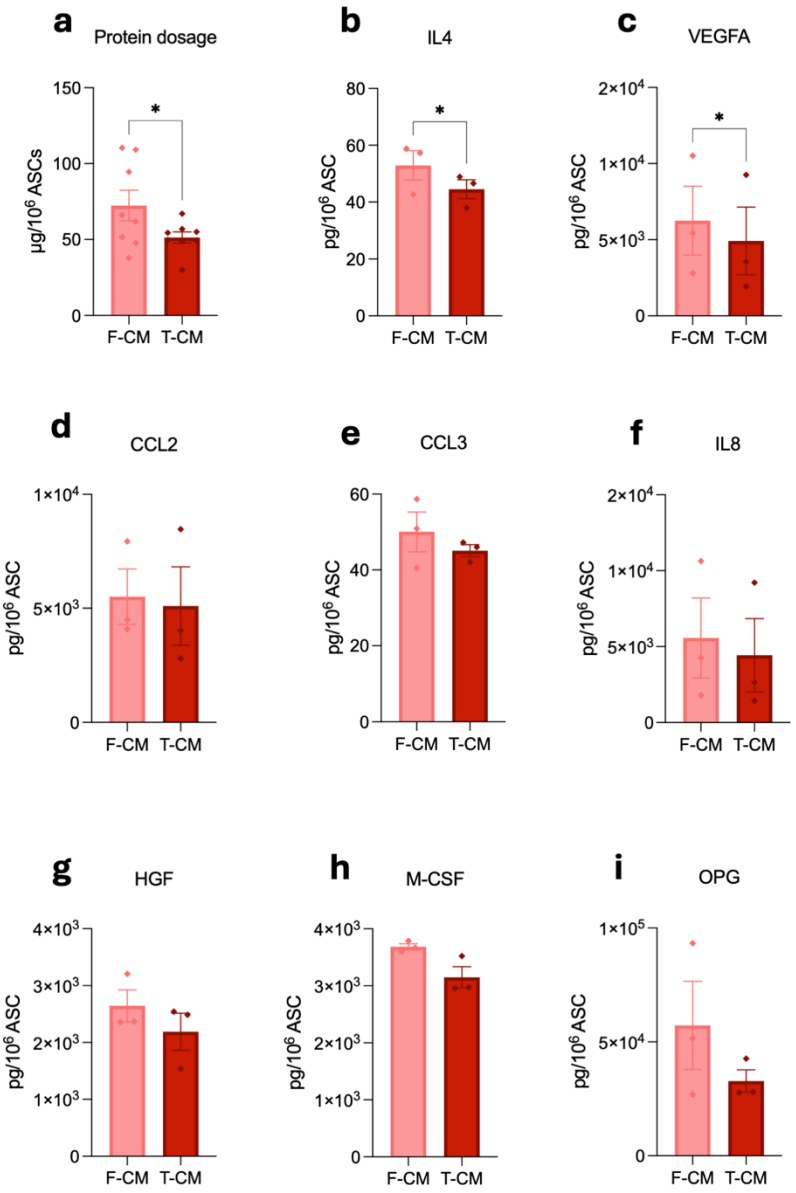

Figure 8 – Effect of pre-concentration freezing on protein content
a) *Total protein content in CM. Mean ± SEM. n = 8.* ***b–i)*** *Levels of selected proteins measured by Luminex in three independent pools of F-CM and T-CM:* ***b)*** *IL-4,* ***c)*** *VEGFA,* ***d)*** *CCL2,* ***e)*** *CCL3,* ***f)*** *IL-8,* ***g)*** *HGF,* ***h)*** *M-CSF, and* ***i)*** *OPG. Data presented as mean ± SEM. n = 3.*

From cytofluorimetric analysis data, the two media present the same percentages of markers positivity (>95% for CD63, >90% CD81, =11% CD9) (Fig.9a). The NTA revealed that, although the total content was not affected, the distribution

seems to be shifted towards smaller particles (Fig. 9b, c). Analysing the NTA specifics particles data, we observed a significant reduction in mode, mean, D10 and D50 sizes (Fig. 9d-g), with D90 showing a reduction trend as well. Additionally, the SPAN index was calculated to address sample polydispersity (D90-D10/D50), and it is comparable between the two groups (Fig. 9i).

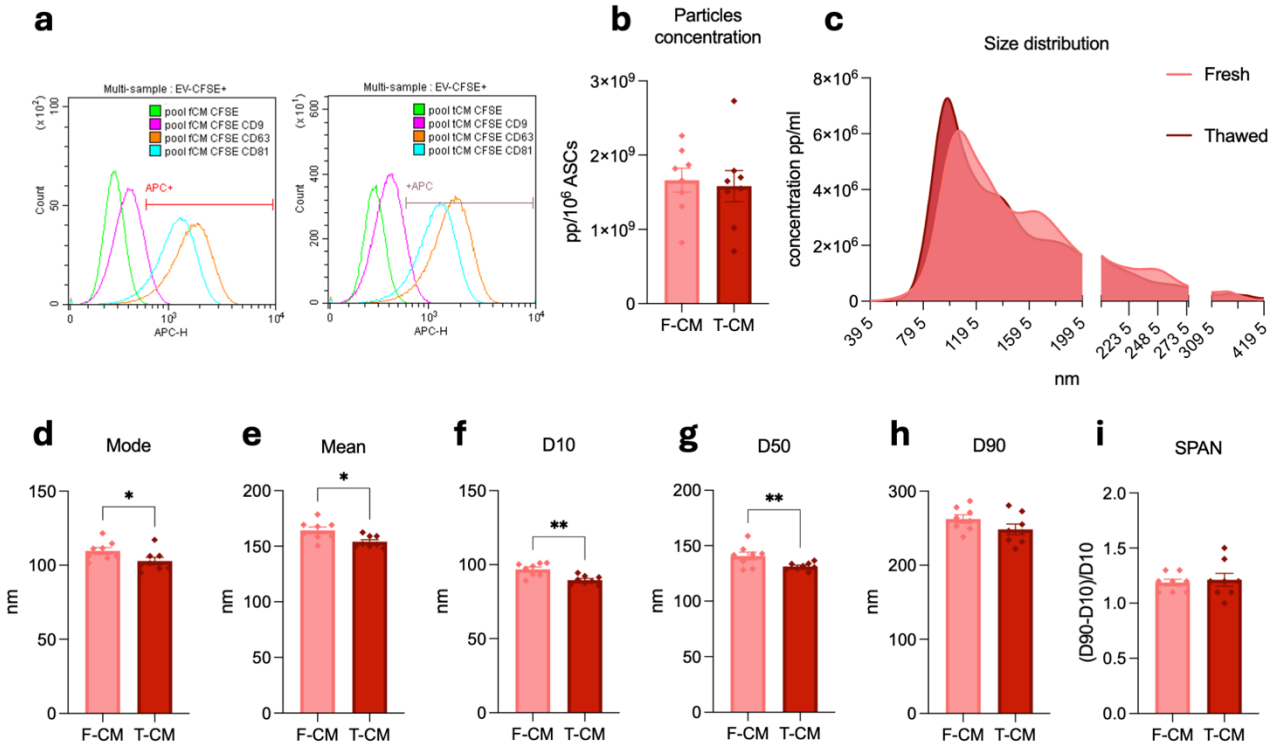

Figure 9 – Effect of pre-concentration freezing in particles distribution
a) *Flow cytometry overlay histograms of canonical EV-positive markers (CD63, CD81, CD9* ***b)*** *Total particle quantification (NTA), normalized per 10^6 ASCs. Mean ± SEM. n = 8.* ***c)*** *NTA-derived size distribution curves for pooled F-CM and T-CM.* ***d–i)*** *NTA-based comparisons of size parameters between F-CM and T-CM:* ***d)*** *Mode,* ***e)*** *Mean,* ***f)*** *D10,* ***g)*** *D50,* ***h)*** *D90,* ***i)*** *SPAN index. Mean ± SEM. n = 8.*

In collaboration with the LABION from Fondazione Don Carlo Gnocchi, we performed the Raman spectroscopy analysis of the media. From the spectra analysis it is possible to appreciate signals related to protein secondary structures—amide I (~1650 cm^{-1}) and amide III (1240–1300 cm^{-1})—along with lipid-associated bonds, making precise molecular attribution complex. However spectral ranges do not completely overlap: T-CM has greater intensity in the 700-1100 and 1200-2000 cm^{-1} ranges, whereas F-CM is higher in intensity in the 2800-3000 cm^{-1} range (Fig. 10a). Indeed, the multivariate analysis states F-CM and T-CM are two significantly different products (Fig. 10b). More in depth, the area under the curve (AUC) was assessed in

spectral ranges of biochemical meaning, specifically in the amide regions (AUC 1600–1690 and AUC 1200–1300; Figure 10c, d), lipid-associated bands (AUC 2750–3040; Figure 10e), and nucleic acid regions (AUC 720–800; Figure 10f). To further dissect these variations, the protein-to-lipid (P/L) and nucleic acid-to-protein (NA/P) ratios were calculated. T-CM displayed an increased P/L ratio (Figure 7g–h), reflecting a relative shift in protein and lipid content. Similarly, a higher NA/P ratio (Figure 7i–j) in T-CM suggests a greater presence of nucleic acids, potentially due the release of nucleic acids from vesicles compromised by freeze–thaw stress. This is consistent with the known tendency of encapsulated nucleic acids to contribute minimally to the spectral profile unless particle integrity is compromised.

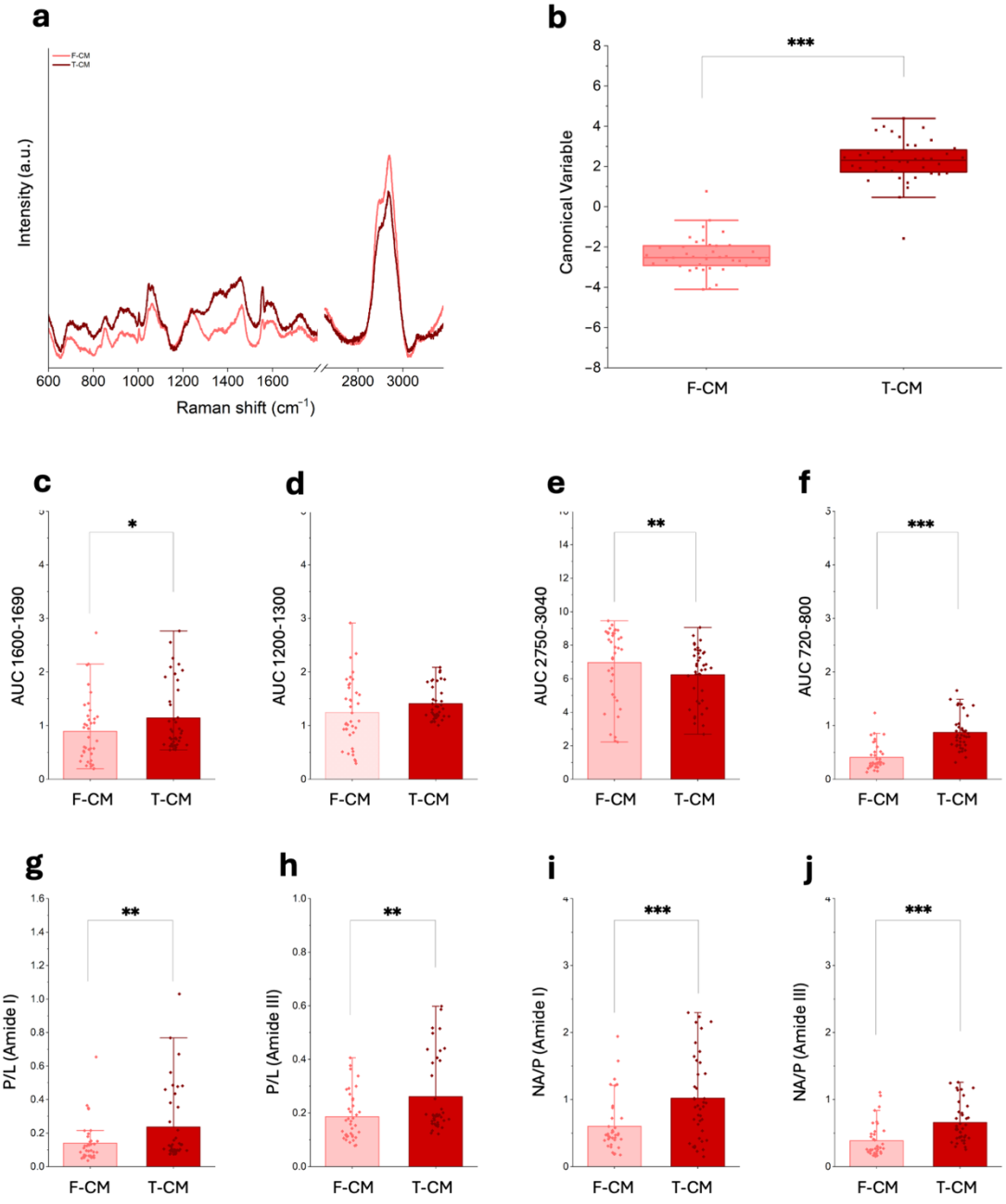

Figure 10 – Raman spectroscopy analysis of pre-concentration freezing effects on CM composition

a) *Representative Raman spectra of pooled F-CM and T-CM.* ***b)*** *Canonical variable plot illustrating group separation. n=4.* ***c-f)*** *Quantification of the area under specific spectral regions:* ***c)*** *amide I,* ***d)*** *amide III,* ***e)*** *lipid associated regions, and* ***f)*** *nucleic acids associated regions.* ***g, h)*** *Ratio of spectral areas: protein-to-lipid ratio based on amide I and amide III, respectively.* ***i, j)*** *nucleic acid-to-protein ratio based on amide I and amide III, respectively.*

Per last, we performed functional evaluation assays, namely MMP activity and chemotaxis assay, which are currently used also as part of the quality evaluation. The MMP activity in CE explants, strongly induced by TNFα and IL-1β, was significantly

reduced by both media, suggesting that the main players in exerting this effect – TIMPs– are retained (Fig. 11a). The THP-1 recruitment proved that even in this case F-CM and T-CM are equally able to attract cells (Fig. 11b).

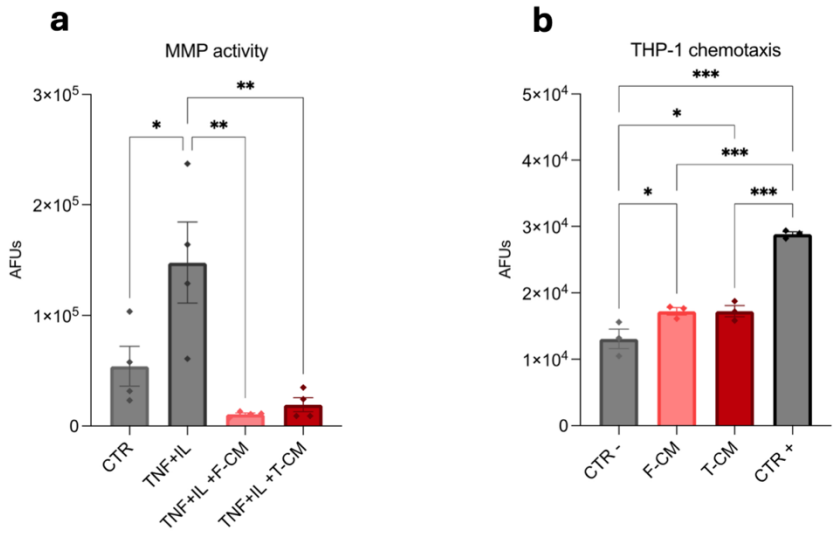

Figure 11 – Effect of pre-concentration freezing on CM functionality
a) *MMP activity in day 3 cartilage explants supernatants following cytokine stimulation and treatment with F-CM or T-CM. Data expressed in arbitrary fluorescence units (AFUs). Mean ± SEM. n = 4.* ***b)*** *Cell migration assay: fluorescence intensity of THP-1 cells attracted by CM, positive or negative control after 24 hours. Data expressed in AFUs. Mean ± SEM. n = 3.*

7.1.2 Evaluation of best timing and priming protocol

In order to obtain a richer CM, specifically containing molecules able to counteract an inflamed environment and phenotype, we tested a combination of collection timing and cytokine priming on ASCs. The experimental set-up comprehended the collection at 24 and 72 hours, whilst the cytokine stimuli were: 1) none (CTR), 2) TNFα 10ng/ml (TNF), 3) IL-1β 10ng/ml (IL), and 4) TNF+IL.

At first, ASCs were stimulated for 5 minutes and then the activation of key signalling pathways was evaluated at 0, 30, and 60 minutes (Fig.12a). Cytokine stimulation induced a rapid and transient activation of the NF-κB and AKT pathways, since phosphorylated NFκB and phosphorylated AKT expression strongly increased at 30' and decreased after 60' in parallel with IκBα degradation. Total (non-phosphorylated) NF-κB and AKT levels remained largely stable, suggesting that the modulation primarily occurs at the activation level rather than through changes in protein abundance. In line with this data, the protein expression of classical

inflammatory markers, COX2 and IDO, was importantly induced (Fig.12b). In this case the evaluation occurred at 24 and 72 hours, and confirmed that the cytokine stimuli, specifically IL and TNF+IL, efficiently sustained the expression of these markers over time. Conclusively, the brief 5' priming with inflammatory cytokines activated the inflammatory response in ASCs, with effects persisting up to 72 hours after exposure.

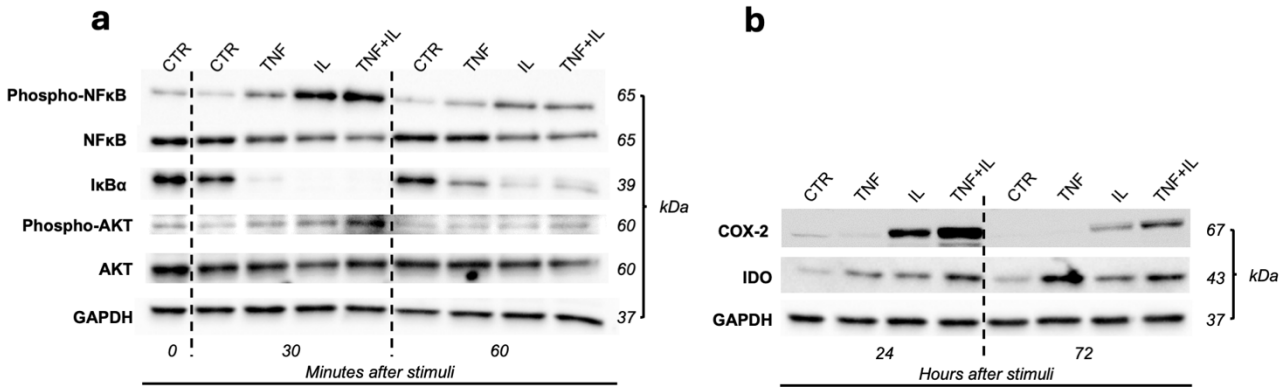

Figure 12 – Effects of inflammatory priming on the activation of signalling pathways
a) *Representative western blot images showing activation of intracellular signalling pathways in ASCs at 0, 30, and 60 minutes after a brief (5 minutes) cytokine stimulus.*
b) *Representative Western blot of inflammatory markers 24 and 72 hours after stimulation*

Subsequently, the CM obtained from all experimental conditions were analysed for total protein content, particle concentration, and the presence of specific bioactive factors and lipid families. The aim was to identify the optimal collection timing and priming strategy to maximize CM yield and potentially enhance its biological efficacy. Cytokine priming consistently increased total protein content compared to the control at both 24 and 72 hours, with no significant differences among the primed groups (Fig.13a). At 72 hours, the TNF and TNF+IL conditions showed a marked increase in particle concentration (Fig. 13b), while the IL group did not display any relevant change compared to its 24-hour counterpart or the 72-hour control.

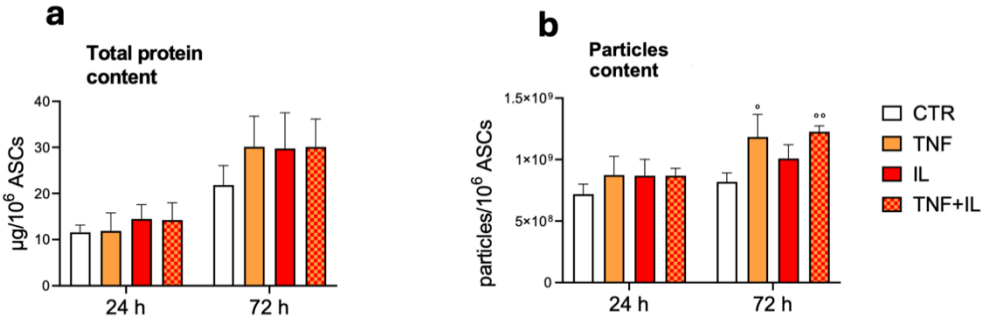

Figure 13 – Protein and particles quantification: impact of collection timepoint and priming protocol

a) *Quantification of total protein CM content.* ***b)*** *Particles quantification. Mean ± SEM. n = 4. Statistical significance vs. corresponding 24 h is shown as °/°°p ≤ 0.05/0.01. All data are normalized on 10^6 donor ASCs.*

The effect of the priming protocol and later collection time was particularly evident on the secretion of VEGF, CCL2, IL-8, Thrombospondin-2, IL-6, and BDNF (Figure 14a–f), with IL, and particularly TNF+IL, at 72hours being the most promising groups. Although no significant differences can be detected between these groups, the specific factors are consistently more abundant in the 72h-TNF+IL group. These results suggest that 72h-TNF+IL represents the most efficient priming protocol.

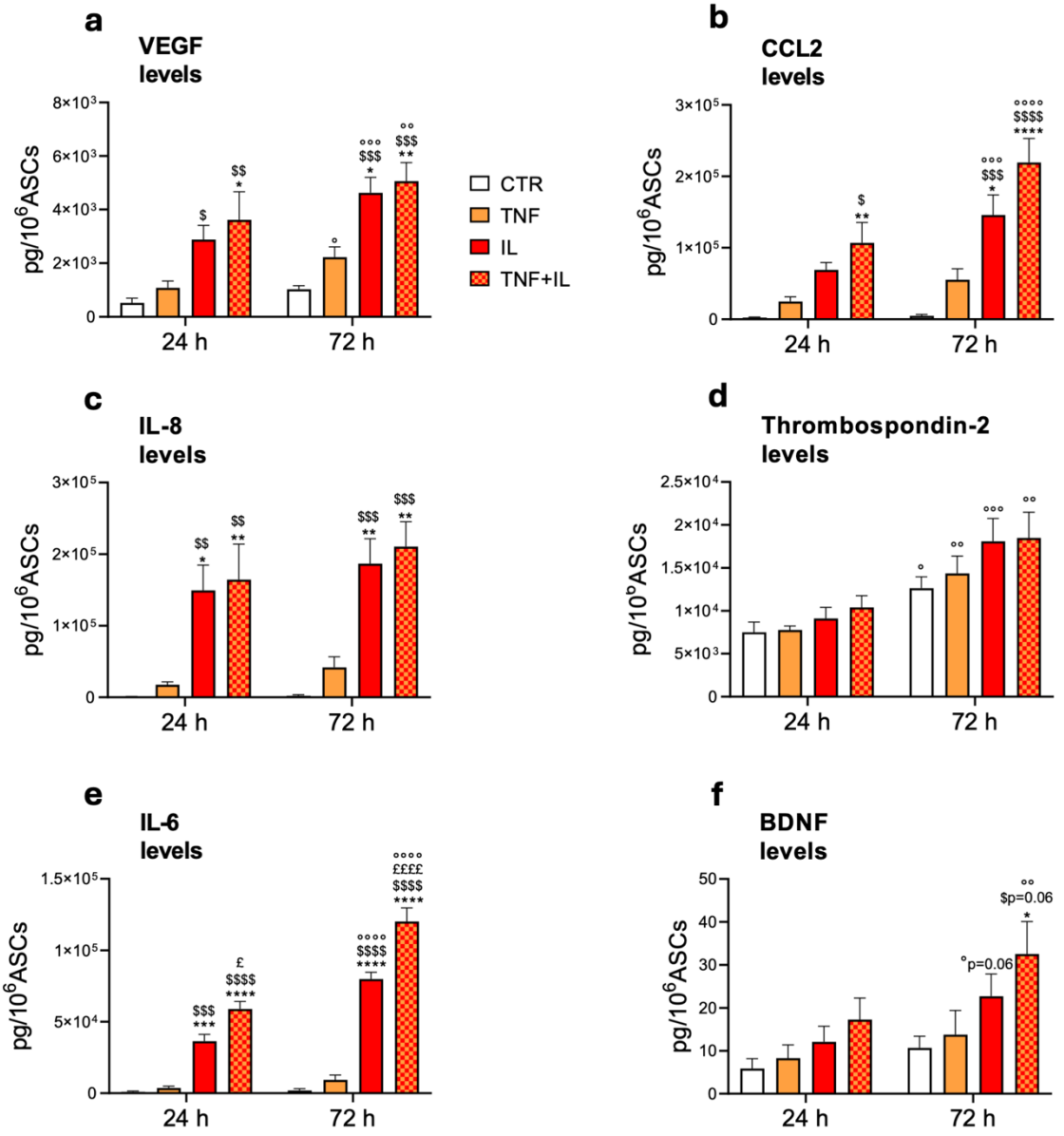

Figure 14 – Selection of optimal priming protocol: part I
a–f) *Levels of selected soluble factors significantly enriched in CM collected at 72-hours following stimulation with TNF+IL, compared to other protocols:* ***a)*** *VEGF,* ***b)*** *CCL2,* ***c)*** *IL-8,* ***d)*** *Thrombospondin-2,* ***e)*** *IL-6, and* ***f)*** *BDNF. Mean ± SEM. n = 4. Statistical significance vs. corresponding 24 h is shown as °/°°/°°°/°°°°$p \leq 0.05/0.01/0.001/0.0001$, vs. corresponding CTR as */**/***/**** $p \leq 0.05/0.01/0.001/0.0001$, vs. corresponding TNF as $/$$/$$$/$$$$ $p \leq 0.05/0.01/0.001/0.0001$, vs. corresponding IL as £/££££ $p \leq 0.05/0.0001$. All data are normalized on 10^6 donor ASCs*

Several other factors were analysed, but the effects of time or priming were not as strong and consistent as for these preceding. TGF-β1 and Angiogenin levels are mainly influenced by timing (Fig. 15a, b). The other factors, especially IL-1ra, seem to be affected primarily by cytokine priming (Fig15c-g).

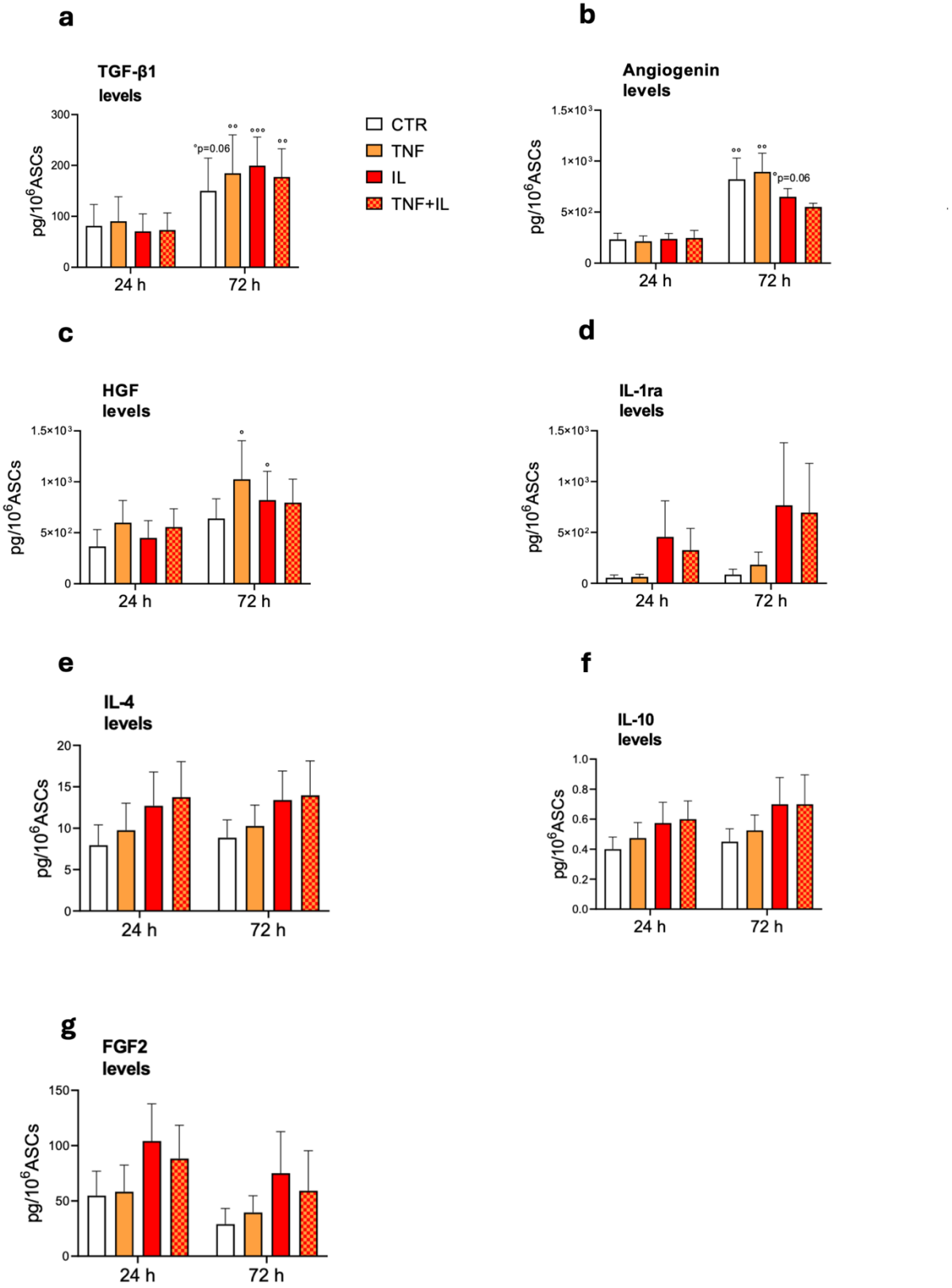

Figure 15 – Selection of optimal priming protocol: part II
a-g) *Levels of specific proteins that were impacted less by the 72h-double stimuli protocol:* ***a)*** *TGF-β1,* ***b)*** *Angiogenin,* ***c)*** *HGF,* ***d)*** *IL-1ra,* ***e)*** *IL-4,* ***f)*** *IL-10, and* ***g)*** *FGF2.*

Mean± SEM. n=4. All data are normalized on 10^6 donor ASCs. Statistical significance vs. corresponding 24 h is shown as °/°°/°°°/°°°°p ≤ 0.05/0.01/0.001/0.0001

Ultimately, PGE2 and several lipidic classes were quantified in each group. PGE2 levels were consistent with the trend of increment in the 72h-TNF+IL group (Fig.16a). The families of DHCER, CER, SM, LacCer, GB3, FA and EICO were quantified in mass spectrometry and showed a clear enrichment in 72h groups, with the TNF+IL group reaching the highest levels in all classes, except for Sphingomyelins (SM) (Fig.16b).

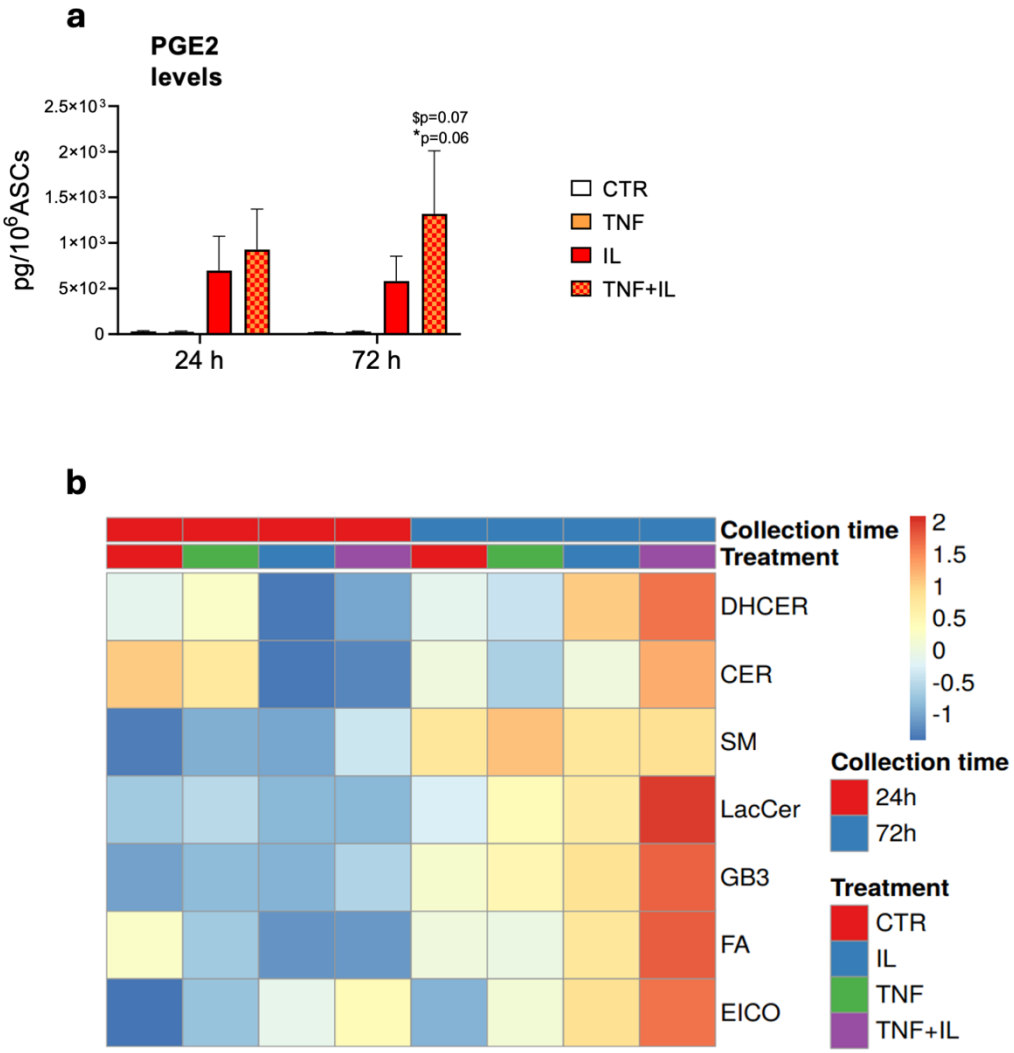

Figure 16 – Selection of optimal priming protocol: part III (lipids)
a) *PGE2 levels. Mean ± SEM. n=4. Statistical significance vs. corresponding CTR as * p ≤ 0.05, vs. corresponding TNF as $ p ≤ 0.05.* ***b)*** *Heatmap of lipid quantified through mass spectrometry, divided per priming protocol and lipidic classes (DHCER = Dihydroceramides; CER = Ceramides; SM = Sphingomyelins; LacCer = Lactosyleramides; GB3 = Globotriaosylceramides; FA = Fatty Acids; EICO= Eicosanoids). All data are normalized on 10^6 donor ASCs.*

7.1.3 pCM comparison to CM

Since the 72h-TNF+IL group was the most promising in terms of protein, particles and lipids enrichment, it was selected for further analysis and directly compared to the 72h control group (laboratory standard). Based on previous results, the 24-hour timepoint was excluded from this comparison. From this point forward, the 72h-CTR will be referred to as CM, while the primed version will be pCM. Direct comparison between the two groups unravels that in terms of protein and particle content, pCM is significantly enriched compared to CM (Fig.17a, b). The differences in particle distribution are clearly visible in the Fig.17c panel, where the pCM (orange) produce a significantly higher peak compared to CM (black). HGF and Thrombospondin-2 data were re-analysed and shown to be significantly higher in pCM (Fig.17d, e). Additionally, the analysis of specific lipid subclasses within the EICO family revealed a consistent increase in pCM, with DHA (3.6-fold), EPA (1.4-fold), and AA (2.9-fold) all showing higher concentrations compared to CM (Fig.17f). A pool of CM and pCM was analysed with the protein array, to qualitatively compare specific protein levels. The membranes can detect 80 proteins; out of them we selected only the ones that underwent a substantial change (at least 2-fold or 0.5-fold change). The analysis revealed that CM and pCM differ in protein content, e.g. ENA-78, IL-6, and IL-8. Interestingly, the cytokines used to prime the ASCs were absent in the pCM (Fig.17g). Ultimately, specific factors were quantified with Luminex technology. The results show that pCM, compared to CM, is consistently more enriched in immunomodulatory and growth factors, with C-GSF showing the most important increase (211-fold) (Fig.17h, right panel is in log10 scale).

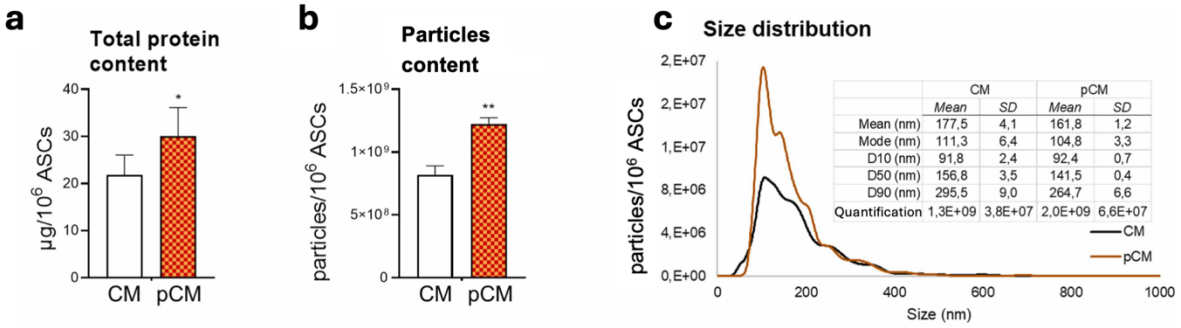

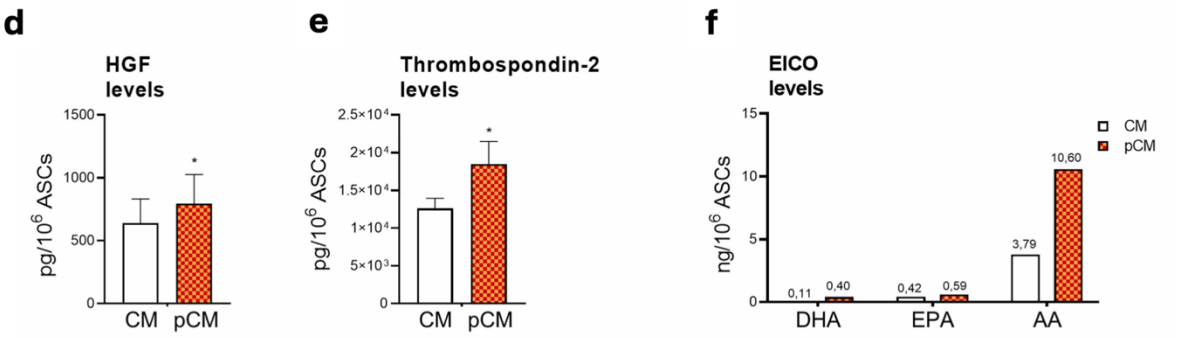

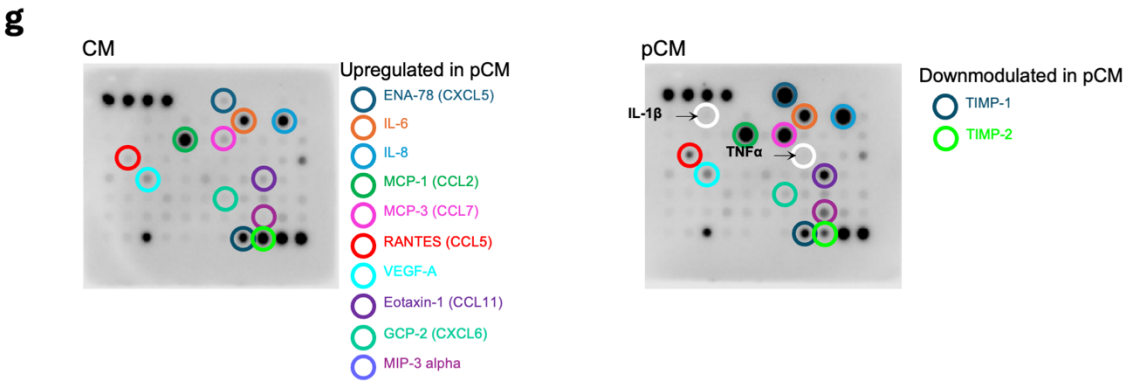

h

pg/10⁶ ASCs	CM mean	CM SEM	pCM mean	pCM SEM
CCL2	6,2E+03	3,6E+03	1,3E+05	3,2E+04
CCL3	24,0	5,9	139,5	24,3
CXCL1	3,1E+03	3,8E+02	1,9E+05	2,9E+02
G-CSF	17,8	3,0	3784,1	701,8
HGF	1,0E+03	6,6E+01	2,2E+03	2,4E+02
IFN-γ	2,6	0,9	3,0	0,7
IL-10	2,6	0,8	2,8	0,8
IL-1ra	53,8	9,9	244,4	39,7
IL-4	17,2	5,1	25,0	1,2
IL-8	1,5E+03	5,8E+02	1,3E+05	2,4E+04
M-CSF	2,5E+03	4,3E+02	4,0E+03	2,6E+02
OPG	2,1E+04	2,7E+03	2,7E+04	6,8E+02
TIMP-1	1,2E+06	1,9E+03	1,5E+06	1,1E+05
VEGF-A	2,8E+03	1,4E+03	8,1E+03	2,9E+03

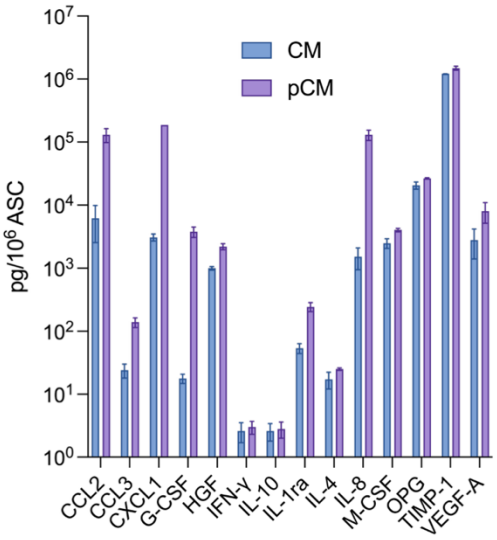

Figure 17 – Additional differences between CM and primed CM
a) *Total protein content of CM (72h-CTR) and pCM (72h-TNF+IL). Mean±SEM. n=4.* ***b)*** *Particles quantification. Mean±SEM. n=4.* ***c)*** *Particles size distribution, with table specifying CM and pCM NTA results.* ***d)*** *HGF. Mean±SEM. n=4* ***e)*** *Thrombospondin-2. Mean±SEM. n=4* ***f)*** *Eicosanoids quantification in CM and pCM pools.* ***g)*** *Protein array membranes comparing the expression levels of 80 cytokines between CM and pCM pools. Proteins were considered differently enriched if they showed a x0.5 or x2 variation between CM and pCM.* ***h)*** *Table with quantified factors in CM and pCM with relative abundances. To the right, a histogram representing the tabled data, in logarithmic scale. Mean±SEM. n=2. All data, except for panel g), are normalized on 10^6 donor ASCs. Statistical significance is represented as */** p-value <0.05/0.01.*

7.2 Implementation of ex vivo cartilage explant culture

To better replicate cartilage in vitro, it was necessary to address issues related to the reproducibility of tissue architecture and cellularity within the laboratory model. For this reason, a cartilage explant culture model was implemented, making use of native tissue to test the CM.

7.2.1 Model validation

The initial experimental groups were designed to identify the most suitable inflammatory stimulus for inducing an OA-like phenotype in the model. Analysis of the supernatants showed that both tested cytokines (TNFα and IL-1β) increased both MMP activity and NO release, with their combination exerting a synergistic effect that significantly amplified these modulations (Fig. 18a, b). No significant differences were observed in the release of sGAGs into the medium across the experimental groups (Fig. 18c). Gene expression analysis of inflammatory, catabolic, and anabolic markers revealed that the combined stimulus strongly upregulated Prostaglandin-endoperoxide synthase-2 (*PTGS2)* (Fig. 18d) and, together with IL-1β, induced the expression of *MMP3* (Fig. 18e). The expression of SRY-box transcription factor 9 (*SOX9*), a pro-chondrogenic gene, showed a moderate increase in response to the individual cytokines but was reduced following the combined stimulation (Fig. 18f). These results indicate that the combination of TNF and IL-1β represents the most effective condition to induce an OA-like phenotype in cartilage explants.

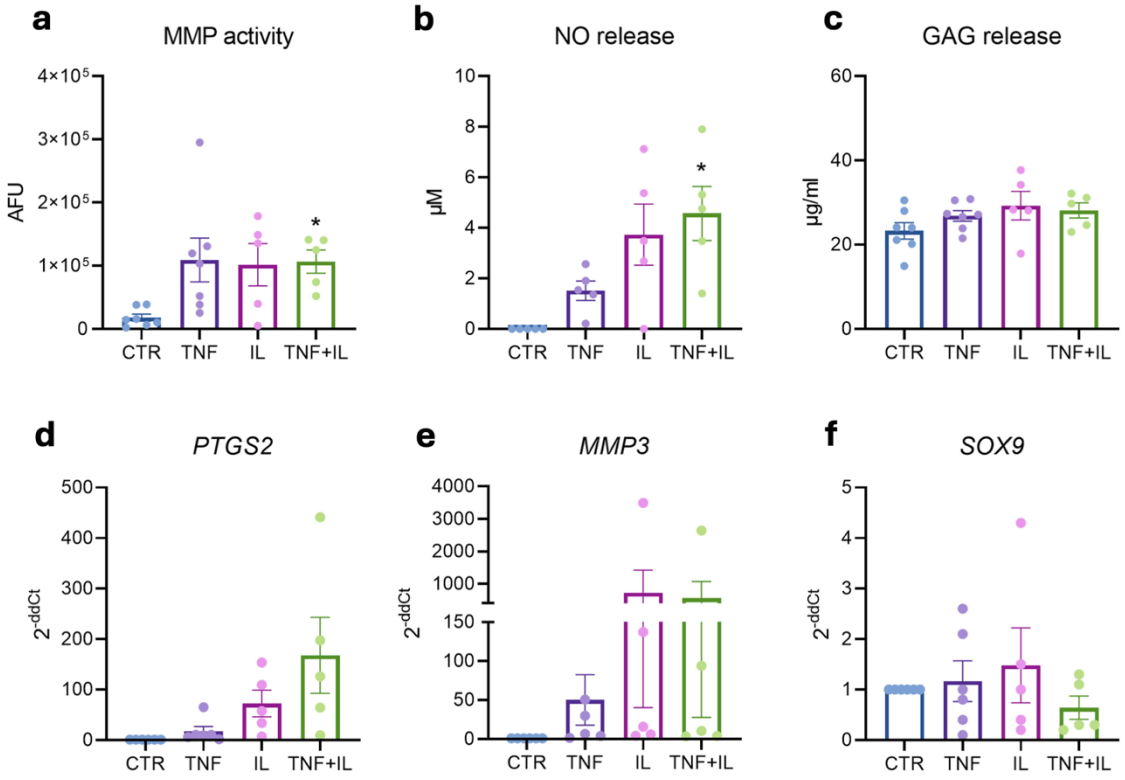

Figure 18 – Effects of cytokine stimulation on cartilage explants
a) *MMP activity in supernatants of cartilage explants following 3 days of stimulation with pro-inflammatory cytokines. Data expressed in AFUs.* ***b)*** *Nitric oxide (NO) levels in explant supernatants under the same conditions.* ***c)*** *Release of sulphated glycosaminoglycans (sGAGs) from the cartilage explants after stimulation.* ***d–f)*** *Gene expression analysis of inflammation- and cartilage-related targets under different stimuli:* ***d)*** *PTGS2,* ***e)*** *MMP3,* ***f)*** *SOX9. Results normalized to housekeeping gene expression. All data are represented as mean ± SEM. n = 5-7. Statistical significance vs CTR is represented as * p-value<0.05*

7.2.2 CM testing against OA catabolic and inflammatory markers

The next step was to evaluate the effect of CM on the pathological alterations induced in the model. Cartilage explants were stimulated with the combination of cytokines (TNF+IL) and treated with CM (TNF+IL+CM). The MMP activity results confirmed that the inflammatory stimulus effectively induced catabolic activity compared to the control and demonstrated that CM significantly reduced this abnormal activation (-74%) (Fig. 19a). In contrast, the effect on NO levels indicated that CM was not sufficient to counteract this strong induction (Fig. 19b). Similarly, sGAG levels did not reflect the expected catabolic effect induced by the cytokines or the protective effect of CM (Fig. 19c). Gene expression analysis showed that the inflammatory marker *PTGS2* and the catabolic markers *MMP3* and *MMP13* were strongly induced

by the cytokines and slightly reduced by CM treatment (-54% and -21%, respectively) (Fig. 19d–f). Unexpectedly, the addition of CM in the presence of TNF + IL exerted a negative effect on the expression of the chondrogenic markers *SOX9* and *COL2A1* (Fig. 19g, h).

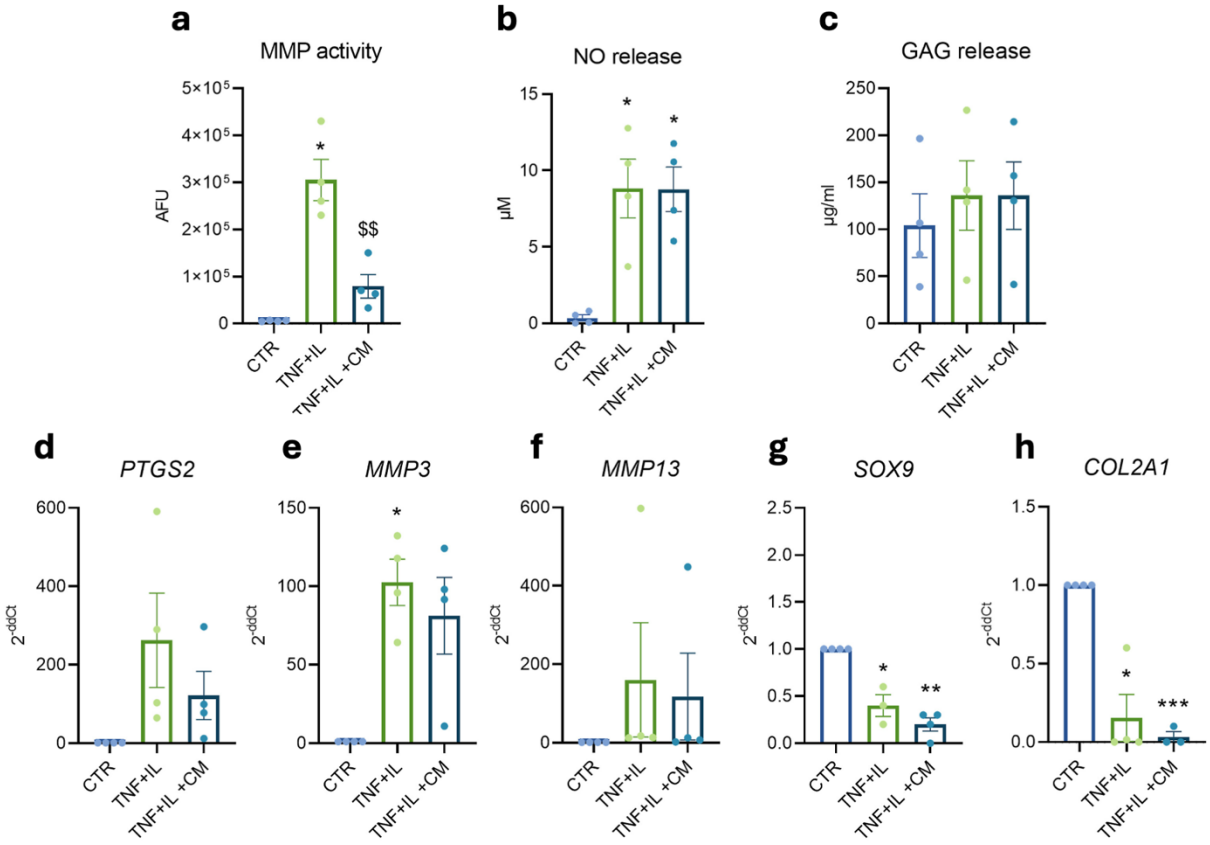

Figure 19 – Effects of CM treatment on cytokine-stimulated cartilage explants *__a)__ MMP activity in supernatants of explants exposed to CM and/or inflammatory cytokines, after 3 days. Data in AFUs. __b)__ NO release. __c)__ sGAG release. __d–h)__ Gene expression analysis of __d)__ PTGS2, __e)__ MMP3, __f)__ MMP13, __g)__ SOX9, __h)__ COL2A1. Expression levels normalized to housekeeping genes. All data are represented as mean ± SEM. n = 4. Statistical significance vs CTR is represented as */**/*** p-value<0.05/0.01/0.001.*

Given that CM is enriched in immunoregulatory factors, its effects were also evaluated in hypertrophic synovial membrane explants deriving from OA patients, a tissue naturally enriched in immune components. In this setting, CM was tested both alone and in combination with the inflammatory stimulus (TNF+IL). The results showed that CM alone reduced inflammatory markers, including NO release (-67%), *PTGS2* expression (-77%), and COX2 expression (-90%). Consistently, CM also attenuated the pathological upregulation of these markers induced by TNF+IL (Fig. 20a–d).

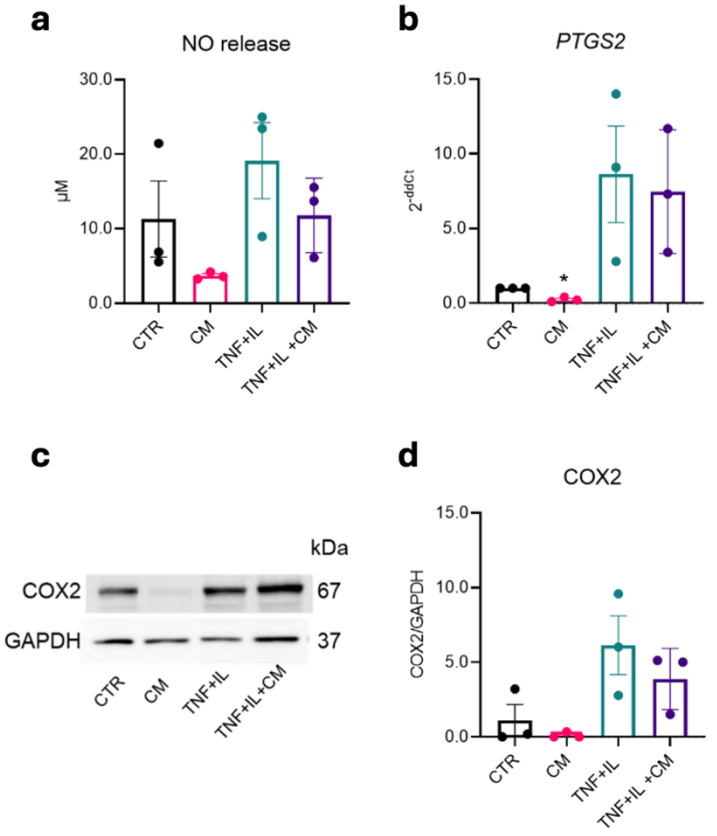

Figure 20– Effects of inflammation and CM treatment on synovial membrane explants

a-d) *Expression of inflammatory markers in synovial membrane supernatants, with or without TNF+IL and/or CM:* ***a)*** *NO levels,* ***b)*** *PTGS2 gene expression,* ***c)*** *Representative Western blot showing COX-2 protein expression, and* ***d)*** *relative densitometric quantifications. n=3. Significance versus CTR is shown as * p≤0.05*

7.2.3 Co-culture of CE and SM

Separate experiments were conducted using a co-culture model combining cartilage explants (CE) and synovial membrane (SM). The rationale of this setup was to investigate CE–SM crosstalk under inflammatory conditions. In this model, CM was compared with the anti-inflammatory drug dexamethasone (DEX). CE and SM were placed in the same well but separated by a transwell membrane insert, reflecting their anatomical separation within the joint. Supernatant analysis after 48h showed that CM was as effective as DEX in inhibiting MMP activity, causing -59% and -61% reduction, respectively (Fig.21 a). sGAG release was unaffected by either treatment (Fig.21 b, right panel), while the time-dependent loss of GAGs during culture was evident (Fig.21 b, left panel). NO release was strongly reduced by DEX, whereas CM had no effect compared to control (Fig.21 c).

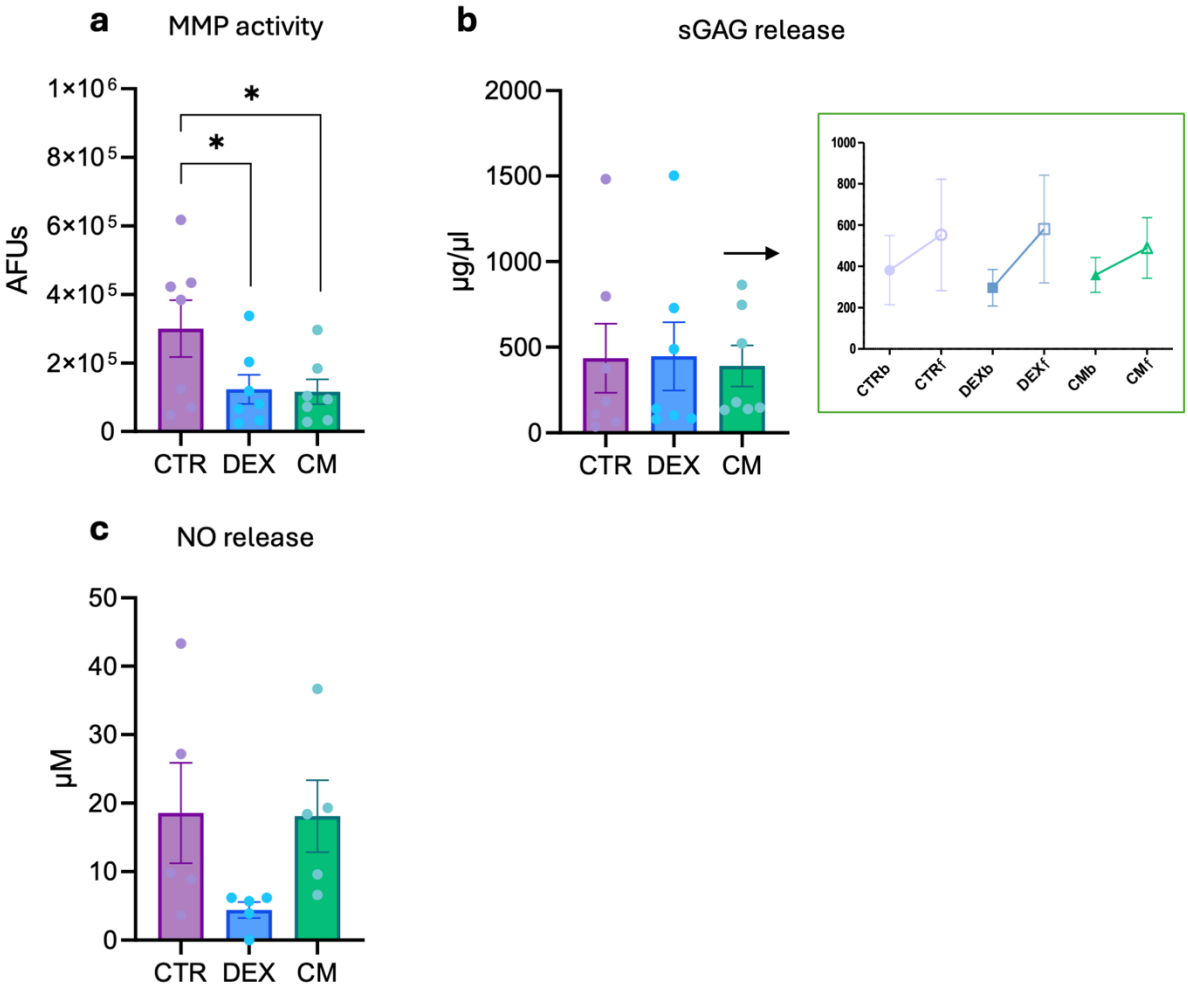

Figure 21– Comparison between dexamethasone and CM effect in the CESM model

a) *MMP activity in supernatants of cartilage and synovial membrane co-cultured explants, exposed to dexamethasone (DEX) or CM, after 48 hours. Data in AFUs.* ***b)*** *sGAG released in the supernatants after 48 hours ((left panel) and showed as basal (b) (prior any treatment) versus final (f) (right panel). N=7.* ***c)*** *NO release in supernatant after 48 hours. n=5. Significance is shown as * p≤0.05*

Gene expression analysis was performed on both CE and SM. In CE, DEX markedly reduced the expression of inflammatory genes (Prostaglandin-endoperoxide synthase-2, *PTGS2*, and *IL1B*) and catabolic genes (*MMP3*, *MMP13*) (Fig.22 a-d). No consistent effect was observed on *TIMP1* and Aggrecan (*ACAN*), (Fig.22 e-f). By contrast, DEX reduced the expression of *COL2A1* and to a minor extent *SOX9* suggesting that DEX might influence matrix-related genes. CM significantly reduced *MMP3* expression but also decreased *COL2A1* and *SOX9* expression (Fig. 22 c, g-h).

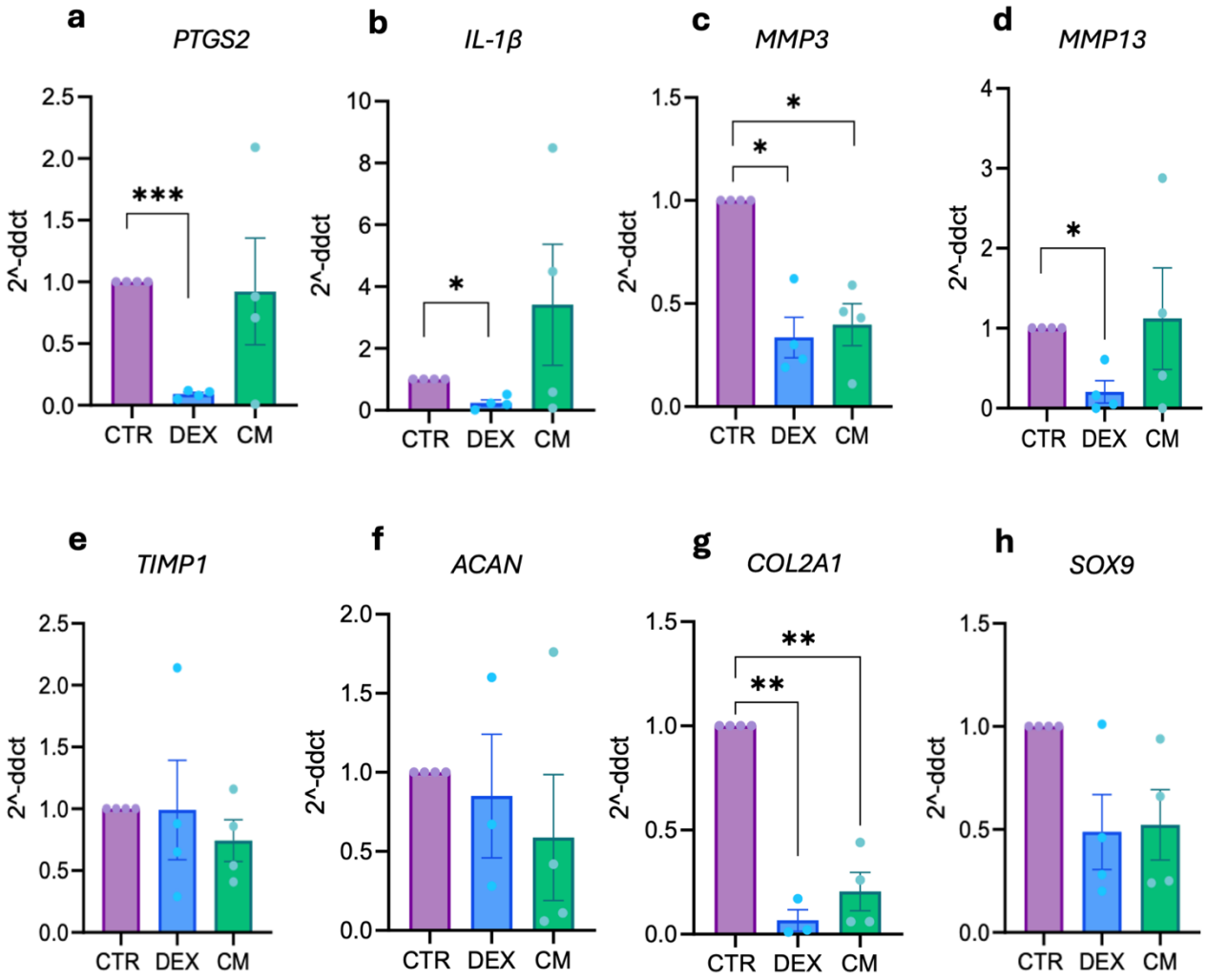

Figure 22– Effects of DEX and CM on CE gene expression in the co-culture model

a, b) *Gene expression of inflammatory-related markers.* ***c-e)*** *Gene expression of extracellular matrix remodelling markers.* ***f-h)*** *Gene expression of cartilage markers. Results are obtained from samples co-cultured and treated for 48 hours. n=4. Significance is shown as * p≤0.05, *** p≤0.001*

In SM, DEX consistently downregulated *PTGS2*, *IL1B*, *MMP3*, and *MMP13* (Fig.23 a d), without affecting *TIMP1* (Fig.23 e). DEX also significantly decreased Vascular Endothelial Growth Factor alpha (*VEGFA*) expression, a marker of OA synovial membrane (SM) associated with the severity of the pathology. Among genes related to tissue homeostasis and repair, DEX did not alter Fibrionectin-1 (*FN1*) and Connective tissue growth factor (*CTGF*) *expression* (Fig.23 f-h). In this setting, CM did not significantly modulate these genes, compared to control (Fig.23 a-h).

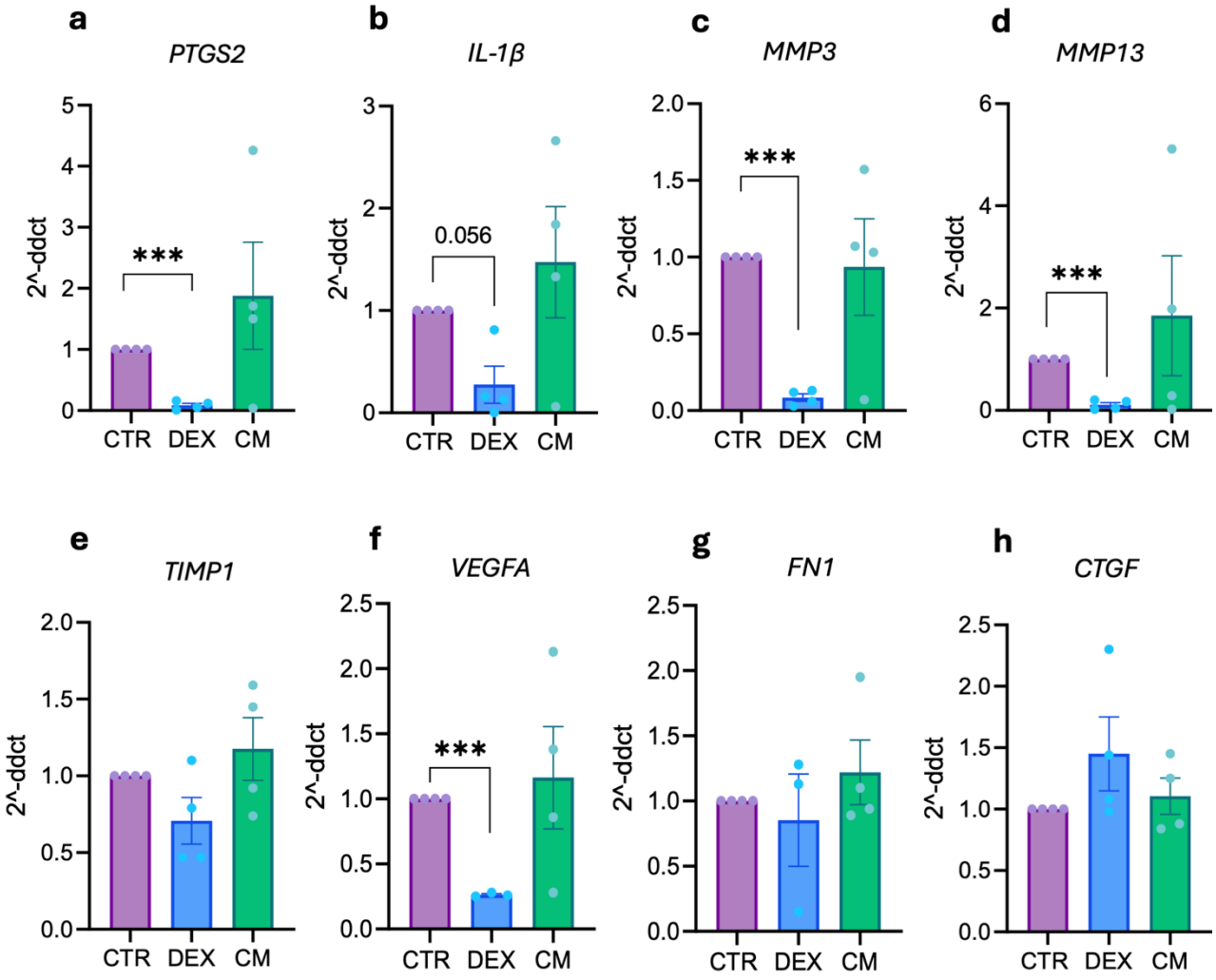

Figure 23– Effects of DEX and CM on SM gene expression in the co-culture model

a, b) *Gene expression of inflammatory-related markers.* ***c-e)*** *Gene expression of matrix remodelling markers.* ***f-h)*** *Gene expression of angiogenesis and tissue fibrosis-related markers. Results are obtained from samples co-cultured and treated for 48 hours. n=4. Significance is shown as ** p≤0.01, *** p≤0.001*

7.3 Osteochondral explant model

OA is a whole-joint pathology; therefore, the objective of this disease modelling is to incorporate all relevant joint tissues. Building upon a previously described osteochondral model (110), we implemented a double-compartment osteochondral model that enables the use of tissue-specific culture media and allows the targeted application of inflammatory stimuli or treatments to a specific compartment (Fig.24 a, b). In this setup, OCh explants were maintained using cartilage- and bone-specific media, while the inflammatory stimulus (TNF+IL) was applied exclusively to the

cartilage compartment. Treatments with CM or pCM were also administered in the cartilage compartment to simulate an intra-articular injection, which represents the most clinically relevant route of administration for this type of therapeutic approach.

7.3.1 Model validation

The first step was to validate the model in terms of both compartmentalization efficacy and the selection of tissue-specific markers to assess individual tissue responses. Marker evaluation was performed after three days and included viability/metabolic activity for both tissues, MMP activity and sGAG release for cartilage, and alkaline phosphatase (ALP) and tartrate-resistant acidic phosphatase (TRAP) activities and osteocalcin (OC) release for bone. Viability was significantly higher in bone compared to cartilage, consistent with the higher metabolic activity of bone tissue (Fig. 24c). Both MMP activity and sGAG release were significantly higher in the cartilage compartment (Fig. 24d, e), while bone-related markers were appropriately more expressed in the bone compartment (Fig. 24f–h). These results confirm that the compartmentalization is effective over the 3-day culture period and that the selected markers are suitable for assessing tissue-specific responses.

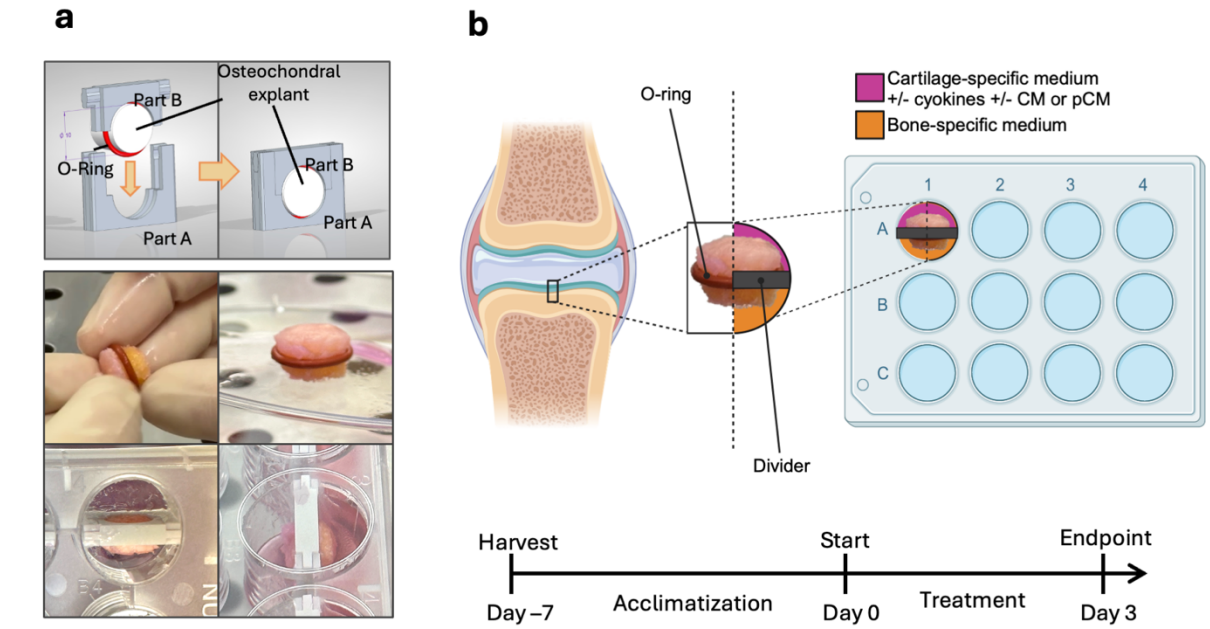
a
Part B
Osteochondral explant
O-Ring
Part B
Part A
Part A
b
O-ring
Cartilage-specific medium
+/- cyokines +/- CM or pCM
Bone-specific medium
1
2
3
4
A
B
C
Divider
Harvest
Start
Endpoint
Day –7
Acclimatization
Day 0
Treatment
Day 3

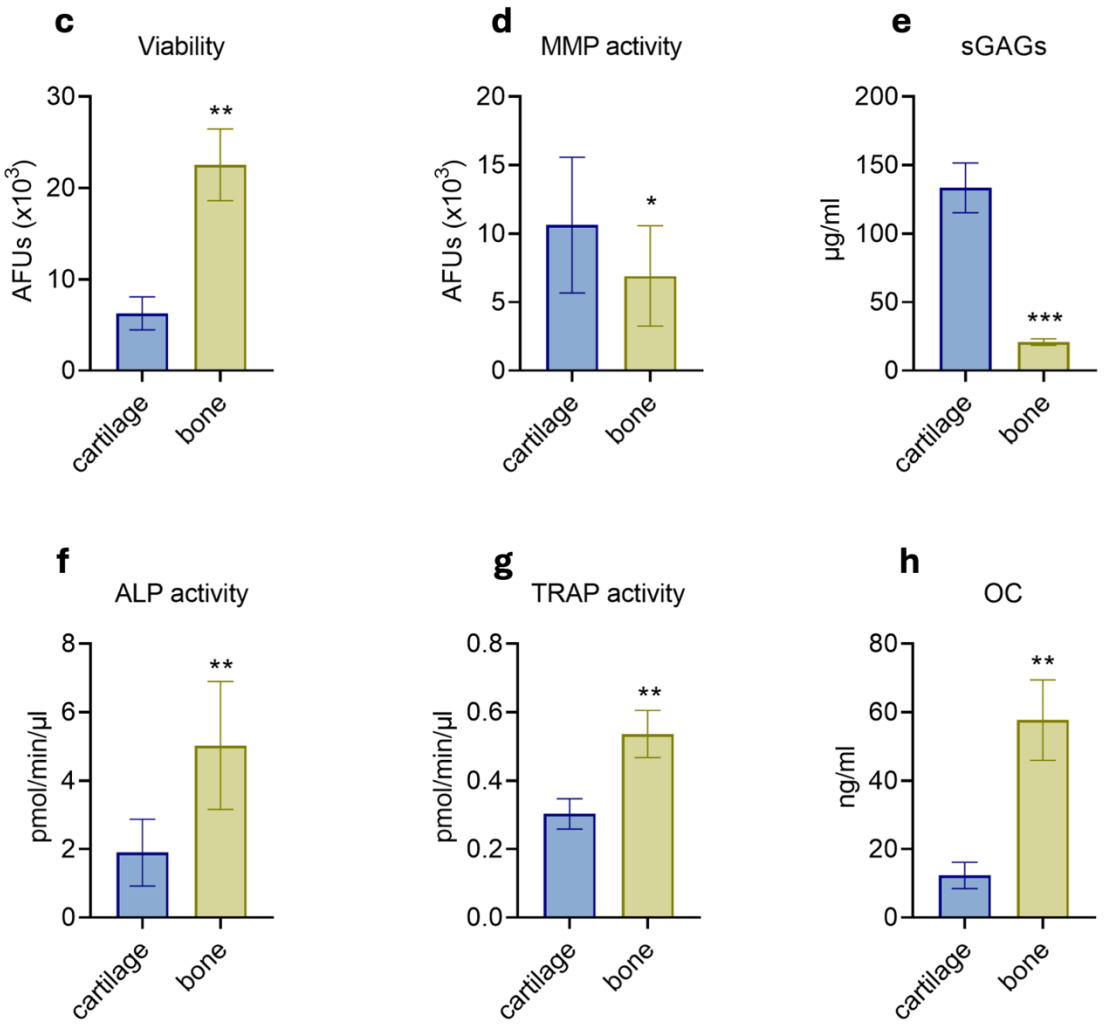
c
Viability
AFUs (x10³)
30
20
10
0
**
cartilage
bone
d
MMP activity
AFUs (x10³)
20
15
10
5
0
*
cartilage
bone
e
sGAGs
µg/ml
200
150
100
50
0
***
cartilage
bone
f
ALP activity
pmol/min/µl
8
6
4
2
0
**
cartilage
bone
g
TRAP activity
pmol/min/µl
0.8
0.6
0.4
0.2
0.0
**
cartilage
bone
h
OC
ng/ml
80
60
40
20
0
**
cartilage
bone

Figure 24 – Validation of compartmentalization
a) *Project of the 3D-printed insert (upper panel), and representative images of the step-by-step inclusion of OCh explants within the insert (lower panel).* ***b)*** *Experimental set-up and timeline.* ***c)*** *Tissue viability in both cartilage and bone compartments after 3 days of culture, assessed using the AlamarBlue assay. Data expressed in AFUs x10^3. n = 12.* ***d)*** *MMP activity in supernatants. AFUs. n=9.* ***e)*** *sGAG release. Mean±SEM. n=7.* ***f)*** *Alkaline phosphatase (ALP) activity. Data expressed in U/µl, where U is pmol/min. n=9.* ***g)*** *Tartrate-resistant acid phosphatase (TRAP) activity. n=13.* ***h)*** *Osteocalcin (OC) levels in supernatants. n = 9. All data derive from day 3 supernatants and are represented as mean± SEM, with bone data normalized on weight in grams. Statistical significance is represented as */**/*** p-value≤0.05/0.01/0.001*

7.3.2 CM and pCM administration as a treatment

The effects of CM and pCM treatments were then assessed. Briefly, tissue viability was assessed at Day 0 –afterwards the OCh housing but prior any treatment– and at the endpoint (Day 3). As already observed, cartilage viability is always inferior to the bone one, and ulteriorly significantly decreases after 3 days, independently from the experimental group, while the bone remains viable during all the experimental timeline (Fig.25a, b).

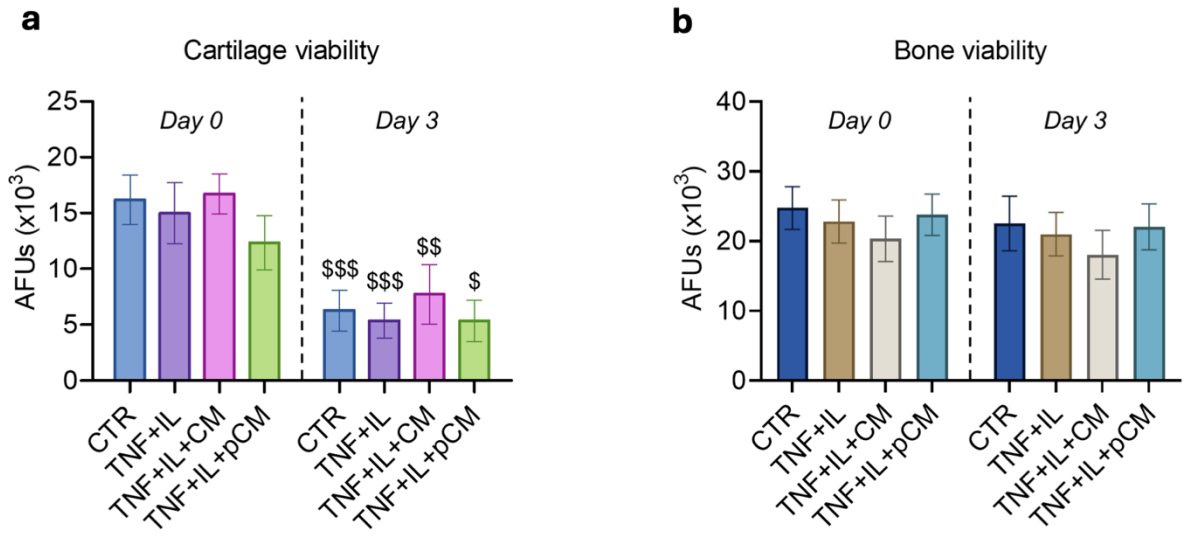

Figure 25 – Metabolic activity/viability in both compartments
Tissue viability was evaluated through AlamarBlue assay, in both ***a)*** *cartilage and* ***b)*** *bone compartments, at day 0 and day 3. Data expressed in AFUsx10^3. Mean±SEM. n=12. Statistical significance vs. Day 0 is represented with $/$$/$$$ p-value<0.05/0.01/0.001.*

The results further showed that TNF+IL significantly induced MMP activity in the cartilage compartment, while both CM, and more effectively pCM, exerting an inhibitory effect on this marker (Fig. 26a). As observed previously on cartilage explants, sGAG levels did not align with the MMP results, showing only a minimal increase in the groups exposed to cytokines compared to the control (Fig. 26b). The protein expression of MMP3 –for catabolism– and COL2A1 –for anabolism– were also assessed. The cytokines exposure triggers an increase in MMP3 expression, without evident effects by CM and pCM treatments (Fig. 26c). Conversely, COL2A1expression is reduced by cytokines, unaffected by CM, but mildly restored by pCM treatment (Fig.26d). In the bone compartment, the markers remained unaffected by the conditions applied to the cartilage side. The only appreciable change, although not statistically significant, was a slight modulation in ALP activity, suggesting the possibility of cross-communication between the two tissues (Fig. 26e-g). As for the validation part, tissue specific markers were assessed also in the opposite compartment: no signs of leakage or modulation were observed (Supplementary Figure 1).

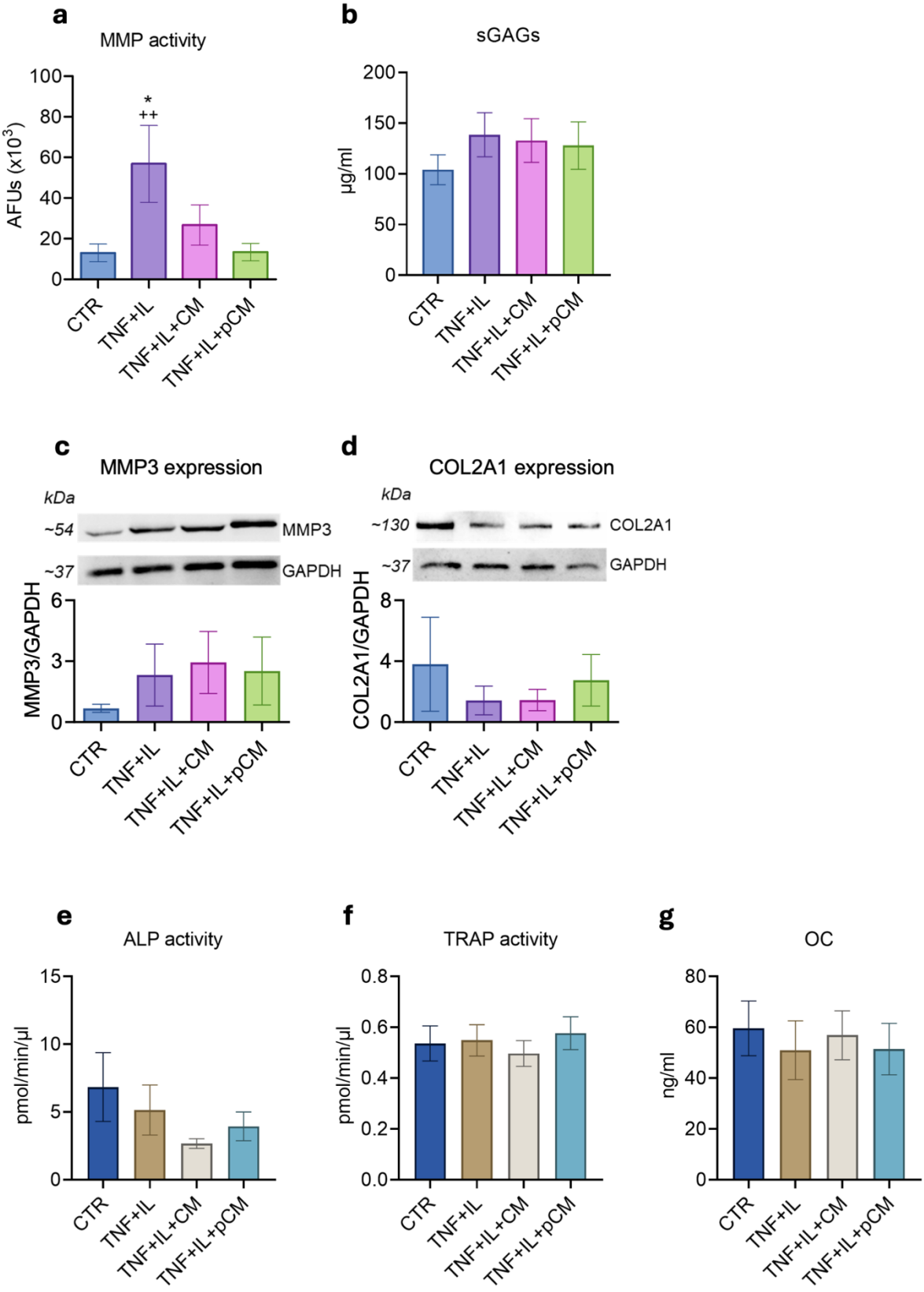

Figure 26 – Results of CM/pCM and/or inflammatory stimulus on tissue specific markers

a, b) *Markers of cartilage health state at the endpoint:* ***a)*** *MMP activity and* ***b)*** *sGAG release. All data are represented as mean ± SEM. Statistical significance is*

*represented by * vs CTR and ⁺ vs TNF+IL+pCM (*/⁺⁺p-value≤0.05/0.01). n=13* ***c, d)*** *Densitometry of protein expression in cartilage tissue:* ***c)*** *MMP3 (n=5) and* ***d)*** *COL2A1 (n=4) expression normalised on GAPDH as the housekeeping. Both bar plots are shown together with a representative western blot image.* ***e-g)*** *Markers of bone metabolic state at the endpoint:* ***e)*** *ALP activity,* ***f)*** *TRAP activity, and* ***g)*** *OC levels. All data are represented as mean ± SEM. Bone data are normalized on explant weight in g. n=13*

7.4 CM effects on bone turnover markers (collaboration)

In collaboration with The Laboratory for Joint & Bone Engineering - University of Ferrara, we tested CM in a model of bone turnover. Based on previous, we analysed the content of CM in relation to bone tissue. The main bone-related biological terms identified through the STRING analysis are reported in Fig. 27a, with the corresponding network shown in Fig. 27b. Building on these findings, CM was repeatedly administered to a co-culture of osteoblasts and monocytes—serving as osteoclast precursors—during the 14-days long process of micromass formation. Analysis of the supernatants showed that, in the presence of CM, ALP activity increased while osteocalcin release decreased (Fig. 27c, d), which may suggest a shift towards an early osteogenic response and deposition of mineralized matrix. Analyses of the micromasses revealed that CM significantly reduced TRAP expression (Fig. 27e, first panel), indicating an inhibitory effect on osteoclast differentiation. Additionally, CM enhanced the expression of several osteogenic markers, including a significant upregulation of OPN and ARS (Fig. 27e).

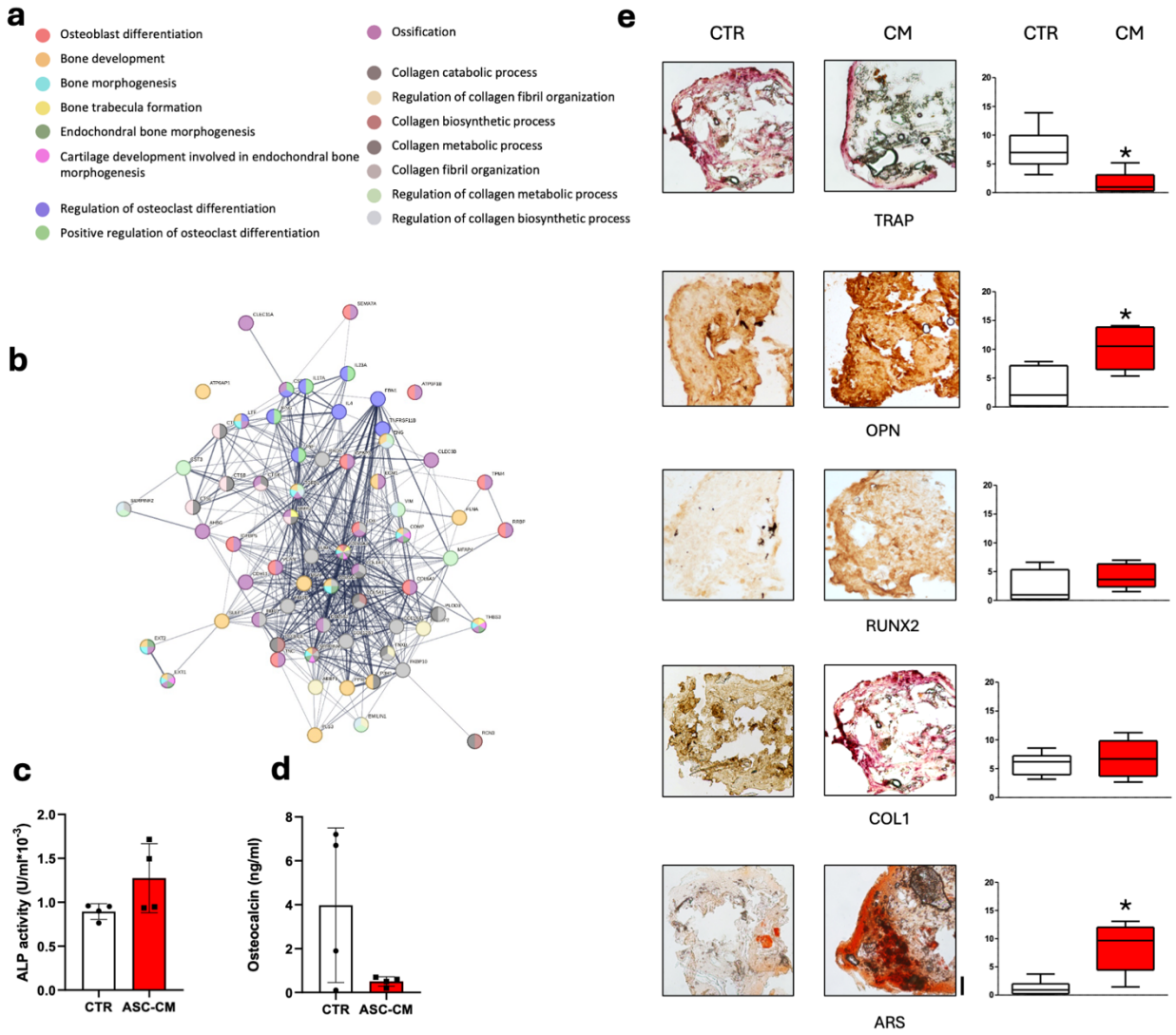

Figure 27 – Effects of CM in a bone remodelling model

a) *Bone-related GO biological processes associated with proteins quantified in CM.* ***b)*** *Bone-related STRING protein–protein interaction network of CM-derived proteins.* ***c)*** *ALP activity in supernatants of 3D bone micromasses cultured with CM or left untreated.* ***d)*** *OC levels under the same conditions. Mean ± SEM. n = 4.* ***e)*** *Representative images and quantification of histological staining of 3D bone micromasses, untreated or treated with CM. Assessed markers: TRAP, OPN, RUNX2, COL1, and Alizarin Red S (ARS). Mean ± SEM. Statistical significance vs CTR is represented as * p-value<0.05.*

8. Discussion and conclusions

8.1 Conditioned medium

Cell-derived products such as conditioned medium (CM) represent promising biotherapeutics for a wide range of pathologies, from osteoarthritis (OA) to COVID-19 (118,119). CM can be produced easily from ASCs. It is possible to tailor the production protocol to obtain different final products, but it is important to account for every minimal change in the pipeline since it can alter the final composition.

8.1.1 Production

The success of cell-free therapies based on mesenchymal stromal cell (MSC)-derived secretome critically depends on the upstream parameters governing cell sourcing and expansion. Among all MSC sources, adipose tissue represents one of the most advantageous due to its abundance, ease of access, and minimal donor site morbidity (120). One of the main advantages of exploiting adipose stem cells (ASCs) for allogeneic CM production, is that they can be easily harvested from healthy –often young– donors as surgical waste following liposuction or other aesthetic procedures, and they grow under standard culture conditions that are readily optimizable and suitable for scale-up (121). Moreover, liposuction procedures, often performed for cosmetic purposes, provide a high-yield, minimally invasive harvest of ASCs, positioning adipose tissue as a superior and sustainable MSC source for translational applications (122). In addition to availability, ASCs possess a high proliferation rate and phenotypic stability during early passages, allowing for efficient expansion and batch standardization. Following standard characterization, the ASCs populations used for CM production showed differentiation ability, colony formation and expression of canonical markers. In literature, ASCs are appreciated for their capability to preserve these abilities even at later passages and different growth settings (123), therefore making them ideal candidates for scaling-up processes. Nonetheless, conventional expansion protocols often rely on animal-derived serum, introducing safety concerns and batch variability. Several groups have proposed optimized protocols involving xeno-free (124) or human platelet lysate-based media (125), which support ASC expansion while preserving multipotency and secretory profiles. The shift to standardized, xeno-free conditions is a prerequisite for clinical-grade production and

aligns with current good manufacturing practices (cGMP). Scalability and cost-efficiency are further critical for the industrial and clinical feasibility of secretome-based products. Compared to bone marrow–derived MSCs, ASCs can be isolated in larger quantities and expanded more rapidly, reducing the number of passages required and thus minimizing senescence-associated alterations (126). This accelerates manufacturing timelines and reduces overall production costs. Moreover, the secretome protein/particles yield per cell has been reported to be higher in ASCs than in other MSC types, supporting their suitability for large-scale CM production (127,128). Automation, bioreactor-based expansion systems, and the adoption of closed systems for culture and secretome collection will further improve yield consistency and reduce contamination risks (129). Precise regulation of these upstream variables—tissue source, expansion protocol, and scalability—are fundamental to ensure the reproducibility, affordability, and effectiveness of CM as a therapeutic platform. Addressing them strategically is essential before tackling downstream process control or product functionalization. Cell-derived therapies rely on the concerted action of proteins, lipids, and EVs, but this very complexity makes them highly sensitive to upstream manufacturing choices.

8.1.1.1 Importance of standardization

In our experience, inter-donor variability had negligible impact on total particles and protein yields, suggesting our culture and collection standard operating procedures (SOPs) yield reproducible outputs. In fact, the results on standard CM revealed that we obtain quite coherent batches, independently from donor sex, age or cell passage. Other studies investigated that; for example, Trotzier et al. reported that donor age had no impact on the concentrations of cytokines, angiogenic and growth factors, or MMP (130). However, contrasting opinions emerges from literature research, as reviewed by Pinheiro-Machado (131): several donor characteristics were investigated as potential confounding factors for secretome analyses –age, sex, BMI, and anatomical origin– revealing that there is no consensus. Interestingly, in the same review, even the protocols were addressed as source of bias in the results, ranging from collection method to protein analyses, remarking the importance of a clear communication of procedures to allow data replication. In a previous work, we demonstrated that our protocol allows for a standardized CM production (132).

Eventually, among further suggestions in literature to ensure batch reproducibility, there is the use of bioreactors, since they can help in reducing operator actions, guarantee stability in growth conditions and product yield (133). Nonetheless, broad literature echoes that even small changes—oxygen tension, serum source, cell confluency—can dramatically alter MSC secretomes (29). Therefore, SOPs should be consistent and well documented, to ensure product standardization starting from its manufacture. Among critical procedural steps, pre-concentration freezing at –80 °C resulted in ≈ 25% decrease in total protein and in specific quantified factors. Studies have shown that freezing and thawing represent critical steps for proteins, lipids, nucleic acids, and vesicles, and more comprehensively, for biologics preservation (134). Consequently, the cold-chain processes in CM production pose significant challenges. Some proteins are especially vulnerable at ultra-low temperatures (e.g., –80 °C), likely because of the cryo-concentration effect: as ice forms, solutes—including proteins—become concentrated in the remaining liquid phase, altering solvent exposure, promoting structural changes, and driving aggregation and eventual precipitation (135). Eventually, this makes harder a reliable protein quantification, leading to possible biased reduced levels. Furthermore, data suggested a shift in the size distribution toward smaller EVs (mean and mode reduced) in thawed-CM (T-CM), compared to fresh CM (F-CM). These alterations are consistent with studies reporting protein aggregation and vesicle rupture due to ice-crystal formation (136). Even Raman spectroscopy highlighted variations in composition, that led to the identification of two completely different products, by PCA. Despite these changes, even at the level of putative effector concentrations, T-CM retained chemotactic and anti-catabolic activities comparable to F-CM. Nevertheless, the observed compositional drift underscores the need for the addition of cryoprotectants or controlled-rate freezing to preserve CM integrity (137), as recommended in EV preservation guidelines (138,139).

8.1.1.2 How cell priming impacts final product composition

CM, as a cell-derived product, is susceptible to alterations based on culture conditions, and researcher are exploiting this feature to “train” cells to deal to pathological environments and boost their therapeutic efficacy (140). In this project, ASCs were primed with inflammatory cytokines to mimic the inflammatory

environment typical of OA joints. Our results demonstrate that a 5-minute priming with IL-1β and TNFα triggers robust activation of both the NF-κB and AKT signalling axes—phosphorylation peaks at 30 min—leading to sustained upregulation of COX2 and IDO that persists up to 72 hours. This is consistent with the fact that ASCs sense their surroundings and have a memory of them (141), meaning that even a brief stimulus can trigger their immunomodulatory response, as it would happen when exposed to inflammatory environments (142,143). Priming—using stimuli such as IFNγ, TNFα, or IL-1β—has been applied in several contexts. Indeed, inflammatory cytokines can enhance the immunosuppressive effect of ASCs secrete (144). In this project, donor ASCs underwent various priming protocols –leveraging different cytokine stimulation and collection timing– to identify the one leading to a product enriched in bioactive factors. The 72-hour TNF+IL stimulation protocol yielded conditioned medium (CM) with the highest overall protein and particle content. Moreover, beyond the effects of inflammatory priming itself, the timing of collection modulated the abundance of individual components: CM harvested at 72 hours following TNF+IL exposure was significantly enriched in proteins, particles and lipid species. Multiplex profiling revealed significant enrichment of HGF, TGF-β1, PGE2, VEGF-A, CCL2, IL-6, IL-8, and BDNF—all critical modulators of immunoregulation, angiogenesis, and neuro-modulation in OA contexts (145). Similarly, in the work of Calligaris et al, 2024 (146), they compared CM from IFNγ-primed cells to control CM and found enrichment in gene ontology (GO) terms related to proliferation, tissue regeneration, immunomodulation, and angiogenesis. Likewise, in equine BMSCs, priming with TNFα, IL-1β, or IFNγ induced changes in immunomodulatory gene expression and altered cytokine levels in the CM (147). Moreover, TIMP-1 was highly present in both CM and pCM, with the latter expressing a slightly higher concentration. This is important in our specific therapeutical context and will be discussed in terms of beneficial effects in the dedicated section (*8.2.1 Anticatabolic effects in cartilage).*

Notably, pCM also exhibited a 3.6-fold increase in DHA, 1.4-fold in EPA, and 2.9-fold in AA. These ω-3 and ω-6 fatty acids are precursors to specialized pro-resolving mediators (SPMs) such as resolvins and lipoxins, which orchestrate inflammation resolution (148) To our knowledge, this is among the first reports quantifying lipidome shifts in cytokine-primed ASC secretome, underscoring lipids as a third functional axis alongside proteins and nucleic acids.

8.1.1.3 Regulatory implications

Tailoring CM through upstream manipulations—such as cytokine priming, hypoxic culture, or collection timing—enhances therapeutic potency but undoubtedly adds layers of complexity under Good Manufacturing Practice (GMP). Each added step requires validated protocols, qualified raw materials, and additional in-process controls to demonstrate product consistency (149). Harmonizing flexibility (customisable priming) with compliance (validated, reproducible workflows) will be a central translational challenge. For example, introduction of a 5-minute cytokine priming step would require qualification of cytokine source, endotoxin testing, and demonstration that residual priming agents are removed below acceptable limits, as it currently happens for cell-based therapies (150). These requirements prolong process validation, increase documentation burden, and escalate manufacturing costs. At the same time, regulatory frameworks demand rigid standardization to ensure safety and reproducibility. Agencies such as the FDA and EMA expect fixed, unchanging manufacturing flows once a product enters clinical trials. Any process change—from cell passage number to storage conditions—requires comparability studies and potentially new clinical data (151). This rigidity can conflict with the inherent flexibility needed to optimize CM for different indications or patient subgroups. Reconciling these opposing demands will require a modular approach to GMP: establishing a core, validated “platform” process for CM production, then defining controlled complementary modules (e.g., priming, freezing, concentration methods) with predefined acceptance criteria. By pre-approving these modules during development, one can maintain regulatory compliance while preserving the ability to tailor CM composition for specific therapeutic contexts.

8.1.1.4 Considerations for CM broad-scale administration

Considering ASC plasticity and CM vast production protocol modifications, a key question emerges: Can a “universal” CM serve all clinical needs, or must we embrace customizable protocols tailored to specific patient subgroups? A universal CM—a single, standardized product—offers clear advantages in terms of manufacturing simplicity, regulatory approval, and cost control. With one validated process, quality control parameters remain constant, comparability studies are minimized, and scale-up is straightforward. However, our data and broader MSC-

secretome literature highlight substantial biological heterogeneity. For example, a CM optimized for anti-inflammatory activity may underperform in contexts requiring angiogenesis or inflammation-induced tissue regeneration (152). By contrast, customizable CM protocols—incorporating specific priming regimens, collection timings, or concentration methods—enable the generation of indication-focused secretomes. In OA, our 5-min TNF+IL priming yielded an immunomodulatory profile ideally suited to modulate joint inflammation and cartilage catabolism. Beyond pathology tailored production, future considerations should encompass the possibility to implement a CM banking system, leveraging the fact that donor-matching is not required (23). The feasibility of a CM bank is further underscored by studies in which allogeneic CM—often derived from hypoimmunogenic sources such as umbilical-cord (153) or peripheral-blood MSCs—has been administered alongside, or directly compared to, autologous CM (NCT04876326). Indeed, in a rat model comparing allogeneic versus autologous secretome administration, the allogeneic CM showed no signs of toxicity, supporting its safety profile for off-the-shelf use (154). Finally, as reported by Foo JB, Looi QH, Chong PP, et al. in 2021 (155), there is a positive trend in clinical trials exploiting cell-free therapies, among which several with allogeneic CM (NCT04134676, NCT04314661), with 34, 35, 5 and 2 studies in phases I, II, III and IV, respectively.

8.1.2 Quality assessment

To perform a batch quality control (QC) some techniques can be applied. First of all, batch-to-batch consistency means that each production lot must reliably meet predefined compositional and functional benchmarks to guarantee predictable therapeutic effects. Based on our experience, we could define these benchmarks statistically: acceptance ranges could be set at mean ±SEM of total protein and EV particle count–that in our case falls between 64.4±6.2 μg/10^6 cells and 1.5 x10^9±1.5x10^8 particles/10^6 cells, respectively– and any outlier batch is flagged for further investigation. Using rapid Bradford and nanoparticle tracking assays (NTA) as first-pass screens allows us to detect outliers in production, with minimal CM volume. This approach is in line with recommendations from the EV field, where biophysical metrics serve as essential indicators before committing to more complex analyses (156). By integrating these early QC gates into our workflow, we ensure that only

batches likely to retain full potency advance to detailed functional testing, streamlining development and aligning with regulatory expectations for reproducibility in cell-derived therapeutics. Freezing steps, unavoidable in CM logistics, introduce compositional variability and potential loss of bioactive molecules. Our findings demonstrated a significant reduction in total protein content, specific factors such as IL-4 and VEGFA, and alteration in EV size distribution in CM cold stored before further processing. The MISEV guidelines addressed this issue, suggesting the addition of detailed manipulation passages and procedure to evaluate its effects on EV properties (156).

8.1.2.1 Raman spectroscopy for QC

Raman spectroscopy provides a rapid, label-free “molecular fingerprint” of CM that captures broad changes in proteins, lipids, and nucleic acids without targeting individual analytes (116). In our study, comparing fresh CM to thawed CM revealed a decrease in the amide I band (1,600–1,690 cm^{-1}) alongside an increase in lipid-associated peaks (2,800–3,040 cm^{-1}), and principal component analysis cleanly separated the two groups. Because Raman spectra reflect the ensemble of biomolecules, even subtle shifts—such as partial protein denaturation or vesicle membrane disruption—become immediately apparent (116,157). This global sensitivity makes Raman an ideal in-process QC tool: it requires only a few microliters of CM (~10µl) and may efficiently be employed to flags batches whose overall composition drifts outside established spectral tolerances, all without consuming precious material.

8.1.2.2 Potency assays based on intended effect

Potency assays that directly reflect CM’s intended therapeutic effects are essential for demonstrating batch quality and guiding clinical dosing. As an example, in our workflow we employ assays that measure CM efficacy in MMP activity, a well-known hallmark of OA pathology. The identification of informative potency assays depends on the pathology, but also on the attribution of a factor-effect causality that can correlate the presence –possibly also the concentration– of specific bioactive factors to a desired effect (158). However, as perfectly summarised by Sagaradze et al. (159), CM is neither a biological nor a cell-product –from a regulatory

stance– however existing guidelines for potency assay for such products can pave the way for CM own ones.

8.1.3 Establishing a QC framework

A robust QC framework for CM production should be structured in different escalating tiers. At the basic level, we monitor total protein content and EV particle number—fast, low-volume assays that flag major deviations in secretome composition. The intermediate level employs targeted multiplex assays (e.g., Luminex) to quantify a selected panel of cytokines and growth factors—IL-6, TIMP-1, VEGF-A—that directly reflect CM's mechanism of action. Finally, the advanced tier comprises effect-based potency assays—anti-catabolic MMP inhibition in cartilage explants and anti-inflammatory COX2/NO suppression in synovial tissue—that confirm each batch delivers its intended biological function. To ensure accuracy and comparability, every assay should include well-characterized internal standards (e.g. reference CM/pool) and positive controls (e.g. TIMP-1 for MMP activity or IL-10 for NO reduction). This layered approach maps directly onto regulatory expectations: agencies such as the FDA and EMA require demonstrated identity, purity, and potency for all biologics, making both analytical QC and functional potency assays mandatory for GMP compliance and clinical trial registration (160). Translating experimental tools into regulatory-approved assays will involve formal method qualification—establishing precision, accuracy, linearity, and robustness—followed by validation under cGMP conditions. By aligning each QC tier with clear acceptance criteria and documented validation plans, it is possible to bridge laboratory assays to the rigorous standards demanded for cell-derived therapeutics, ensuring CM products enter the clinic with proven safety, consistency, and efficacy. Inevitably, QC applies also to the donor cells. The current guidelines for human somatic cell therapy medicinal product require –at each passage– viability, identity, growth, activity and purity (161). Additionally, microbiological and viral-related assay are needed, if applicable. In a work from Perpiñá et al. (162) they establish a step-by-step quality control protocol, for the production of the master and working cell banks. Those two extremely important components were tested for viability, purity, morphology and microbiological sterility (as well as microbiological sterility of the process per se). Additionally, to determine the health state of the cells it would be preferable to assess their senescence –

especially in cases in which the final product is their secretome. Indeed, senescence induces the change in the secretory phenotype –namely, senescence associated secretory phenotype– that could bring unwanted functional alterations (163). Since the secretome characterisation is already part of the workflow, a good point to introduce could be the donor cell senescence evaluation, in order to define “safe expansion ranges” and avoid to further expand populations that are not promising. Several assays could serve this purpose, and it is safe to say that one may not suffice (164). The proliferation rate should always be monitored by carefully annotating the metrics relative to population doublings, doubling time, as well as adopting more complex methods (such as the evaluation of Ki67 and PCNA). Evaluating cell-cycle inhibitors and oxidative stress markers also provides important indicators of cellular senescence. Lysosomial alteration can be monitored by SA-β-galactosidase staining (165). Additional methods are DNA-related, such as telomere length evaluation and DNA damage quantification, or morphology-related. An example of the latter is the measurement of cells size, and in this field the use of AI is particularly promising since there are already studies reporting the automation of this process performed on clinical grade stem cells (166).

8.1.4 Dosing, route of administration, and formulation

Optimal dosing and delivery of CM remain key unknowns on the path to clinical application. Preclinical studies have yet to define the therapeutic window of secretome-based therapies. In the review of Giovannelli et al. (167), several cell-free clinical trials were considered, and each one was testing a different posology: concentration, number of doses, timing, route of administration. Concerning OA, the questions are: dose, local (intra-articular) or systemic administration, single or repeated doses. Furthermore, the formulation is also a crucial point. Formulation strategies such as freeze-drying CM with cryoprotectants (e.g., trehalose) could enable long-term storage and rapid on-site reconstitution (168), while hydrogel embedding (for example, hyaluronic acid or PEG-based matrices) can prolong intra-articular residence time, promote sustained release, and shield CM components from rapid clearance (169).

8.1.5 Ethical and safety concerns

As a biologic product derived from ASCs, CM raises critical ethical and safety considerations. Immunogenicity must be evaluated, even though CM lacks living cells, it contains above average physiological levels of immunomodulatory factors, that in exceeding doses can induce immunoparalysis and harm the receiving organism (170). Tumorigenicity is less of a concern for acellular products, yet cautious patient selection and long-term surveillance are needed to rule out unforeseen proliferative responses (171). Donor selection and screening protocols—mirroring blood or tissue donation—should include infectious disease testing (e.g., HIV, hepatitis), HLA profiling, and screening for oncogenic viruses. This as part of both operator and receiving patient safety. Comprehensive traceability and informed consent processes are essential to maintain transparency and public trust, as it happens for normal organ donation (172).

8.1.6 Xenofree production of CM: collaboration with REMEDI, University of Galway

The translation of CM into clinical practice begins with the production protocol. As extensively discussed before, the need to standardise CM production is a crucial aspect, ensuring a reproducible and comparable output even when manufactured across different laboratories. To align our protocol more closely with GMP-grade standards, I conducted a proof-of-concept batch production in the laboratory of Professor Frank Barry at the Regenerative Medicine Institute (REMEDI), University of Galway. The objective was to produce CM from human ASC under xenofree conditions, which are essential to eliminate the risks associated with animal-derived products, such as batch-to-batch variability, immunogenic contaminants, and potential transmission of pathogens. Working xenofree not only aligns with regulatory expectations for advanced therapeutic products but also ensures greater reproducibility, safety, and ethical acceptability of the final product. Furthermore, xenofree processes carry a lower environmental footprint, an increasingly relevant consideration for large-scale manufacturing. By improving sustainability and reducing dependency on costly animal-derived reagents, such protocols can also enhance scalability and economic attractiveness, ultimately making CM a more viable candidate for pharmaceutical development and industrial investment.

The ASCs were previously isolated and expanded within the Centre for Cell Manufacturing of Ireland (CCMI), in full compliance with GMP requirements. A

proprietary xenofree medium (WIPO: WO2015121471A1) was employed, available in two formulations: PurStem II for BMSC culture and PurStem III for ASC. These media support cell expansion by providing all essential factors. For CM production, cells were cultured using PurStem III until passage 5. Once confluent, and in accordance with our standard protocol, they underwent a 72-hour starvation period achieved by withdrawing xenofree supplementation from the standard medium. This xenofree formulation has already been validated for GMP-compliant production of EVs and secretome, where it successfully maintained cell phenotype and proliferation. Notably, the derived products have demonstrated protective and restorative effects in in vitro cartilage models (173,174). In future experiments, we will compare the features and efficacy of CM obtained from these cells with our standard preparations to identify common and unique features and assess the feasibility of xeno-free media for CM production.

8.2 Ex vivo models

8.2.1 Anti-catabolic effect in cartilage

The most promising and consistent results of CM were on MMP activity in cartilage. Cartilage degradation in OA is driven by a feed-forward loop of pro-inflammatory cytokines and matrix-degrading enzymes, most notably MMP-13 and ADAMTS5 (175). MMP-13 initiates collagen II cleavage at specific triple–helix sites, creating collagen fragments that are further degraded by other proteases (104), while ADAMTS5 cleaves aggrecan, leading to loss of cartilage hydration and biomechanical resilience (176). In our cartilage and osteochondral explant models, combined TNFα+IL-1β stimulation increased total MMP activity in a pathological way. This is confirmed by other studies, reporting how inflammatory cytokines induced a pro-catabolic and anti-chondrogenic OA-like environment (144). In CE and OCh models, CM (and pCM) treatment reduced MMP activity to levels of unstimulated controls, demonstrating robust suppression of the catabolic cascade. In the CESM co-culture, CM lowered MMP activity in supernatants to an extent similar to dexamethasone, confirming its protective effect against matrix degradation. When looking at transcriptional and translational regulation, however, differences emerged. In CE and OCh models, CM had only limited effects on MMP gene and protein expression. Differently, in CESM, CM significantly reduced MMP3 expression, consistently with

the results in van Buul et al work, where MSC secretome had a inhibiting effect on pro-catabolic genes (177). The discrepancy between CM effects on MMP activity and gene/protein expression suggest that CM mainly exerts a downstream modulation, compared to cytokines or dexamethasone, that respectively increase or decrease MMP activity by affecting these enzyme expression. This could represent an advantage for the use of CM. Dexamethasone for instance acts upstream through the glucocorticoid receptor (178). This regulation which is responsible for the well-known anti-inflammatory action also leads to significant drawbacks both at local (179) and systemic level (180). Mechanistically, CM's ability to inhibit MMPs may stems from coordinated actions of multiple secretome fractions. CM and, to an even greater extent, pCM, strongly inhibit cytokine-induced MMP activity in cartilage. Soluble TIMPs exert their inhibitory function directly binding to activated MMPs or by inhibiting their activation (181). Their high levels in CM/pCM undoubtedly contribute to this effect, but we have also quantified other MMP inhibitors—such as α-1-antitrypsin and α-2-macroglobulin (A2M)—that can take part in the process. A2M functions as a broad-spectrum "trap" for cartilage-degrading proteases—including MMPs and ADAMTS—attenuating OA progression in preclinical models (182), which offers a plausible contributor to the strong activity-level effects we observed. The presence of multiple, overlapping inhibitors likely initiates a redundant mechanism of MMP suppression. Moreover, there are data regarding also the transcriptional inhibition, performed by EV-associated miRNAs—such as miR-140 or miR-125b— that have been reported to downregulate MMP-13 and ADAMTS5 (183,184). Although our current dataset did not profile individual miRNAs, the functional outcomes can be due to a pleiotropic mode of action. Finally, defining the minimal TIMP concentration or miRNA signature is required for effective cartilage protection, as well as for potency assay development and dose optimization. Targeting MMPs –specifically MMP-13– is at the basis of several novel OA therapeutic approaches, exploiting monoclonal antibodies and inhibitors of this enzyme to establish a novel generation of disease-modifying OA drugs (DMOADs) (185,186). These results underscore CM's promise as one of them, considering that the ones currently in trial are aimed at restoring matrix homeostasis (187). In order to assess a real DMOAD effect by CM, studies are needed with longer timepoints addressing earlier stages and disease progression. To do so, it is necessary to start with the right model: explants tissue have shorter lifespan, therefore

they may not represent the best model for prolonged studies. However they retain native tissue characteristics, which lack in simpler models considered suitable for DMOADs investigation (188). In the future studies, it will be also necessary to further investigate the effects of CM on the expression of anabolic cartilage markers, which in our models resulted often reduced (similarly to dexamethasone), in order to determine whether this reflects feedback mechanisms or direct modifications induced by the treatments.

8.2.2 Overview of anti-inflammatory effect

Osteoarthritis is now understood to involve not only mechanical wear but also a chronic, low-grade inflammatory process that exacerbates joint damage and pain. Central to this inflammatory milieu are cytokines such as IL-1β, TNF-α, and IL-6: IL-1β and TNF-α activate synoviocytes and macrophages to produce matrix-degrading enzymes and inflammatory mediators (189), while IL-6 acts as a pro-inflammatory and pain-sensitizing factor, since it promotes both prostaglandin synthesis and nociceptor neuron sensitization (190). CM has an anti-inflammatory effect on synovial membrane and cartilage. In our settings, human synovial explants challenged with TNF-α+IL-1β, increased *PTGS2* and COX2 expression and nitric oxide output, reflecting synovitis-like conditions. A certain degree of *PTGS2* modulation, but more importantly at NO level, was present also in cartilage explants. Treatment with CM brought *PTGS2* levels down and reduced NO release, demonstrating robust suppression of key inflammatory pathways. Supernatant analyses in CESM however, revealed that while DEX strongly suppressed NO release, CM did not significantly affect this parameter. Gene expression further confirmed the anti-inflammatory potency of DEX, which reduced *PTGS2* and *IL1B* expression in both CE and SM. In contrast, CM did not decrease inflammatory gene expression. Taken together, these observations suggest that in this co-culture setting, CM lacks a robust and consistent anti-inflammatory effect compared to DEX, which has a homogenous effect independently from the inter-donor variability, both at transcriptional level as well as in terms of NO release. These data suggest CM activity may be context dependent, indeed in other settings, CM was able to strongly reduce NO levels (191). Beyond these readouts, Luminex profiling and proteomic studies of CM revealed above standard physiological concentrations of cytokines and chemokines. This broad cytokine content, suggests that CM could

modulate the inflammatory network at multiple nodes, rather than simply antagonizing a single target (192). These findings are consistent with a study that reports that MSC secretome inhibited the expression of pro-inflammatory cytokines, chemokines, and chemokine receptors in the LPS-stimulated macrophages, without toxicity drawbacks on them (86). Therefore, a hypothetical mechanism of action for the anti-inflammatory function of CM, should encompass gene and protein expression, as well as extracellular activity. Because synovitis is driven by complex interactions among immune cells, stromal cells, and cartilage, incorporating immune-competent models will be crucial to fully elucidate CM's mechanisms. Such approaches would clarify how CM's combination of soluble factors and EV-encapsulated ones orchestrates immune cell behaviour, informs dosing strategies, and predicts clinical efficacy in OA patients, whose joints present a complex immunological environment. More importantly, the CM mode of action should be compared with other anti-inflammatory drugs by evaluating the therapeutic trade-off between benefits—such as slowing disease progression and relieving symptoms—and risks, including systemic exposure associated with biological or conventional therapies. The only comparisons available are with other CM formulations, as in the Kalhor et al. work (193) were CM from three different cell sources –adipose tissue, bone marrow, and menstrual blood– was tested in an in vitro model of inflammatory bowel disease. Further, other studies investigate the CM against damages induced by approved pharmacological therapies. As an example, in the work of Xia et al. (194) the CM is investigated for NSAIDs-induced gastric ulcers repair using plain DMEM as the control; including a conventional therapeutic agent in their comparison would have better highlighted CM's relative efficacy. Lately, we have conducted comparison studies of CM anticatabolic and anti-inflammatory efficacy versus dexamethasone, in a co-culture model of cartilage and synovial membrane explants, starting from the previous model developed by Chan et al in 2022 (109).

8.2.3 Effects of bone metabolism

Although our osteochondral explant model did not reveal overt CM-induced changes in cartilage–bone crosstalk, a growing body of evidence supports CM's utility in bone regenerative medicine. In particular, adipose-derived MSC secretomes are rich in factors such as VEGF, HGF, IGF-1, OPG, and bone morphogenetic proteins (BMP-2, BMP-4) (195), which collectively regulate osteoblast proliferation,

differentiation, and mineralization via the RANKL–OPG axis and Wnt/β-catenin signalling pathways. For example, Soleimanifar et al. demonstrated that ASC-CM alone could induce osteogenic differentiation of human induced pluripotent stem cells on polycaprolactone scaffolds—promoting alkaline phosphatase activity, mineral deposition, and upregulation of RUNX2 and osteocalcin—at levels comparable to standard osteogenic media (196). Likewise, recent reviews highlight that MSC-CM enhances osteoblast activity, stimulates endothelial migration for neovascularization, and accelerates bone defect healing in animal models (197). In our own bone-turnover co-culture system, CM administration increased alkaline phosphatase activity while reducing osteocalcin release —consistent with enhanced osteoblastic matrix-deposition activity and delayed late-stage differentiation— and suppressed TRAP expression in osteoclast precursors, resulting in enhanced osteopontin expression and alizarin red S deposition. These findings underscore CM's multifaceted pro-matrix deposition and pro-mineralization functions and suggest its broader applicability not only in OA but also in reconstructive scenarios such as maxillofacial surgery, where balanced bone remodelling and angiogenesis are critical.

8.2.4 Usefulness of ex vivo model in precision medicine research

Human ex vivo explants derived directly from OA patients bridge the gap between simplified in vitro assays and complex in vivo models, offering a more clinically relevant platform, whilst maintaining species-specificity. By using native cartilage and synovial tissues, our explant studies preserve critical features—three-dimensional extracellular matrix organization, layered chondrocyte distribution—that standard monolayer cultures cannot replicate. These factors profoundly influence cell behaviour: for example, matrix stiffness and integrin signalling modulate MMP expression (198,199), and oxygen gradients within cartilage affect cytokine responses and NO release (200). As such, human explants capture the pathophysiological milieu of OA more faithfully than rodent or bovine systems, as discussed in the chapter "*4.5.2 In vivo models"*.

Despite these advantages, explant models have inherent limitations. First, most available tissues come from late-stage OA patients undergoing joint replacement, precluding assessment of CM's preventive or early-intervention potential (i.e. patients with KL grade 1-2). Specifically, in our studies, patients were diagnosed with a KL

grade 3 OA, therefore cartilage was preserved only in small area, not subjected to load pressure. This also intrinsically causes high levels of variability even within the same donor, as previously reported by Werner et al. (201). Second, healthy, non-arthritic control tissues are rarely accessible, making it difficult to define a true "baseline" response. Third, we observed considerable inter-donor variability in both MMP inhibition and NO suppression (ranging from significant reduction to almost null effect), possibly related to differences in patient age, disease severity, or other treatments that can confound data interpretation. Building from these data, it is possible to infer the existence of "responders" and "non-responders" explants to CM treatment. The definition of statistical thresholds in functional assay outputs along with donors characteristics –KL grades, comorbidities, supplementation, sex and age– can lay the basis for a scoring system to predict patient response to CM. Moreover, these hypothetical correlations should be investigated in a broad population, with verified data collection, ultimately to link explant outcomes with patient demographics and clinical features to identify predictive biomarkers of CM efficacy. In the long term, such an integrated approaches and QC-potency database could serve as a preclinical diagnostic tool, predicting individual patient responses to CM formulations. By assigning future trial participants to known responder groups based on reference explants or biomarker profiling, clinical studies could enhance efficacy readouts, reduce placebo exposure, and accelerate CM's path to clinical adoption as a personalized regenerative therapy.

8.3 Conclusive remarks and implications to ease therapeutic translation of CM

Together, our findings support a dual strategy for the clinical translation of CM—first, optimizing its efficacy through cell priming and, second, minimizing process-induced variability by rigorously standardizing all manufacturing steps—from precise documentation of cell passage number to controlled freeze–thaw cycles and concentration methods. CM offers distinct advantages over cellular therapies: it can be collected easily at scale, does not contain live cells, and thus avoids the safety and logistical hurdles of cell transplantation. However, CM composition is highly sensitive to upstream variables, so every passage and process detail must be recorded and controlled. Although priming can produce a more "powerful" CM enriched in cytokines, chemokines, and growth factors, excessive potency carries the risk of adverse

immune reactions, underscoring that more is not always better. Importantly, CM's therapeutic activity arises from a redundant, pleiotropic mechanism that could uncouples functional outcome from the level of a single component. In our ex vivo models, CM almost universally reduced MMP activity in cartilage tissues—although individual explants varied in their degree of response, the overall, statistically significant downward trend confirms CM's true anti-catabolic efficacy and validates MMP activity testing as a robust potency assay. Additionally, CM suppressed nitric oxide release and upstream inflammatory pathways in synovial tissues, underscoring its anti-inflammatory potential. Beyond joint applications, CM also promoted bone matrix deposition and mineralization in a co-culture system, suggesting utility in reconstructive fields such as maxillofacial surgery. While human explants provide physiologically relevant models, they exhibit significant inter- donor variability, reflecting patient age, disease stage, and prior treatments. Rather than view this variability as an obstacle, we propose harnessing it by linking donor demographics and functional assay readouts to identify "responder" phenotypes, enabling pre-stratification of patients in future clinical trials.

Further examination of the secretome's effects should focus on "dissecting" the contribution of its individual components to the overall biological activity. This step is critical for establishing an appropriate dosing strategy based on the intended therapeutic effect, including the identification of key active component(s) to support dose–response assessments. The same rationale—applied inversely—can be used to identify components that may pose safety concerns or elicit undesirable effects, thereby enabling the determination of a maximum safe dose that avoids introducing harmful concentrations of such molecules. The distinction between the soluble and vesicular fractions, in terms of their relative contribution to activity, is more challenging to establish. Isolation of EVs from the whole secretome is required, followed by comprehensive characterisation, including membrane and internal markers, nucleic acid content, and the associated protein corona. Moreover, experimental comparisons between the whole secretome, the isolated EV fraction, and an EV-depleted fraction will provide greater clarity on the specific therapeutic impact attributable to EVs. From a manufacturing and regulatory perspective, the introduction of additional isolation steps must be justified with robust scientific evidence, as such steps increase process complexity and may introduce risks already described (e.g., variability, manipulation,

and standardization challenges). Therefore, before selecting a whole secretome–based approach or an EV-only approach, several considerations must be addressed, including whether the whole secretome demonstrates equivalent or superior efficacy, and whether the isolated EV fraction confers advantages relevant to product consistency, standardization, or process feasibility. Ultimately, translating CM into a viable, personalized regenerative therapy will require multi-omics characterization, rigorous process control, and mechanism-driven functional assays in models that closely mirror human physiology, ensuring that every variable—from priming to delivery—is understood and controlled.

9. Acknowledgments

I am grateful to my tutor, co-tutor and supervisor for scientific guidance and constructive discussions throughout this work. I also thank my colleagues at Laboratory of Biotechnological Applications for their valuable assistance and collaboration. This work was supported by the PhD program in Experimental Medicine of the University of Milan; by IRCCS Istituto Ortopedico Galeazzi (Ricerca Corrente by the Italian Ministry of Health); and by the University of Milan, Department of Biomedical, Surgical and Dental Sciences.

10. References

1. Caplan AI. What's in a Name? Tissue Engineering Part A. 2010 Aug;16(8):2415–7.

2. Caplan AI. Mesenchymal Stem Cells: Time to Change the Name! Stem Cells Translational Medicine. 2017 June 1;6(6):1445–51.

3. Phinney DG, Prockop DJ. Concise Review: Mesenchymal Stem/Multipotent Stromal Cells: The State of Transdifferentiation and Modes of Tissue Repair—Current Views. Stem Cells. 2007 Nov 1;25(11):2896–902.

4. Friedenstein AJ, Chailakhjan RK, Lalykina KS. The development of fibroblast colonies in monolayer cultures of guinea-pig bone marrow and spleen cells. Cell Tissue Kinet. 1970 Oct;3(4):393–403.

5. Česnik AB, Švajger U. The issue of heterogeneity of MSC-based advanced therapy medicinal products–a review. Front Cell Dev Biol. 2024 July 26;12:1400347.

6. Zuk PA, Zhu M, Ashjian P, De Ugarte DA, Huang JI, Mizuno H, et al. Human Adipose Tissue Is a Source of Multipotent Stem Cells. Mol Biol Cell. 2002 Dec;13(12):4279–95.

7. Barry FP, Murphy JM. Mesenchymal stem cells: clinical applications and biological characterization. The International Journal of Biochemistry & Cell Biology. 2004 Apr 1;36(4):568–84.

8. Dominici M, Le Blanc K, Mueller I, Slaper-Cortenbach I, Marini FC, Krause DS, et al. Minimal criteria for defining multipotent mesenchymal stromal cells. The International Society for Cellular Therapy position statement. Cytotherapy. 2006 Jan 1;8(4):315–7.

9. Viswanathan S, Shi Y, Galipeau J, Krampera M, Leblanc K, Martin I, et al. Mesenchymal stem versus stromal cells: International Society for Cell & Gene Therapy (ISCT®) Mesenchymal Stromal Cell committee position statement on nomenclature. Cytotherapy. 2019 Oct;21(10):1019–24.

10. Maguire G. Stem cell therapy without the cells. Communicative & Integrative Biology. 2013 Nov 9;6(6):e26631.

11. Kadri N, Amu S, Iacobaeus E, Boberg E, Le Blanc K. Current perspectives on mesenchymal stromal cell therapy for graft versus host disease. Cell Mol Immunol. 2023 June;20(6):613–25.

12. Markovic BS, Kanjevac T, Harrell CR, Gazdic M, Fellabaum C, Arsenijevic N, et al. Molecular and Cellular Mechanisms Involved in Mesenchymal Stem Cell-Based Therapy of Inflammatory Bowel Diseases. Stem Cell Rev and Rep. 2018 Apr 1;14(2):153–65.

13. Wang D, Zhang H, Liang J, Li X, Feng X, Wang H, et al. Allogeneic Mesenchymal Stem Cell Transplantation in Severe and Refractory Systemic Lupus Erythematosus: 4 Years of Experience. Cell Transplant. 2013;22(12):2267–77.

14. Deszcz I. Stem Cell-Based Therapy and Cell-Free Therapy as an Alternative Approach for Cardiac Regeneration. Stem Cells International. 2023;2023(1):2729377.

15. Bowles-Welch AC, Jimenez AC, Stevens HY, Frey Rubio DA, Kippner LE, Yeago C, et al. Mesenchymal stromal cells for bone trauma, defects, and disease: Considerations for manufacturing, clinical translation, and effective treatments. Bone Reports. 2023 June 1;18:101656.

16. Le H, Xu W, Zhuang X, Chang F, Wang Y, Ding J. Mesenchymal stem cells for cartilage regeneration. J Tissue Eng. 2020 Aug 26;11:2041731420943839.

17. Caplan AI, Correa D. The MSC: An Injury Drugstore. Cell Stem Cell. 2011 July 8;9(1):11–5.

18. Gnecchi M, Danieli P, Malpasso G, Ciuffreda MC. Paracrine Mechanisms of Mesenchymal Stem Cells in Tissue Repair. In: Gnecchi M, editor. Mesenchymal Stem Cells: Methods and Protocols [Internet]. New York, NY: Springer; 2016 [cited 2025 Apr 29]. p. 123–46. Available from: https://doi.org/10.1007/978-1-4939-3584-0_7

19. Harrell CR, Fellabaum C, Jovicic N, Djonov V, Arsenijevic N, Volarevic V. Molecular Mechanisms Responsible for Therapeutic Potential of Mesenchymal Stem Cell-Derived Secretome. Cells. 2019 May 16;8(5):467.

20. Vizoso FJ, Eiro N, Cid S, Schneider J, Perez-Fernandez R. Mesenchymal Stem Cell Secretome: Toward Cell-Free Therapeutic Strategies in Regenerative Medicine. International Journal of Molecular Sciences. 2017 Sept;18(9):1852.

21. Chouw A, Facicilia G, Sartika CR, Faried A, Milanda T. Factors Influencing the Therapeutic Potential of the MSC-derived Secretome. Regen Eng Transl Med. 2022 Sept 1;8(3):384–93.

22. Rani S, Ryan AE, Griffin MD, Ritter T. Mesenchymal Stem Cell-derived Extracellular Vesicles: Toward Cell-free Therapeutic Applications. Molecular Therapy. 2015 May 1;23(5):812–23.

23. Gunawardena TNA, Rahman MT, Abdullah BJJ, Abu Kasim NH. Conditioned media derived from mesenchymal stem cell cultures: The next generation for regenerative medicine. J Tissue Eng Regen Med. 2019 Apr;13(4):569–86.

24. Flamant S, Loinard C, Tamarat R. MSC beneficial effects and limitations, and MSC-derived extracellular vesicles as a new cell-free therapy for tissue regeneration in irradiated condition. Environmental Advances. 2023 Oct 1;13:100408.

25. Noronha N de C, Mizukami A, Caliári-Oliveira C, Cominal JG, Rocha JLM, Covas DT, et al. Priming approaches to improve the efficacy of mesenchymal stromal cell-based therapies. Stem Cell Research & Therapy. 2019 May 2;10(1):131.

26. Giannasi C, Morte ED, Cadelano F, Valenza A, Casati S, Cas MD, et al. Boosting the therapeutic potential of cell secretome against osteoarthritis: Comparison of cytokine-based priming strategies. Biomedicine & pharmacotherapy = Biomedecine & pharmacotherapie [Internet]. 2024 Jan;170. Available from: https://pubmed.ncbi.nlm.nih.gov/38042116/

27. Fathi-Kazerooni M, Fattah-Ghazi S, Darzi M, Makarem J, Nasiri R, Salahshour F, et al. Safety and efficacy study of allogeneic human menstrual blood stromal cells secretome to treat severe COVID-19 patients: clinical trial phase I & II. Stem Cell Research & Therapy. 2022 Mar 7;13(1):96.

28. Rosochowicz MA, Lach MS, Richter M, Suchorska WM, Trzeciak T. Conditioned Medium – Is it an Undervalued Lab Waste with the Potential for Osteoarthritis Management? Stem Cell Rev and Rep. 2023 July 1;19(5):1185–213.

29. Chouaib B, Haack-Sørensen M, Chaubron F, Cuisinier F, Collart-Dutilleul PY. Towards the Standardization of Mesenchymal Stem Cell Secretome-Derived Product Manufacturing for Tissue Regeneration. Int J Mol Sci. 2023 Aug 9;24(16):12594.

30. Niada S, Giannasi C, Gualerzi A, Banfi G, Brini AT. Differential proteomic analysis predicts appropriate applications for the secretome of adipose-derived mesenchymal stem/stromal cells and dermal fibroblasts. Stem Cells International. 2018;2018.

31. Deng C, He Y, Feng J, Dong Z, Yao Y, Lu F. Conditioned medium from 3D culture system of stromal vascular fraction cells accelerates wound healing in diabetic rats. Regen Med. 2019 Oct;14(10):925–37.

32. Ernault AC, Verkerk AO, Bayer JD, Aras K, Montañés-Agudo P, Mohan RA, et al. Secretome of atrial epicardial adipose tissue facilitates reentrant arrhythmias by myocardial remodeling. Heart Rhythm. 2022 Sept 1;19(9):1461–70.

33. Margiana R, Markov A, Zekiy AO, Hamza MU, Al-Dabbagh KA, Al-Zubaidi SH, et al. Clinical application of mesenchymal stem cell in regenerative medicine: a narrative review. Stem Cell Research & Therapy. 2022 July 28;13(1):366.

34. Oikonomopoulos A, van Deen WK, Manansala AR, Lacey PN, Tomakili TA, Ziman A, et al. Optimization of human mesenchymal stem cell manufacturing: the effects of animal/xeno-free media. Sci Rep. 2015 Nov 13;5:16570.

35. Giannasi C, Niada S, Della Morte E, Casati SR, De Palma C, Brini AT. Serum starvation affects mitochondrial metabolism of adipose-derived stem/stromal cells. Cytotherapy. 2023 July;25(7):704–11.

36. Da Silva K, Kumar P, Choonara YE. The paradigm of stem cell secretome in tissue repair and regeneration: Present and future perspectives. Wound Repair and Regeneration. 2025;33(1):e13251.

37. Ferreira JR, Teixeira GQ, Santos SG, Barbosa MA, Almeida-Porada G, Gonçalves RM. Mesenchymal Stromal Cell Secretome: Influencing Therapeutic Potential by Cellular Pre-conditioning. Front Immunol. 2018 Dec 4;9:2837.

38. Cadelano F, Giannasi C, Gualerzi A, Gerli M, Niada S, Della Morte E, et al. Pre-Concentration Freezing Alters the Composition of Mesenchymal Stem/Stromal Cell-Conditioned Medium. Biology (Basel). 2025 Feb 10;14(2):181.

39. Caplan AI, Ricordi C. Improving the regulatory framework for cell therapy does not equate to deregulation. CellR4 Repair Replace Regen Reprogram. 2016;4(4):e2109.

40. Singh N, Choonara YE, Kumar P. Method standardization of secretome production, collection, and characterization: New insights and challenges. Regenerative Therapy. 2025 June 1;29:466–73.

41. Yoon J, Lee S, Kim MJ, Kim JH. Brief summary of the regulatory frameworks of regenerative medicine therapies. Front Pharmacol [Internet]. 2025 Jan 22 [cited 2025 June 9];15. Available from: https://www.frontiersin.org/journals/pharmacology/articles/10.3389/fphar.2024.1486812/full

42. Guideline on quality, non-clinical and clinical requirements for investigational advanced therapy medicinal products in clinical trials - Scientific guideline | European Medicines Agency (EMA) [Internet]. 2019 [cited 2025 May 18]. Available from: https://www.ema.europa.eu/en/guideline-quality-non-clinical-clinical-requirements-investigational-advanced-therapy-medicinal-products-clinical-trials-scientific-guideline

43. Iglesias-Lopez C, Agustí A, Obach M, Vallano A. Regulatory Framework for Advanced Therapy Medicinal Products in Europe and United States. Front Pharmacol. 2019 Aug 30;10:921.

44. Thauvin B, Olmos E, Madec E, Simon C, Branchu J, Chebil L. Bead to Bead Transfer, an Efficient Strategy to Scale-up the Mesenchymal Stromal Cells-Derived Secretome Bioproduction. Biotechnology and Bioengineering [Internet]. [cited 2025 Sept 5];n/a(n/a). Available from: https://onlinelibrary.wiley.com/doi/abs/10.1002/bit.70042

45. Tang S, Zhang C, Oo WM, Fu K, Risberg MA, Bierma-Zeinstra SM, et al. Osteoarthritis. Nat Rev Dis Primers. 2025 Feb 13;11(1):1–22.

46. Blewis ME, Nugent-Derfus GE, Schmidt TA, Schumacher BL, Sah RL. A model of synovial fluid lubricant composition in normal and injured joints. Eur Cell Mater. 2007 Mar 6;13:26–39.

47. Yue S, Zhai G, Zhao S, Liang X, Liu Y, zheng J, et al. The biphasic role of the infrapatellar fat pad in osteoarthritis. Biomedicine & Pharmacotherapy. 2024 Oct 1;179:117364.

48. Poole AR. Osteoarthritis as a Whole Joint Disease. HSS J. 2012 Feb;8(1):4–6.

49. Motta F, Barone E, Sica A, Selmi C. Inflammaging and Osteoarthritis. Clinic Rev Allerg Immunol. 2023 Apr 1;64(2):222–38.

50. Rezuș E, Cardoneanu A, Burlui A, Luca A, Codreanu C, Tamba BI, et al. The Link Between Inflammaging and Degenerative Joint Diseases. International Journal of Molecular Sciences. 2019 Jan;20(3):614.

51. Bruyère O, Cooper C, Pelletier JP, Maheu E, Rannou F, Branco J, et al. A consensus statement on the European Society for Clinical and Economic Aspects of Osteoporosis and Osteoarthritis (ESCEO) algorithm for the management of knee osteoarthritis—From evidence-based medicine to the real-life setting. Seminars in Arthritis and Rheumatism. 2016 Feb 1;45(4, Supplement):S3–11.

52. Gao Y, Zhang Y, Liu X. Rheumatoid arthritis: pathogenesis and therapeutic advances. MedComm. 2024;5(3):e509.

53. Wu D, Luo Y, Li T, Zhao X, Lv T, Fang G, et al. Systemic complications of rheumatoid arthritis: Focus on pathogenesis and treatment. Front Immunol. 2022 Dec 22;13:1051082.

54. Denniston AK, Gayed M, Carruthers D, Gordon C, Murray PI. Chapter 80 - Rheumatic Disease. In: Ryan SJ, Sadda SR, Hinton DR, Schachat AP, Sadda SR, Wilkinson CP, et al., editors. Retina (Fifth Edition) [Internet]. London: W.B. Saunders; 2013 [cited 2025 May 13]. p. 1415–40. Available from: https://www.sciencedirect.com/science/article/pii/B9781455707379000801

55. MSD Manual Professional Edition [Internet]. [cited 2025 May 13]. Evaluation of the Patient With Joint Symptoms - Musculoskeletal and Connective Tissue Disorders. Available from: https://www.msdmanuals.com/professional/musculoskeletal-and-connective-tissue-disorders/approach-to-the-patient-with-joint-symptoms/evaluation-of-the-patient-with-joint-symptoms

56. Kellgren JH, Lawrence JS. Radiological assessment of osteo-arthrosis. Ann Rheum Dis. 1957 Dec;16(4):494–502.

57. Braun HJ, Gold GE. Diagnosis of Osteoarthritis: Imaging. Bone. 2012 Aug;51(2):278–88.

58. Oliviero F, Mandell BF. Synovial fluid analysis: Relevance for daily clinical practice. Best Practice & Research Clinical Rheumatology. 2023 Mar 1;37(1):101848.

59. Deng M, Tang C, Yin L, Jiang Y, Huang Y, Feng Y, et al. Clinical and omics biomarkers in osteoarthritis diagnosis and treatment. J Orthop Translat. 2025 Jan 22;50:295–305.

60. Marot V, Murgier J, Carrozzo A, Reina N, Monaco E, Chiron P, et al. Determination of normal KOOS and WOMAC values in a healthy population. Knee Surg Sports Traumatol Arthrosc. 2019 Feb;27(2):541–8.

61. Rigoglou S, Papavassiliou AG. The NF-κB signalling pathway in osteoarthritis. Int J Biochem Cell Biol. 2013 Nov;45(11):2580–4.

62. Choi MC, Jo J, Park J, Kang HK, Park Y. NF-κB Signaling Pathways in Osteoarthritic Cartilage Destruction. Cells. 2019 July 17;8(7):734.

63. Ye Y, Zhou J. The protective activity of natural flavonoids against osteoarthritis by targeting NF-κB signaling pathway. Front Endocrinol (Lausanne). 2023 Mar 14;14:1117489.

64. Hong X, Liu X, Li B, Shi S, Xiao K, Xu T, et al. Glaucocalyxin A delays the progression of OA by inhibiting NF-κB and MAPK signaling pathways. Journal of Orthopaedic Surgery and Research. 2024 Mar 18;19(1):188.

65. Gill AK, McCormick PJ, Sochart D, Nalesso G. Wnt signalling in the articular cartilage: A matter of balance. International Journal of Experimental Pathology. 2023;104(2):56–63.

66. Zhou Y, Wang T, Hamilton JL, Chen D. Wnt/β-catenin Signaling in Osteoarthritis and in Other Forms of Arthritis. Curr Rheumatol Rep. 2017 Sept;19(9):53.

67. Zhai G, Doré J, Rahman P. TGF-β signal transduction pathways and osteoarthritis. Rheumatol Int. 2015 Aug 1;35(8):1283–92.

68. Mariani E, Pulsatelli L, Facchini A. Signaling Pathways in Cartilage Repair. International Journal of Molecular Sciences. 2014 May;15(5):8667–98.

69. Yao Q, Wu X, Tao C, Gong W, Chen M, Qu M, et al. Osteoarthritis: pathogenic signaling pathways and therapeutic targets. Sig Transduct Target Ther. 2023 Feb 3;8(1):1–31.

70. Guo P, Alhaskawi A, Adel Abdo Moqbel S, Pan Z. Recent development of mitochondrial metabolism and dysfunction in osteoarthritis. Front Pharmacol. 2025 Feb 13;16:1538662.

71. Miller RE, Scanzello CR, Malfait AM. An Emerging Role for Toll-like Receptors at the Neuroimmune Interface in Osteoarthritis. Semin Immunopathol. 2019 Sept;41(5):583–94.

72. Zhao Z, Li Y, Wang M, Zhao S, Zhao Z, Fang J. Mechanotransduction pathways in the regulation of cartilage chondrocyte homoeostasis. J Cell Mol Med. 2020 May;24(10):5408–19.

73. López-Otín C, Blasco MA, Partridge L, Serrano M, Kroemer G. Hallmarks of aging: An expanding universe. Cell. 2023 Jan 19;186(2):243–78.

74. Coryell PR, Diekman BO, Loeser RF. Mechanisms and therapeutic implications of cellular senescence in osteoarthritis. Nat Rev Rheumatol. 2021 Jan;17(1):47–57.

75. Oo WM, Hunter DJ. Repurposed and investigational disease-modifying drugs in osteoarthritis (DMOADs). Therapeutic Advances in Musculoskeletal. 2022 Jan 1;14:1759720X221090297.

76. Intra-articular Therapies for Knee Osteoarthritis: Current Update | Current Treatment Options in Rheumatology [Internet]. [cited 2025 May 15]. Available from: https://link.springer.com/article/10.1007/s40674-023-00207-x?utm_source=getftr&utm_medium=getftr&utm_campaign=getftr_pilot&getft_integrator=sciencedirect_contenthosting

77. Katz JN. Total joint replacement in osteoarthritis. Best Practice & Research Clinical Rheumatology. 2006 Feb 1;20(1):145–53.

78. Salmon JH, Rat AC, Achit H, Ngueyon-Sime W, Gard C, Guillemin F, et al. Health resource use and costs of symptomatic knee and/or hip osteoarthritis. Osteoarthritis and Cartilage. 2019 July 1;27(7):1011–7.

79. Brumat P, Kunšič O, Novak S, Slokar U, Pšenica J, Topolovec M, et al. The Surgical Treatment of Osteoarthritis. Life. 2022 July;12(7):982.

80. Blaga FN, Nutiu AS, Lupsa AO, Ghiurau NA, Vlad SV, Ghitea TC. Exploring Platelet-Rich Plasma Therapy for Knee Osteoarthritis: An In-Depth Analysis. Journal of Functional Biomaterials. 2024 Aug;15(8):221.

81. Boada-Pladellorens A, Avellanet M, Pages-Bolibar E, Veiga A. Stromal vascular fraction therapy for knee osteoarthritis: a systematic review. Ther Adv Musculoskelet Dis. 2022;14:1759720X221117879.

82. Keeling LE, Belk JW, Kraeutler MJ, Kallner AC, Lindsay A, McCarty EC, et al. Bone Marrow Aspirate Concentrate for the Treatment of Knee Osteoarthritis: A Systematic Review. Am J Sports Med. 2022 July;50(8):2315–23.

83. Yin H, Li M, Tian G, Ma Y, Ning C, Yan Z, et al. The role of extracellular vesicles in osteoarthritis treatment via microenvironment regulation. Biomaterials Research. 2022 Oct 5;26(1):52.

84. Yang H, Tian W, Wang S, Liu X, Wang Z, Hou L, et al. TSG-6 secreted by bone marrow mesenchymal stem cells attenuates intervertebral disc degeneration by inhibiting the TLR2/NF-κB signaling pathway. Laboratory Investigation. 2018 June 1;98(6):755–72.

85. Elkhenany HA, Linardi RL, Ortved KF. Differential modulation of inflammatory cytokines by recombinant IL-10 in IL-1β and TNF-α– stimulated equine chondrocytes and synoviocytes: impact of washing and timing on cytokine responses. BMC Veterinary Research. 2024 Dec 2;20(1):546.

86. Jin QH, Kim HK, Na JY, Jin C, Seon JK. Anti-inflammatory effects of mesenchymal stem cell-conditioned media inhibited macrophages activation in vitro. Sci Rep. 2022 Mar 19;12(1):4754.

87. Qi H, Liu DP, Xiao DW, Tian DC, Su YW, Jin SF. Exosomes derived from mesenchymal stem cells inhibit mitochondrial dysfunction-induced apoptosis of chondrocytes via p38, ERK, and Akt pathways. In Vitro Cell Dev Biol Anim. 2019 Mar;55(3):203–10.

88. González-González A, García-Sánchez D, Alfonso-Fernández A, Haider KH, Rodríguez-Rey JC, Pérez-Campo FM. Regenerative Medicine Applied to the Treatment of Musculoskeletal Pathologies. In: Haider KH, editor. Handbook of Stem Cell Therapy [Internet]. Singapore: Springer Nature; 2022 [cited 2025 May 21]. p. 1123–58. Available from: https://doi.org/10.1007/978-981-19-2655-6_50

89. Bartolotti I, Roseti L, Petretta M, Grigolo B, Desando G. A Roadmap of In Vitro Models in Osteoarthritis: A Focus on Their Biological Relevance in Regenerative Medicine. J Clin Med. 2021 Apr 28;10(9):1920.

90. Jung YK, Shin D, Park D, Kim J, Han S. Breakdown of the extracellular matrix recapitulates osteoarthritic phenotypes in 3d-hydrogel model: the validation of in vitro cell culture model of osteoarthritis. Osteoarthritis and Cartilage. 2020 Apr 1;28:S186.

91. Samvelyan HJ, Hughes D, Stevens C, Staines KA. Models of Osteoarthritis: Relevance and New Insights. Calcif Tissue Int. 2021 Sept;109(3):243–56.

92. Mirazi H, Wood ST. Microfluidic chip-based co-culture system for modeling human joint inflammation in osteoarthritis research. Front Pharmacol [Internet]. 2025 Apr 9 [cited 2025 June 12];16. Available from: https://www.frontiersin.org/journals/pharmacology/articles/10.3389/fphar.2025.1579228/full

93. Banh L, Cheung KK, Chan MWY, Young EWK, Viswanathan S. Advances in organ-on-a-chip systems for modelling joint tissue and osteoarthritic diseases. Osteoarthritis and Cartilage. 2022 Aug 1;30(8):1050–61.

94. Glasson SS, Blanchet TJ, Morris EA. The surgical destabilization of the medial meniscus (DMM) model of osteoarthritis in the 129/SvEv mouse. Osteoarthritis and Cartilage. 2007 Sept 1;15(9):1061–9.

95. Fang H, Huang L, Welch I, Norley C, Holdsworth DW, Beier F, et al. Early Changes of Articular Cartilage and Subchondral Bone in The DMM Mouse Model of Osteoarthritis. Sci Rep. 2018 Feb 12;8(1):2855.

96. Tawonsawatruk T, Sriwatananukulkit O, Himakhun W, Hemstapat W. Comparison of pain behaviour and osteoarthritis progression between anterior cruciate ligament transection and osteochondral injury in rat models. Bone Joint Res. 2018 May 5;7(3):244–51.

97. Pitcher T, Sousa-Valente J, Malcangio M. The Monoiodoacetate Model of Osteoarthritis Pain in the Mouse. J Vis Exp. 2016 May 16;(111):53746.

98. Kuyinu EL, Narayanan G, Nair LS, Laurencin CT. Animal models of osteoarthritis: classification, update, and measurement of outcomes. Journal of Orthopaedic Surgery and Research. 2016 Feb 2;11(1):19.

99. Helminen HJ, Säämänen A -M., Salminen H, Hyttinen MM. Transgenic mouse models for studying the role of cartilage macromolecules in osteoarthritis. Rheumatology. 2002 Aug 1;41(8):848–56.

100. Christiansen BA, Guilak F, Lockwood KA, Olson SA, Pitsillides AA, Sandell LJ, et al. Non-invasive mouse models of post-traumatic osteoarthritis. Osteoarthritis and Cartilage. 2015 Oct 1;23(10):1627–38.

101. Little CB, Hunter DJ. Post-traumatic osteoarthritis: from mouse models to clinical trials. Nat Rev Rheumatol. 2013 Aug;9(8):485–97.

102. Gregory MH, Capito N, Kuroki K, Stoker AM, Cook JL, Sherman SL. A review of translational animal models for knee osteoarthritis. Arthritis. 2012;2012:764621.

103. Bapat S, Hubbard D, Munjal A, Hunter M, Fulzele S. Pros and cons of mouse models for studying osteoarthritis. Clin Transl Med. 2018 Nov 21;7:36.

104. Loeser RF, Goldring SR, Scanzello CR, Goldring MB. Osteoarthritis: a disease of the joint as an organ. Arthritis and rheumatism. 2012 June;64(6):1697–707.

105. Makris EA, Hadidi P, Athanasiou KA. The knee meniscus: Structure–function, pathophysiology, current repair techniques, and prospects for regeneration. Biomaterials. 2011 Oct 1;32(30):7411–31.

106. Liebers N, Bruch PM, Terzer T, Hernandez-Hernandez M, Paramasivam N, Fitzgerald D, et al. Ex vivo drug response profiling for response and outcome prediction in hematologic malignancies: the prospective non-interventional SMARTrial. Nat Cancer. 2023 Dec;4(12):1648–59.

107. Thorel L, Divoux J, Lequesne J, Babin G, Morice PM, Florent R, et al. The OVAREX study: Establishment of ex vivo ovarian cancer models to validate innovative therapies and to identify predictive biomarkers. BMC Cancer. 2024 June 7;24(1):701.

108. Genestra MAF, Rosselló MA, Munar GR, Calvo J, Gayà A, Monjo M, et al. Comparative effect of platelet- and mesenchymal stromal cell-derived extracellular vesicles on human cartilage explants using an ex vivo inflammatory osteoarthritis model. Bone & joint research. 2023 Oct;12(10):667–76.

109. Chan MWY, Gomez-Aristizábal A, Mahomed N, Gandhi R, Viswanathan S. A tool for evaluating novel osteoarthritis therapies using multivariate analyses of human cartilage-synovium explant co-culture. Osteoarthritis and Cartilage. 2022 Jan 1;30(1):147–59.

110. Giannasi C, Mangiavini L, Niada S, Colombo A, Della Morte E, Vismara V, et al. Human Osteochondral Explants as an Ex Vivo Model of Osteoarthritis for the Assessment of a Novel Class of Orthobiologics. Pharmaceutics. 2022 June;14(6):1231.

111. Siefen T, Lokhnauth J, Liang A, Larsen CC, Lamprecht A. An *ex-vivo* model for transsynovial drug permeation of intraarticular injectables in naive and arthritic synovium. Journal of Controlled Release. 2021 Apr 10;332:581–91.

112. Casati S, Giannasi C, Minoli M, Niada S, Ravelli A, Angeli I, et al. Quantitative Lipidomic Analysis of Osteosarcoma Cell-Derived Products by UHPLC-MS/MS. Biomolecules. 2020 Sept;10(9):1302.

113. Morano C, Zulueta A, Caretti A, Roda G, Paroni R, Dei Cas M. An Update on Sphingolipidomics: Is Something Still Missing? Some Considerations on the Analysis of Complex Sphingolipids and Free-Sphingoid Bases in Plasma and Red Blood Cells. Metabolites. 2022 May;12(5):450.

114. Dei Cas M, Paroni R, Saccardo A, Casagni E, Arnoldi S, Gambaro V, et al. A straightforward LC-MS/MS analysis to study serum profile of short and medium chain fatty acids. Journal of Chromatography B. 2020 Oct 1;1154:121982.

115. Gualerzi A, Niada S, Giannasi C, Picciolini S, Morasso C, Vanna R, et al. Raman spectroscopy uncovers biochemical tissue-related features of extracellular vesicles from mesenchymal stromal cells. Scientific Reports. 2017 Dec;7(1).

116. Gualerzi A, Kooijmans SAA, Niada S, Picciolini S, Brini AT, Camussi G, et al. Raman spectroscopy as a quick tool to assess purity of extracellular vesicle preparations and predict their functionality. Journal of Extracellular Vesicles. 2019 Jan;8(1).

117. Della Morte E, Notarangelo MP, Niada S, Giannasi C, Fortuna F, Cadelano F, et al. Adipose-Derived Stromal Cell Conditioned Medium on Bone Remodeling: Insights from a 3D Osteoblast-Osteoclast Co-Culture Model. Calcif Tissue Int. 2025 Jan 7;116(1):26.

118. Willett NJ, Thote T, Lin ASP, Moran S, Raji Y, Sridaran S, et al. Intra-articular injection of micronized dehydrated human amnion/chorion membrane attenuates osteoarthritis development. Arthritis Res Ther. 2014 Feb 6;16(1):R47.

119. Sengupta V, Sengupta S, Lazo A, Woods P, Nolan A, Bremer N. Exosomes Derived from Bone Marrow Mesenchymal Stem Cells as Treatment for Severe COVID-19. Stem Cells Dev. 2020 June 15;29(12):747–54.

120. Bunnell BA. Adipose Tissue-Derived Mesenchymal Stem Cells. Cells. 2021 Dec;10(12):3433.

121. Oedayrajsingh-Varma MJ, van Ham SM, Knippenberg M, Helder MN, Klein-Nulend J, Schouten TE, et al. Adipose tissue-derived mesenchymal stem cell yield and growth characteristics are affected by the tissue-harvesting procedure. Cytotherapy. 2006 Jan 1;8(2):166–77.

122. Aust L, Devlin B, Foster SJ, Halvorsen YDC, Hicok K, du Laney T, et al. Yield of human adipose-derived adult stem cells from liposuction aspirates. Cytotherapy. 2004 Jan 1;6(1):7–14.

123. Zhao AG, Shah K, Freitag J, Cromer B, Sumer H. Differentiation Potential of Early- and Late-Passage Adipose-Derived Mesenchymal Stem Cells Cultured under Hypoxia and Normoxia. Stem Cells International. 2020;2020(1):8898221.

124. McGrath M, Tam E, Sladkova M, AlManaie A, Zimmer M, de Peppo GM. GMP-compatible and xeno-free cultivation of mesenchymal progenitors derived from human-induced pluripotent stem cells. Stem Cell Res Ther. 2019 Jan 11;10(1):11.

125. Atashi F, Serre-Beinier V, Nayernia Z, Pittet B, Modarressi A. Platelet Rich Plasma Promotes Proliferation of Adipose Derived Mesenchymal Stem Cells via Activation of AKT and Smad2 Signaling Pathways. Journal of Stem Cell Research & Therapy. 2015 Jan 1;05.

126. Mastrolia I, Foppiani EM, Murgia A, Candini O, Samarelli AV, Grisendi G, et al. Challenges in Clinical Development of Mesenchymal Stromal/Stem Cells: Concise Review. Stem Cells Transl Med. 2019 July 16;8(11):1135–48.

127. Fraser JK, Wulur I, Alfonso Z, Hedrick MH. Fat tissue: an underappreciated source of stem cells for biotechnology. Trends in Biotechnology. 2006 Apr 1;24(4):150–4.

128. Kuhbier JW, Weyand B, Radtke C, Vogt PM, Kasper C, Reimers K. Isolation, Characterization, Differentiation, and Application of Adipose-Derived Stem Cells. In: Kasper C, van Griensven M, Pörtner R, editors. Bioreactor Systems for Tissue Engineering II: Strategies for the Expansion and Directed Differentiation of Stem Cells [Internet]. Berlin, Heidelberg: Springer; 2010 [cited 2025 July 13]. p. 55–105. Available from: https://doi.org/10.1007/10_2009_24

129. Melocchi A, Schmittlein B, Sadhu S, Nayak S, Lares A, Uboldi M, et al. Automated manufacturing of cell therapies. Journal of Controlled Release. 2025 May 10;381:113561.

130. Trotzier C, Bellanger C, Abdessadeq H, Delannoy P, Mojallal A, Auxenfans C. Deciphering influence of donor age on adipose-derived stem cells: in vitro paracrine function and angiogenic potential. Sci Rep. 2024 Nov 11;14(1):27589.

131. Pinheiro-Machado E, Getova VE, Harmsen MC, Burgess JK, Smink AM. Towards standardization of human adipose-derived stromal cells secretomes. Stem Cell Rev and Rep. 2023 Oct 1;19(7):2131–40.

132. Giannasi C, Niada S, Della Morte E, Casati S, Orioli M, Gualerzi A, et al. Towards Secretome Standardization: Identifying Key Ingredients of MSC-Derived Therapeutic Cocktail. Stem Cells Int. 2021;2021:3086122.

133. Hansmann J, Groeber F, Kahlig A, Kleinhans C, Walles H. Bioreactors in tissue engineering—principles, applications and commercial constraints. Biotechnology Journal. 2013;8(3):298–307.

134. Elsayed A, Jaber N, Al-Remawi M, Abu-Salah K. From cell factories to patients: Stability challenges in biopharmaceuticals manufacturing and administration with mitigation strategies. Int J Pharm. 2023 Oct 15;645:123360.

135. Mehta SB, Subramanian S, D'Mello R, Brisbane C, Roy S. Effect of protein cryoconcentration and processing conditions on kinetics of dimer formation for a monoclonal antibody: A case study on bioprocessing. Biotechnology Progress. 2019 July;35(4).

136. Maroto R, Zhao Y, Jamaluddin M, Popov VL, Wang H, Kalubowilage M, et al. Effects of storage temperature on airway exosome integrity for diagnostic and functional analyses. Journal of Extracellular Vesicles. 2017 Dec;6(1).

137. Kusuma GD, Barabadi M, Tan JL, Morton DAV, Frith JE, Lim R. To Protect and to Preserve: Novel Preservation Strategies for Extracellular Vesicles. Front Pharmacol [Internet]. 2018 Oct 29 [cited 2025 July 12];9. Available from: https://www.frontiersin.org/journals/pharmacology/articles/10.3389/fphar.2018.01199/full

138. Witwer KW, Buzás EI, Bemis LT, Bora A, Lässer C, Lötvall J, et al. Standardization of sample collection, isolation and analysis methods in extracellular vesicle research. J Extracell Vesicles. 2013;2.

139. Welsh JA, Goberdhan DCI, O'Driscoll L, Buzas EI, Blenkiron C, Bussolati B, et al. Minimal information for studies of extracellular vesicles (MISEV2023): From basic to advanced approaches. J Extracell Vesicles. 2024 Feb;13(2):e12404.

140. Seo Y, Shin TH, Kim HS. Current Strategies to Enhance Adipose Stem Cell Function: An Update. Int J Mol Sci. 2019 Aug 5;20(15):3827.

141. Wang Y, Chen X, Cao W, Shi Y. Plasticity of mesenchymal stem cells in immunomodulation: pathological and therapeutic implications. Nat Immunol. 2014 Nov;15(11):1009–16.

142. Mahmoud M, Abdel-Rasheed M, Galal ER, El-Awady RR. Factors Defining Human Adipose Stem/Stromal Cell Immunomodulation in Vitro. Stem Cell Rev Rep. 2024;20(1):175–205.

143. Cuerquis J, Romieu-Mourez R, François M, Routy JP, Young YK, Zhao J, et al. Human mesenchymal stromal cells transiently increase cytokine production by activated T cells before suppressing T-cell proliferation: effect of interferon-γ and tumor necrosis factor-α stimulation. Cytotherapy. 2014 Feb;16(2):191–202.

144. Domenis R, Cifù A, Quaglia S, Pistis C, Moretti M, Vicario A, et al. Pro inflammatory stimuli enhance the immunosuppressive functions of adipose mesenchymal stem cells-derived exosomes. Sci Rep. 2018 Sept 6;8:13325.

145. Madrigal M, Rao KS, Riordan NH. A review of therapeutic effects of mesenchymal stem cell secretions and induction of secretory modification by different culture methods. J Transl Med. 2014 Oct 11;12:260.

146. Calligaris M, Zito G, Busà R, Bulati M, Iannolo G, Gallo A, et al. Proteomic analysis and functional validation reveal distinct therapeutic capabilities related to priming of mesenchymal stromal/stem cells with IFN-γ and hypoxia: potential implications for their clinical use. Front Cell Dev Biol [Internet]. 2024 May 31 [cited 2025 July 10];12. Available from: https://www.frontiersin.org/journals/cell-and-developmental-biology/articles/10.3389/fcell.2024.1385712/full

147. Jammes M, Contentin R, Audigié F, Cassé F, Galéra P. Effect of pro-inflammatory cytokine priming and storage temperature of the mesenchymal stromal cell (MSC) secretome on equine articular chondrocytes. Frontiers in Bioengineering and Biotechnology [Internet]. 2023 Aug 31 [cited 2023 Sept 11];11. Available from: https://discovery.researcher.life/article/effect-of-pro-inflammatory-cytokine-priming-and-storage-temperature-of-the-mesenchymal-stromal-cell-msc-secretome-on-equine-articular-chondrocytes/283357f62020393ebd9a58c6c85556fb

148. Serhan CN, Chiang N, Dalli J. The resolution code of acute inflammation: Novel pro-resolving lipid mediators in resolution. Semin Immunol. 2015 May;27(3):200–15.

149. EudraLex - Volume 4 - European Commission [Internet]. 2025 [cited 2025 July 12]. Available from: https://health.ec.europa.eu/medicinal-products/eudralex/eudralex-volume-4_en

150. Human cell-based medicinal products - Scientific guideline | European Medicines Agency (EMA) [Internet]. 2008 [cited 2025 July 12]. Available from: https://www.ema.europa.eu/en/human-cell-based-medicinal-products-scientific-guideline

151. Wixmerten A, Miot S, Bittorf P, Wolf F, Feliciano S, Hackenberg S, et al. Good Manufacturing Practice-compliant change of raw material in the manufacturing process of a clinically used advanced therapy medicinal product-a comparability study. Cytotherapy. 2023 May;25(5):548–58.

152. Gao M, Guo H, Dong X, Wang Z, Yang Z, Shang Q, et al. Regulation of inflammation during wound healing: the function of mesenchymal stem cells and strategies for therapeutic enhancement. Front Pharmacol [Internet]. 2024 Feb 15 [cited 2025 July 12];15. Available from: https://www.frontiersin.org/journals/pharmacology/articles/10.3389/fphar.2024.1345779/full

153. Lee M, Jeong SY, Ha J, Kim M, Jin HJ, Kwon SJ, et al. Low immunogenicity of allogeneic human umbilical cord blood-derived mesenchymal stem cells in vitro and in vivo. Biochem Biophys Res Commun. 2014 Apr 18;446(4):983–9.

154. Wuschko S, Gugerell A, Chabicovsky M, Hofbauer H, Laggner M, Erb M, et al. Toxicological testing of allogeneic secretome derived from peripheral mononuclear cells (APOSEC): a novel cell-free therapeutic agent in skin disease. Sci Rep. 2019 Apr 3;9(1):5598.

155. Foo JB, Looi QH, Chong PP, Hassan NH, Yeo GEC, Ng CY, et al. Comparing the Therapeutic Potential of Stem Cells and their Secretory Products in Regenerative Medicine. Stem Cells Int. 2021;2021:2616807.

156. Théry C, Witwer KW, Aikawa E, Alcaraz MJ, Anderson JD, Andriantsitohaina R, et al. Minimal information for studies of extracellular vesicles 2018 (MISEV2018): a position statement of the International Society for Extracellular Vesicles and update of the MISEV2014 guidelines. Journal of Extracellular Vesicles. 2018 Dec 1;7(1):1535750.

157. Chandra A, Kumar V, Garnaik UC, Dada R, Qamar I, Goel VK, et al. Unveiling the Molecular Secrets: A Comprehensive Review of Raman Spectroscopy in Biological Research. ACS Omega. 2024 Dec 24;9(51):50049–63.

158. Gimona M, Brizzi MF, Choo ABH, Dominici M, Davidson SM, Grillari J, et al. Critical considerations for the development of potency tests for therapeutic applications of mesenchymal stromal cell-derived small extracellular vesicles. Cytotherapy. 2021 May;23(5):373–80.

159. Sagaradze G, Monakova A, Efimenko A. Potency Assays for Mesenchymal Stromal Cell Secretome-Based Products for Tissue Regeneration. International Journal of Molecular Sciences. 2023 Jan;24(11):9379.

160. Salmikangas P, Carlsson B, Klumb C, Reimer T, Thirstrup S. Potency testing of cell and gene therapy products. Front Med (Lausanne). 2023 May 5;10:1190016.

161. New guidelines on good manufacturing practices for advanced therapies | European Medicines Agency (EMA) [Internet]. 2017 [cited 2025 Nov 21]. Available from: https://www.ema.europa.eu/en/news/new-guidelines-good-manufacturing-practices-advanced-therapies

162. Perpiñá U, Herranz C, Martín-Ibáñez R, Boronat A, Chiappe F, Monforte V, et al. Cell Banking of HEK293T cell line for clinical-grade lentiviral particles manufacturing. Translational Medicine Communications. 2020 Nov 19;5(1):22.

163. Alves-Paiva RM, Nascimento S do, De Oliveira D, Coa L, Alvarez K, Hamerschlak N, et al. Senescence State in Mesenchymal Stem Cells at Low Passages: Implications in Clinical Use. Front Cell Dev Biol [Internet]. 2022 Apr 4 [cited 2025 Nov 21];10. Available from: https://www.frontiersin.org/journals/cell-and-developmental-biology/articles/10.3389/fcell.2022.858996/full

164. González-Gualda E, Baker AG, Fruk L, Muñoz-Espín D. A guide to assessing cellular senescence in vitro and in vivo. FEBS J. 2021 Jan;288(1):56–80.

165. Valieva Y, Ivanova E, Fayzullin A, Kurkov A, Igrunkova A. Senescence-Associated β-Galactosidase Detection in Pathology. Diagnostics (Basel). 2022 Sept 25;12(10):2309.

166. Oja S, Komulainen P, Penttilä A, Nystedt J, Korhonen M. Automated image analysis detects aging in clinical-grade mesenchymal stromal cell cultures. Stem Cell Res Ther. 2018 Jan 10;9(1):6.

167. Giovannelli L, Bari E, Jommi C, Tartara F, Armocida D, Garbossa D, et al. Mesenchymal stem cell secretome and extracellular vesicles for neurodegenerative diseases: Risk-benefit profile and next steps for the market access. Bioactive Materials. 2023 Nov 1;29:16–35.

168. Berni P, Del Bue M, Conti V, Andreoli V, Ramoni R, Angelone M, et al. Clinical evaluation of freeze-dried secretome (lyosecretome) for osteoarthritis: a controlled trial in dogs and preliminary safety assessment in horses. International Journal of Pharmaceutics. 2025 Aug 20;681:125864.

169. Hashemi A, Ezati M, Nasr MP, Zumberg I, Provaznik V. Extracellular Vesicles and Hydrogels: An Innovative Approach to Tissue Regeneration. ACS Omega. 2024 Feb 13;9(6):6184–218.

170. Sari MI, Jusuf NK, Munir D, Putra A, Bisri T, Ilyas S, et al. The Role of Mesenchymal Stem Cell Secretome in the Inflammatory Mediators and the Survival Rate of Rat Model of Sepsis. Biomedicines. 2023 Aug 21;11(8):2325.

171. Zimmerlin L, Park TS, Zambidis ET, Donnenberg VS, Donnenberg AD. Mesenchymal stem cell secretome and regenerative therapy after cancer. Biochimie. 2013 Dec;95(12):2235–45.

172. Panigrahi RR, Mukherjee S, Shaikh ZH, Nomran NM. Leveraging Blockchain for Transparency: A Study on Organ Supply Chains and Transplant Processes. Logistics. 2025 Mar;9(1):9.

173. Palamà MEF, Coco S, Shaw GM, Reverberi D, Ghelardoni M, Ostano P, et al. Xeno-free cultured mesenchymal stromal cells release extracellular vesicles with a “therapeutic” miRNA cargo ameliorating cartilage inflammation in vitro. Theranostics. 2023;13(5):1470–89.

174. Palamà MEF, Shaw GM, Carluccio S, Reverberi D, Sercia L, Persano L, et al. The Secretome Derived From Mesenchymal Stromal Cells Cultured in a Xeno-Free Medium Promotes Human Cartilage Recovery in vitro. Front Bioeng Biotechnol [Internet]. 2020 Feb 14 [cited 2025 Sept 2];8. Available from: https://www.frontiersin.org/journals/bioengineering-and-biotechnology/articles/10.3389/fbioe.2020.00090/full

175. Mehana ESE, Khafaga AF, El-Blehi SS. The role of matrix metalloproteinases in osteoarthritis pathogenesis: An updated review. Life Sciences. 2019 Oct 1;234:116786.

176. Glasson SS, Askew R, Sheppard B, Carito B, Blanchet T, Ma HL, et al. Deletion of active ADAMTS5 prevents cartilage degradation in a murine model of osteoarthritis. Nature. 2005 Mar 31;434(7033):644–8.

177. Buul GM van, Villafuertes E, Bos PK, Waarsing JH, Kops N, Narcisi R, et al. Mesenchymal stem cells secrete factors that inhibit inflammatory processes in short-term osteoarthritic synovium and cartilage explant culture. Osteoarthritis and Cartilage. 2012 Oct 1;20(10):1186–96.

178. Black RM, Flaman LL, Lindblom K, Chubinskaya S, Grodzinsky AJ, Önnerfjord P. Tissue catabolism and donor-specific dexamethasone response in a human osteochondral model of post-traumatic osteoarthritis. Arthritis Research & Therapy. 2022 June 10;24(1):137.

179. Pirri C, Sorbino A, Manocchio N, Pirri N, Devito A, Foti C, et al. Chondrotoxicity of Intra-Articular Injection Treatment: A Scoping Review. International Journal of Molecular Sciences. 2024 Jan;25(13):7010.

180. Tavares LCP, Caetano L de VN, Ianhez M. Side effects of chronic systemic glucocorticoid therapy: what dermatologists should know. Anais Brasileiros de Dermatologia. 2024 Mar 1;99(2):259–68.

181. Arpino V, Brock M, Gill SE. The role of TIMPs in regulation of extracellular matrix proteolysis. Matrix Biology. 2015 May 1;44–46:247–54.

182. Wang S, Wei X, Zhou J, Zhang J, Li K, Chen Q, et al. Identification of α2-macroglobulin as a master inhibitor of cartilage-degrading factors that attenuates the progression of posttraumatic osteoarthritis. Arthritis Rheumatol. 2014 July;66(7):1843–53.

183. Lara-Barba E, Araya MJ, Hill CN, Bustamante-Barrientos FA, Ortloff A, García C, et al. Role of microRNA Shuttled in Small Extracellular Vesicles Derived From Mesenchymal Stem/Stromal Cells for Osteoarticular Disease Treatment. Front Immunol. 2021 Nov 1;12:768771.

184. Hoshi H, Akagi R, Yamaguchi S, Muramatsu Y, Akatsu Y, Yamamoto Y, et al. Effect of inhibiting MMP13 and ADAMTS5 by intra-articular injection of small interfering RNA in a surgically induced osteoarthritis model of mice. Cell Tissue Res. 2017 May;368(2):379–87.

185. Hu Q, Ecker M. Overview of MMP-13 as a Promising Target for the Treatment of Osteoarthritis. Int J Mol Sci. 2021 Feb 9;22(4):1742.

186. Zheng S, Hunter DJ, Xu J, Ding C. Monoclonal antibodies for the treatment of osteoarthritis. Expert Opinion on Biological Therapy. 2016 Dec 1;16(12):1529–40.

187. Cho Y, Jeong S, Kim H, Kang D, Lee J, Kang SB, et al. Disease-modifying therapeutic strategies in osteoarthritis: current status and future directions. Exp Mol Med. 2021 Nov;53(11):1689–96.

188. Makarczyk MJ, Gao Q, He Y, Li Z, Gold MS, Hochberg MC, et al. Current Models for Development of Disease-Modifying Osteoarthritis Drugs. Tissue Eng Part C Methods. 2021 Feb 1;27(2):124–38.

189. Arango Duque G, Descoteaux A. Macrophage Cytokines: Involvement in Immunity and Infectious Diseases. Front Immunol [Internet]. 2014 Oct 7 [cited 2025 July 13];5. Available from: https://www.frontiersin.org/journals/immunology/articles/10.3389/fimmu.2014.00491/full

190. Pinho-Ribeiro FA, Verri WA, Chiu IM. Nociceptor Sensory Neuron-Immune Interactions in Pain and Inflammation. Trends Immunol. 2017 Jan;38(1):5–19.

191. Simental-Mendía M, Lozano-Sepúlveda SA, Pérez-Silos V, Fuentes-Mera L, Martínez-Rodríguez HG, Acosta-Olivo CA, et al. Anti-inflammatory and anti-catabolic effect of non-animal stabilized hyaluronic acid and mesenchymal stem cell-conditioned medium in an osteoarthritis coculture model. Mol Med Rep. 2020 May;21(5):2243–50.

192. Yano F, Takeda T, Kurokawa T, Tsubaki T, Chijimatsu R, Inoue K, et al. Effects of conditioned medium obtained from human adipose-derived stem cells on skin inflammation. Regenerative Therapy. 2022 June 1;20:72–7.

193. Kalhor N, Fazaeli H, Asl FD, Sheikholeslami A, Hoseini SJE, Sheykhhasan M. A Comparative Study on the Effects of Mesenchymal Stem Cells and Their Conditioned Medium on Caco-2 Cells as an In Vitro Model for Inflammatory Bowel Disease. International Journal of Cell Biology. 2024;2024(1):1022338.

194. Xia X, Chan KF, Wong GTY, Wang P, Liu L, Yeung BPM, et al. Mesenchymal stem cells promote healing of nonsteroidal anti-inflammatory drug-related peptic ulcer through paracrine actions in pigs. Science Translational Medicine. 2019 Oct 30;11(516):eaat7455.

195. Giannasi C, Cadelano F, Della Morte E, Baserga C, Mazzucato C, Niada S, et al. Unlocking the Therapeutic Potential of Adipose-Derived Stem Cell Secretome in Oral and Maxillofacial Medicine: A Composition-Based Perspective. Biology. 2024 Dec;13(12):1016.

196. Soleimanifar F, Hosseini FS, Atabati H, Behdari A, Kabiri L, Enderami SE, et al. Adipose-derived stem cells-conditioned medium improved osteogenic differentiation of induced pluripotent stem cells when grown on polycaprolactone nanofibers. J Cell Physiol. 2019 July;234(7):10315–23.

197. Ivanisova D, Bohac M, Culenova M, Smolinska V, Danisovic L. Mesenchymal-Stromal-Cell-Conditioned Media and Their Implication for Osteochondral Regeneration. International Journal of Molecular Sciences. 2023 Jan;24(10):9054.

198. Werb Z, Tremble PM, Behrendtsen O, Crowley E, Damsky CH. Signal transduction through the fibronectin receptor induces collagenase and stromelysin gene expression. J Cell Biol. 1989 Aug;109(2):877–89.

199. Jin H, Jiang S, Wang R, Zhang Y, Dong J, Li Y. Mechanistic Insight Into the Roles of Integrins in Osteoarthritis. Front Cell Dev Biol [Internet]. 2021 June 18 [cited 2025 July 13];9. Available from: https://www.frontiersin.org/journals/cell-and-developmental-biology/articles/10.3389/fcell.2021.693484/full

200. Fermor B, Weinberg JB, Pisetsky DS, Guilak F. The influence of oxygen tension on the induction of nitric oxide and prostaglandin E2 by mechanical stress in articular cartilage. Osteoarthritis and Cartilage. 2005 Oct 1;13(10):935–41.

201. Werner NC, Stoker AM, Bozynski CC, Keeney JA, Cook JL. Characterizing correlations among disease severity measures in osteochondral tissues from osteoarthritic knees. Journal of Orthopaedic Research. 2021;39(5):1103–12.

202. Wang C, Jiang C, Yang Y, Xi C, Yin Y, Wu H, et al. Therapeutic potential of HUC-MSC-exos primed with IFN-γ against LPS-induced acute lung injury. Iran J Basic Med Sci. 2024;27(3):375–82.

203. Murphy N, Treacy O, Lynch K, Morcos M, Lohan P, Howard L, et al. TNF-α/IL-1β-licensed mesenchymal stromal cells promote corneal allograft survival via myeloid cell-mediated induction of Foxp3+ regulatory T cells in the lung. FASEB J. 2019 Aug;33(8):9404–21.

204. Ozkan S, Isildar B, Ercin M, Gezginci-Oktayoglu S, Konukoglu D, Neşetoğlu N, et al. Therapeutic potential of conditioned medium obtained from deferoxamine preconditioned umbilical cord mesenchymal stem cells on diabetic nephropathy model. Stem Cell Res Ther. 2022 Sept 2;13(1):438.

205. Priya K, Rawat S, Das D, Chaubey M, Thacker H, Giri K, et al. Autoimmunity and clinical pathology amelioration in SLE by dexamethasone primed mesenchymal stem cell derived conditioned media. Stem Cell Res Ther. 2025 Mar 29;16(1):158.

206. Caneparo C, Baratange C, Chabaud S, Bolduc S. Conditioned medium produced by fibroblasts cultured in low oxygen pressure allows the formation of highly structured capillary-like networks in fibrin gels. Sci Rep. 2020 June 9;10(1):9291.

207. Kim KH, Kim YS, Lee S, An S. The effect of three-dimensional cultured adipose tissue-derived mesenchymal stem cell–conditioned medium and the antiaging effect of cosmetic products containing the medium. Biomedical Dermatology. 2019 Dec 31;4(1):1.

208. Parate D, Kadir ND, Celik C, Lee EH, Hui JHP, Franco-Obregón A, et al. Pulsed electromagnetic fields potentiate the paracrine function of mesenchymal stem cells for cartilage regeneration. Stem Cell Research & Therapy. 2020 Feb 3;11(1):46.

11. List of figures and tables

12. Appendix

Supplementary Figure 1– Results of CM/pCM and/or inflammatory stimulus in the opposite compartment

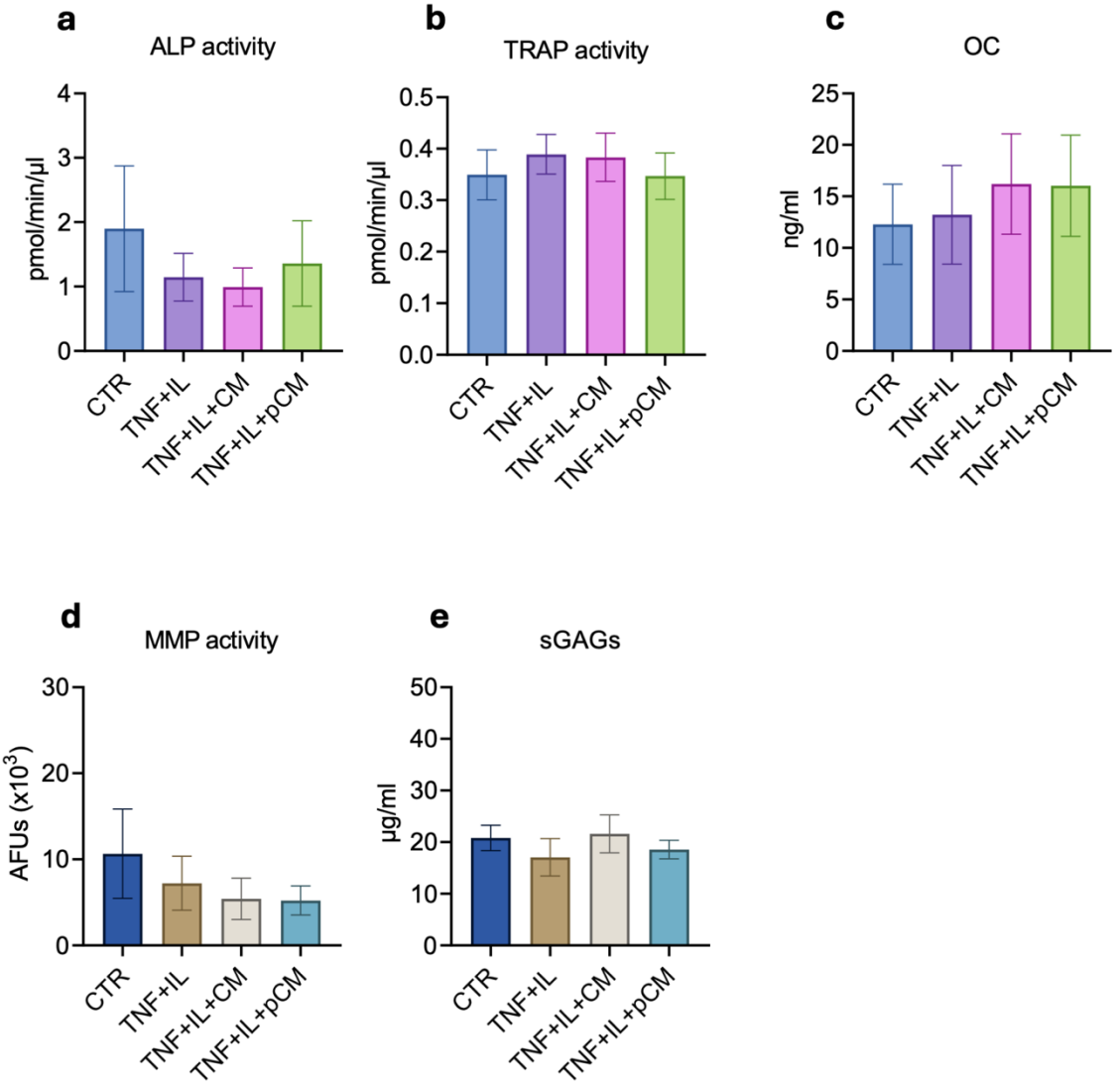

Supplementary Figure 1 – Results of CM/pCM and/or inflammatory stimulus in the opposite compartment

a, b) *Markers of cartilage health state in the bone side at the endpoint:* ***a)*** *MMP activity and* ***b)*** *sGAG release.* ***c, e)*** *Markers of bone metabolic state in the cartilage side at the endpoint:* ***c)*** *ALP activity,* ***d)*** *TRAP activity, and* ***e)*** *OC levels. All data are represented as mean ± SEM. Bone data are normalized on explant weight in g.*

Supplementary Table 1: Preconditioning strategies

Type of conditioning	Specific stimuli	Effects	Pathology/ condition Investigated	Citation
Biological	TNF-α and IL-1β	Increased secretion of anti-inflammatory factors (e.g., IL-4, IL-10, TGF-β) and growth factors (e.g., HGF, VEGF, BDNF, FGF2)	Osteoarthritis	Giannasi et al., 2022 (26)
	IFN-γ	Enhanced anti-ROS and anti-inflammatory activity through downregulation of NFkB, IDO1 and PGE-2	Acute lung injury	Wang et al., 2024 (202)
	TNF-α and IL-1β	Improved corneal allograft survival through NO-mediated T cell regulation	Corneal allograft rejection	Murphy et al., 2019 (203)
Chemical	Deferoxamine (DFX)	Mimics hypoxia, enhancing VEGF and GDNF secretion	Diabetic nephropathy	Ozkan et al., 2022 (204)
	Dexamethasone	Protective effects on organs, amelioration of multi-tissue symptomatology, and inhibition of pathological immune responses	Systemic Lupus Erythematosus	Priya et al., 2025 (205)
Physical	Hypoxia (1–5% O_2)	Increased secretion of pro-survival and pro-angiogenic factors (e.g., VEGF, HGF, IL-6)	Ischemic conditions, wound healing	Caneparo et al., 2020 (206)
	3D Culture	Enhanced expression of collagen and ECM amelioration, improved efficacy in dermis treatments	Dermis and skin ageing	Kim et al., 2020 (207)
	Electromagnetic Fields (EMF)	Enhanced regenerative properties, increased growth and pro-chondrogenic factor secretion	Cartilage degeneration	Parate et al., 2020 (208)

Supplementary Table 2: Tissues in OA

OA	Tissue	Physiological role	Early-stage symptoms	Late-stage symptoms
Common tissues	**Articular cartilage**	Provides smooth, low-friction surface for joint movement; absorbs mechanical load	Chondrocyte activation and proliferation Increased synthesis of inflammatory mediators (IL-1β, TNF-α) Upregulation of MMPs and ADAMTSs Loss of matrix homeostasis begins	Chondrocyte apoptosis and senescence Severe loss of proteoglycans and collagen type II Fissuring and erosion of cartilage Exposure of subchondral bone
	Subchondral bone	Supports cartilage, absorbs and distributes mechanical load.	Increased bone remodeling and turnover Subtle thickening of the subchondral plate Bone marrow lesions begin to appear	Subchondral sclerosis Formation of cysts and collapse of bone architecture Development of osteophytes and joint deformity
	Synovial membrane	Produces synovial fluid; maintains joint homeostasis and immune balance	Mild synovial hyperplasia Infiltration of macrophages and low-grade inflammation Increased production of pro-inflammatory cytokines Pain mediator release (e.g., PGE2, NGF)	Persistent synovitis Fibrosis and chronic thickening of synovial lining Amplification of inflammation and joint damage
	Tendon ligament	Maintain joint alignment and stability	Microtrauma and matrix softening Early structural weakening	Ligament laxity and fibre degeneration Mechanical instability worsening joint degeneration
	Periarticular muscles	Provide joint support, enable movement, absorb shock	Altered neuromuscular activation Mild disuse atrophy due to pain	Marked muscle weakness and atrophy Loss of proprioception and shock absorption

				Further functional decline and joint overload
Knee	**Meniscus**	Distribute load, absorb shock, and stabilize the joint	Matrix disorganization	Tearing
			Mild degeneration	Calcification
			Decreased hydration and elasticity	Biomechanical failure
	Patellofemoral cartilage	Facilitates patellar gliding and force transmission in knee extension	Surface softening (chondromalacia)	Cartilage erosion
			Focal thinning	Patellar maltracking and chronic pain
			Activity-related anterior knee pain	
	Cruciate and collateral ligament	Provide anterior-posterior and medial-lateral joint stability	Mild laxity or strain from altered joint loading	Disrupted or absent ligament
			Inflammation of entheses	Movement impairment
	Hoffa's fat pad	Cushions the anterior knee and supports synovial and immune responses	Inflammation (Hoffitis)	Decreased depth and thickness
			Oedema	Inflammatory mediators release
			Increased vascularization	
Hip	**Acetabular labrum**	Enhances joint stability and maintains intra-articular pressure	Labral tearing or fraying	Labrum degeneration and ossification
			Mild instability	Acetabular cartilage exposure
			Pain during rotation or load	Joint stiffness and restricted ROM
	Ligamentum teres	Contributes to hip joint stability and proprioception	Microtears	Degeneration or rupture
			Mild instability	Intra-articular debris
			Inflammation and thickening	Worsening hip pain and functional limitation
	Deep gluteal tendon	Stabilize pelvis and assist in hip abduction	Tendon overload or tendinopathy	Tendon tears
			Lateral hip pain	Muscle atrophy and gait disturbances
Hand		Maintain small joint alignment	Laxity	Joint deformity

	Collateral ligament and joint capsule	and support during motion	Joint discomfort Early joint instability	Loss of fine motor control
	Flexor and extensor tendons	Facilitate finger flexion and extension	Sheath thickening Mild pain on movement	Impaired tendon gliding Reduced grip strength Pain with motion
Spine	**Intervertebral disc**	Provides shock absorption and spinal flexibility	Disc dehydration and reduced height Mild axial back pain	Disc collapse Instability Osteophyte formation Chronic pain
	Facet capsule	Supports facet joint integrity and motion limitation	Capsular thickening Stiffness and discomfort with movement	Capsule fibrosis Joint locking or impingement Reduced mobility
	Ligamentum flavum	Maintains vertebral alignment and returns spine to neutral position	Hypertrophy begins Minimal symptoms	Significant thickening causing spinal stenosis Neurogenic claudication
Temporo-mandibular joint	**Articular disc**	Separates joint surfaces; facilitates smooth jaw movement	Disc displacement with reduction Clicking or mild pain	Degeneration or displacement without reduction Restricted jaw movement Joint sounds and pain
	Capsule and lateral pterygoid insertion	Stabilizes TMJ during opening/closing; assists disc movement	Capsular irritation Muscle spasm or dysfunction	Capsular fibrosis Persistent pain Jaw asymmetry or deviation

13. Dissemination of results

During my PhD I made efforts to disseminate the results of my project both to the scientific community and to the general public. The main way of communication has been the preparation and submission of manuscripts to peer-reviewed international journals, indexed in scientific databases, and publishing only in open access modalities. Additionally, all the data collected for the peer-reviewed publications have been added to the repository Zenodo, in order to facilitate their accessibility and guarantee transparency. I also presented my results in national and international conferences in the field of regenerative medicine and stem cell research, such as the GISM Annual Meeting 2024, where I also received the Young Investigator Award for the presentation of my work on secretome characterization. Some results are still in preparation or are under review and will be presented to journals to increase their visibility and impact.

I disseminated my work also outside the academic field: I participated in outreach events organized by the University of Milan with the aim of informing non-experts and raising awareness about the possible applications of stem cell research in the orthopaedic field. I consider this aspect an important responsibility, that allows us to gather the trust and encouragement from the general public.

13.1 Lay summary (English)

In my PhD project I studied the secretome derived from mesenchymal stem cells, which is the collection of molecules released by these cells in their surrounding environment. This byproduct can play a role in tissue regeneration and in the reduction of inflammation, without the need of transplanting the cells themselves. During my project, I investigated how different variables during its production, such as specific priming strategies on cells or freezing steps after the collection, can change the composition of the secretome and eventually its activity. I also developed laboratory models based on human tissues to test the effects of the secretome on joint tissues: cartilage, synovial membrane and bone. The final aim was evaluating possible applications of secretome in joint diseases and in regenerative medicine. The results of my research may contribute to the development of new strategies to improve treatments for patients with skeletal or joint tissue damage.

13.2 Lay summary (Italiano)

Nel mio progetto di dottorato ho studiato il secretoma derivato da cellule staminali mesenchimali, cioè l'insieme di molecole che queste cellule rilasciano nell'ambiente in cui crescono. Questo sottoprodotto può avere effetti terapeutici nei processi di rigenerazione dei tessuti e nella riduzione dell'infiammazione, senza dover ricorrere al trapianto delle cellule. Nel corso del mio progetto, ho analizzato come alcune variabili nella produzione del secretoma, per esempio particolari stimolazioni sulle cellule o passaggi di gelo-scongelo dopo la raccolta dello stesso, ne possano modificare la composizione e, in alcuni casi, la sua efficacia. Ho anche sviluppato modelli di laboratorio basati su tessuti umani per studiare l'effetto del secretoma sui tessuti caratteristici delle articolazioni: cartilagine, membrana sinoviale e osso. L'obiettivo finale era di valutare le possibili applicazioni del secretoma nelle malattie articolari e nella medicina rigenerativa. I risultati di questo progetto potranno contribuire allo sviluppo di strategie innovative per migliorare la cura di pazienti con danni a tessuti scheletrici o articolari.